FINAL REPORT

APPLICATIONS OF FIBER OPTIC SENSORS IN WEIGH-IN-MOTION (WIM) SYSTEMS FOR MONITORING TRUCK WEIGHTS ON PAVEMENTS AND STRUCTURES

Submitted to:

Dr. Richard Livingston, Program Director
U.S. Department of Transportation's, FHWA
Washington, D.C.

and

Mr. Rais Rizvi, Research Engineer
NM State Highway and Transportation Department
Albuquerque, NM

Submitted by:

Luz-Elena Y. Mimbela, Project Engineer/Manager
Jim Pate, Engineer IV
Scott Copeland, Research Assistant
New Mexico State University
Southwest Technology Development Institute
Box 30001/Dept. 3SOL
Las Cruces, New Mexico 88003

and

Perry M. Kent, VDC Consultant
John Hamrick, VDC Consultant

April 17, 2003

Disclaimer Notice

This document is disseminated under the sponsorship of the Department of Transportation via the New Mexico State Highway and Transportation Department (NMSHTD) in the interest of information exchange. The United States Government assumes no liability for its contents or use thereof.

The contents of this document reflect the views of the contractor and subcontractors, who are responsible for the accuracy of the data presented herein. The contents do not necessarily reflect the official policy of the Department of Transportation or the NMSHTD.

This document does not constitute a standard, specification, or regulation.

The United States Government or the Vehicle Detector Clearinghouse does not endorse products or manufacturers. Vendor and manufacturer's names appear herein only because they are considered essential to the purpose of this document.

EXECUTIVE SUMMARY

The main objective of this project was to investigate emerging technologies and to establish criteria for evaluating fiber optic sensors used to measure actual dynamic loads on pavements and structures. The dynamic load of particular interest for this project was the vertical component of the load caused by vehicles as they move over the pavement or structure, which is referred to as weigh-in-motion (WIM). Therefore, this project was aimed at determining the state-of-the-art of fiber optic WIM systems.

Although WIM systems are commercially available at this time, fiber optic based WIM systems offer the potential to measure actual dynamic loads while offering sensors that are light weight, immune to electromagnetic interferences, offer the ability to be imbedded under hostile environments, and have extremely high bandwidth capability (Udd, 1995). Furthermore, it is anticipated that fiber optic WIM systems, once developed, will eventually be lower in overall cost relative to conventional systems, due to the inherently low cost of the fiber optic sensors.

In addition to the uses of WIM data for assessing useful and safe life of structures and pavements, WIM data can also be utilized as part of the National Intelligent Transportation System (ITS) Architecture, which is a framework for Integrated Transportation into the 21st century (FHWA, 2003). Many states in the U.S. have developed or are developing local ITS Architecture plans and WIM systems can play a major role in providing real-time data that can be used to achieve the goals of these plans.

In order for WIM systems to play a major role in achieving the goals of the national and local ITS Architecture plans, deployment of these systems must be dramatically increased and their real-time monitoring capabilities need to be improved. In order to satisfy the deployment needs and real-time monitoring capabilities of WIM systems for ITS purposes (includes traffic monitoring) lower cost alternatives must be developed with higher bandwidth capacity. Fiber optic sensor WIM systems have the potential to offer these two key capabilities once the technology has been well developed.

Project Objectives

The specific objectives of this project included:

1. Perform a comprehensive review of the literature for fiber optic sensors for measurement of in-motion weight or weigh-in-motion (WIM) applications; performance criteria (precision, accuracy and durability); and applications of weigh-in-motion (WIM) data for fatigue in pavements and structures.
2. Develop recommended criteria for testing and evaluating commercial fiber optic sensors and measurement systems for WIM.
3. Prepare a final report detailing the results of previous two objectives. The final report will present specific recommendations for the use of fiber optic WIM system data to measure actual loads on pavements and structures.

To accomplish the objectives, a multi-task approach was taken using a research team consisting of staff from the Southwest Technology Development Institute (SWTDI), and Perry Kent and John Hamrick; both project consultants with the Vehicle Detector Clearinghouse (VDC). In conducting the state-of-the-art study for this type of technology, the research team decided to collect information using three techniques: 1) literature search and review, 2) attend pertinent conferences, trade shows, etc., and 3) visit field sites where this technology was being used for WIM.

Study Results

The following sections describe the results of objectives 1 and 2 for this study listed previously. Objective three is simply this report. Although all of the three objectives were met, the technology of fiber optic sensors in WIM system applications was not mature or commercially available throughout most of the study.

<u>Literature Review</u>

Table E.1 shows a summary of the results of the state-of-the-art study for fiber optic sensors in WIM system applications determined from a comprehensive review of the literature available on this topic. The accuracy was compared to gross vehicle weight (GVW) and the speed at which the vehicles passed over the sensors. During the state-of-the-art study documentation for a total of ten different studies was reviewed from the following entities:

1. New Mexico State University (NMSU) / Naval Research Laboratory (NRL)
2. Blue Road Research (BRR)
3. Oak Ridge National Laboratories (ORNL)

4. New Jersey Institute of Technology (NJIT)
5. University of Connecticut (UCONN)
6. Florida Institute of Technology (FL Tech)
7. Laboratoire Central des Ponts et Chaussees (LCPC)
8. Virginia Polytechnic Institute and State University - 1990 Strategic Highway Research Program (SHRP) Project
9. Virginia Polytechnic Institute and State University - Project on Using Fiber Optic Sensors for Civil Infrastructure Monitoring
10. United Kingdom Highway Agency's Project

Table E.1. Results of State-of-the-Art Study for Fiber Optic Sensors in WIM System Applications.

Entity – Year	Method	GVW Accuracy Speed	Status
NMSU/NRL – 1998	Multiple Bragg Grating	Not determined	Research – No plans to continue at this point
Blue Road Research (BRR) 1998 to present	Multiple Bragg Grating	Not determined	Research – Field study stage in progress
ORNL – 1990 to 1991	Transparent Rubber	±0.5% to ±3% 5km/hr (3 mph)	Research – No plans to continue at this point
NJIT – 1996	Polarimetry	Lab testing w/o vehicles	Research – No plans to continue at this point
UCONN – 1997 to present	FTDM Dual Core fiber	±4% to ±12% Static (0 mph)	Research – Laboratory testing is ongoing
FL Tech –1999 to present	Microbend	8% to 14% 10-40 mph	Commercial Deployment of Fiber Optic WIM System
LCPC – 1999	Low birefringence single mode optical fiber	±22.5 lbf (lbs) 6.2-9.3 mph	Research – On hold until demand for product is determined
VPI & State University			
SHRP Project – 1990	Extrinsic pressure sensor	Lab testing w/o vehicles	Research – No evidence of plans to continue at this point
Civil Infrastructure Monitoring Project – 1994	Fabry-Perot	Not determined	Research – No evidence of plans to continue at this point
United Kingdom Hwy. Agency – 2002	Interferometry	Not determined	Research – No evidence of plans to continue at this point

The results of the state-of-the-art study for the use of fiber optic sensors in WIM system applications clearly demonstrated that this technology was in the research stages at the time of this study with the exception of FL Tech's microbend sensor WIM system (highlighted). At the beginning of the state-of-the-art study, the FL Tech study was also in the research stage. However, in late 2002 and early 2003 the researchers made a breakthrough and a commercially available fiber optic WIM system was developed and marketed. As of the date of this report a

WIM system using microbend fiber optic sensors (WIM 3000) was commercially available from Optical Sensors and Switches, Inc. and had been deployed in at least one location in the U.S.

Information on performance criteria (precision, accuracy, and durability) for WIM systems using fiber optic sensors is clearly lacking. However, it is obvious that once the technology matures to the demonstration phase, acquiring this type of information should be top priority since this will allow providers of this technology to find a niche for their specific product.

The results of the literature review for applications of WIM data for the determination of fatigue in pavements and structures are described in Chapter 3 of this report. Chapter 3 describes the use of WIM data for determining fatigue on bridges using WIM data vs. simplified the American Association of State Highway Transportation Officials (AASHTO) methods that use estimated values of truck weights (HS15 fatigue truck) and number of trucks crossing the bridge.

The results from this literature review demonstrated that using an HS15 fatigue truck and using GVW's computed with WIM data for determining fatigue in steel bridges yielded similar conservative figures for service life when compared to using actual field measurements of individual stress ranges. One conclusion made from this particular study was to first estimate the fatigue life of a bridge using an HS15 fatigue truck, which would give a conservative estimate. If the safe life was found to be shorter than the desired service life, the fatigue analysis using actual field measurements of individual stress ranges should be performed.

Evaluation and Testing of Fiber Optic WIM Systems

The second objective stated previously of this study for fiber optic sensors in WIM system applications was to develop recommended criteria for testing and evaluating commercial fiber optic sensors and measurement systems for WIM. Chapter 6 of this report describes the use of the American Society for Testing and Materials' (ASTM's) WIM standard E1318-02 for calibration and testing of the entire WIM system (sensors and measurement system combined). The reader is also referred to the *State's Successful Practices Weigh-in-Motion Handbook (WIM Handbook)* by McCall, et al for guidelines on evaluating commercial WIM systems.

The ASTM WIM standard and the WIM Handbook offer criteria for evaluating and testing WIM systems as a whole and do not separate the sensors and the measurement system. For testing only the sensors portion of the system, the users of WIM systems rely on the vendors' guidelines. This will be the case as well for the evaluation and testing of fiber optic sensors in WIM system applications. Furthermore, if there should be a problem with the sensors this will most likely show up as a problem during the calibration and evaluation and testing of the entire WIM system.

Conclusions and Recommendations

Fiber optic sensors in WIM system applications show considerable promise for meeting both traffic monitoring needs and as part of the national and local ITS architecture plans. However, the technology is not mature with only one type of system commercially available and several others in various stages of development. In order to bring the technology of using fiber optic sensors in WIM system application to maturity, additional research must be conducted to advance potential candidates to the field demonstration phase where further evaluation and testing can take place to determine performance criteria (precision, accuracy and durability) in real-life installations.

SWTDI plans to continue its research in this area to bring some of the most advanced fiber optic sensor systems to the field demonstration stage. At the time of this study, SWTDI was a partner in a proposed project to conduct a field demonstration test of at least two fiber optic sensor systems in WIM system applications. However, additional funds are needed to conduct several more field demonstrations of additional potential candidates that might be ready for this stage of development.

TABLE OF CONTENTS

List of Figures

List of Tables

Chapter 1 – Introduction

The main objective of this project was to investigate emerging technologies and to establish criteria for evaluating state-of-the-art fiber optic sensors used to measure actual dynamic loads on pavements and structures. The dynamic load of particular interest for this project was the vertical component of the load caused by vehicles as they move over the pavement or structure, which is referred to as weigh-in-motion (WIM). Therefore, this project was aimed at determining the state-of-the-art of fiber optic WIM systems.

The need for this study was based on the fact that heavy truck loadings result in repetitive stresses that cause fatigue in highway bridges and pavement. The static axle loads measured by conventional weigh stations can be considerably different from actual traffic loadings. On the other hand, WIM systems have the ability to provide actual real-time dynamic loadings on the pavement or structure caused by moving vehicles. For bridges, true real-time WIM data can be analyzed to estimate the probability that the maximum load rating of the bridge is being exceeded or to calculate the fatigue cycles experienced by the structure, which can in turn be used to predict remaining service life (Ansari, 1998). For pavements, WIM data are used to predict remaining service life of the roadway.

Although WIM systems are commercially available at this time, fiber optic based WIM systems offer the potential to measure actual dynamic loads while offering sensors that are light weight, immune to electromagnetic interferences, offer the ability to be imbedded under hostile environments, and have extremely high bandwidth capability (Udd, 1995). Furthermore, it is anticipated that fiber optic WIM systems, once developed, will eventually be lower in overall cost relative to conventional systems, due to the inherently low cost of the fiber optic sensors. Also, several successful structural monitoring applications utilizing fiber optic sensors in bridges had been demonstrated at the time of this research study. Therefore, the potential for utilizing a structural monitoring fiber optic installation for gathering WIM data was great.

The specific objectives of the project included:

- Perform a comprehensive review of the literature for fiber optic sensors for measurement of in-motion weight or weigh-in-motion (WIM) applications; performance criteria (precision, accuracy and durability); and applications of weigh-in-motion (WIM) data for fatigue in pavements and structures.

- Develop recommended criteria for testing and evaluating commercial fiber optic sensors and measurement systems for weigh-in-motion.

- Prepare a final report detailing the results of previous two objectives. The final report will present specific recommendations for the use of fiber optic WIM system data to measure actual loads on pavements and structures.

Chapter 2 – Methods and Approach

To accomplish the objectives described in Chapter 1, a multi-task approach was taken using a research team consisting of staff from SWTDI, and Perry Kent and John Hamrick; both project consultants with the Vehicle Detector Clearinghouse. As stated in the introduction section of this report, this project was aimed at determining the state-of-the-art of fiber optic WIM systems. In conducting a state-of-the-art study for this type of technology, the research team decided to collect information using three techniques: 1) literature search and review, 2) attend pertinent conferences, trade shows, etc., and 3) visit field sites where this technology was being used for WIM. The following sections discuss briefly the three techniques and specific tasks carried out to complete the objectives of the project.

Literature Search and Review

A literature search was conducted for the use of fiber optic sensors in WIM System applications. All research team members conducted literature searches using the world-wide-web, technical libraries, as well as references in previously obtained reports. All pertinent publications in books, conference proceedings and research reports were collected for review.

Collection of Product Information at Conferences

During the course of the project, research team members attended several conference events where either papers on the use of fiber optic sensors in WIM systems were presented and/or vendors of fiber optic sensors were displaying this type of technology. The events that were visited by some of the research team members included:

- The North American Travel Monitoring Exhibition and Conference (NATMEC) 2000,
- The Intelligent Transportation Society of America Tenth Annual Meeting and Exposition (ITS 2000),
- 80th Annual Meeting of the Transportation Research Board (TRB)-2001,
- The International Society for Optical Engineering's (SPIE) 8th Annual International Symposium on Smart Structures and Materials,
- SPIE 6th Annual Symposium on Non-Destructive Evaluation (NDE) for Health Monitoring and Diagnostics, and

3

- The North American Travel Monitoring Exhibition and Conference (NATMEC) 2002.

Field Visits

Based on the results of the literature review and the conference events attended two research projects that were conducting field studies at the time of this study of fiber optic sensors in potential WIM system applications were pinpointed. The two projects were the following:

- "Analysis and Testing of the I-10 Bridge Over University Avenue Using a Fiber Optics Bragg Grating Monitoring System," in Las Cruces, New Mexico, and
- "Interstate 84 Freeway Installation and Horsetail Falls Bridge Installation and Traffic Monitoring," East of Portland, Oregon.

Research team members decided to conduct a site visit of each of the two field sites mentioned previously. Since the New Mexico project was in the final stages at the time of this study, the research team decided to visit this field site first. Therefore, VDC consultants John Hamrick and Perry Kent met the rest of the New Mexico State University research team members in Las Cruces, New Mexico in May 2000. The research team members visited with Dr. Rola Idriss, principal investigator for the New Mexico project, on the results of the traffic monitoring application of the fiber optic Bragg grating system installed on the I-10 Bridge and its potential for WIM applications.

The second site visit was to the Interstate-84 freeway installation and the Horsetail Falls Bridge installation of Blue Road Research (BRR) fiber optic sensors for a traffic monitoring application and structural monitoring application, respectively in the Portland, Oregon vicinity. Three research team members traveled to Portland and met with Dr. Eric Udd, Marley Kunzler and other Blue Road Research staff and with Robert Edgar and Steve Soltez of the Oregon Department of Transportation to tour the I-84 site and the Horsetail Falls Bridge installations. In addition, Dr. Eric Udd, president of BRR gave research team members a tour of the BRR facility and the small-scale installations of the fiber optic sensor used for experimentation prior to full-scale installation.

Chapter 3 – Background on Weigh-in-Motion Systems

This chapter provides background information on the concept and technical aspects of conventional weigh-in-motion (WIM) systems. The information contained in this section will lay the foundation for discussion of fiber optic WIM systems for measuring dynamic loads on pavements and structures as well as the applications of using WIM data to determine fatigue in pavements and structures. The information contained in the sections "Application and Uses" and "Conventional Equipment," was taken from a document prepared for the US Department of Transportation's Federal Highway Administration (FHWA) titled "Summary of Vehicle Detection and Surveillance Technologies," (Mimbela & Klein, 2000).

Highway Weigh-in-Motion (WIM) Concept

To obtain the static weight of a vehicle, a total upward force exactly equal to the downward force of gravity is applied through the motionless (vertical direction) tires of the vehicle and measured simultaneously by scales (force transducers) or a balance. In-motion weighing of a highway vehicle on the other hand, attempts to approximate the static weight of the vehicle, a wheel, an axle, or a group of axles on the vehicle by measuring instantaneously, or during a short period of time, the vertical component of dynamic (continually changing) force that is applied to a smooth, level road surface by the tires of the moving vehicle. The weight of the vehicle does not change when it moves over the road, but the dynamic force applied to the road surface by a rolling tire of the vehicle varies from more than double its static weight when it runs over a bump, thereby exerting a large unbalanced force on the wheel mass, to zero when the tire bounces off the road (Lee & Ferguson, 1983). Results of simple experiments documented by Lee and Ferguson in 1983 demonstrated the following:

- The pattern of wheel force for a given vehicle traveling over the same road surface at the same speed is consistent;
- The mass of the vehicle components affects the magnitude and frequency of dynamic wheel forces and their variation from static weight; and
- The dynamic wheel force is sometimes less than static weight, and sometimes greater.

One hundred percent accurate in-motion weighing is the sum of the vertical forces exerted on a smooth, level surface by the perfectly round and dynamically balanced, rolling wheels of a vehicle at constant speed in a vacuum. None of the vehicle components will be accelerating vertically under these ideal conditions (Lee and Ferguson, 1983). However, such conditions never exist in practice. Some of the factors that affect the tire forces of a moving vehicle are shown in Table 3.1. The closer actual conditions approach ideal conditions, the better the approximation of vehicle weight that can be made by measuring the vertical forces applied to the roadway surface by the tires of a moving vehicle.

Table 3.1. Factors That Affect Wheel Loads of a Moving Vehicle (Lee & Ferguson, 1983).

Roadway Factors	Vehicle Factors	Environment Factors
1. Longitudinal Profile	1. Speed, Acceleration	1. Wind
2. Transverse Profile	2. Axle Configuration	2. Temperature
3. Grade	3. Body Type	3. Ice
4. Cross Slope	4. Suspension System	
5. Curvature	5. Tires	
	6. Load, Load Shift	
	7. Aerodynamic Characteristics	
	8. Center of Gravity	

WIM Systems

A typical weigh-in-motion (WIM) system consists of one or more wheel force transducers (sensors) plus the associated signal processing equipment. Typically, vehicle presence sensors (e.g., inductance loop detectors) or axle passage detectors are also included as part of the WIM system to measure speed, axle spacing, overall vehicle length, and lateral placement as the vehicle passes over the system.

Transducer (Sensor)

The key component of the WIM system is the wheel force transducer (sensor), which converts the vertical component of the force applied to its surface through the tires of a moving vehicle into a proportional signal that can be measured and recorded. To be able to measure the total

vertical force imparted on the transducer by a selected tire, or by a group of tires, on a vehicle, the full tire contact area(s) of interest must be supported completely and simultaneously by the transducer. Next, the transducer must produce a signal, which is exactly proportional to the vertical force applied (Lee & Ferguson, 1983). Furthermore, the signal produced by the transducer must not be affected by the following: 1) tire contact area, stiffness, inflation pressure, nor position on the sensing surface of the transducer, 2) tractive forces, 3) temperature, nor 4) moisture.

As illustrated by Lee and Ferguson, 1983, an ideal force vs. time signal from a wheel force transducer is shown on Figure 3.1. As the tire contact length, L, moves onto the transducer, force increases until the transducer supports the full tire contact area. Force does not change (assuming no vertical movement of the vehicle components) during the time T_{W-L} while the tire contact patch continues to be supported only by the transducer. This is the time when wheel force measurements are possible.

The surface of the wheel force transducer must be exactly even with the surface of the level roadway into which it is installed in order not to create an unbalanced force on the wheel/tire mass as the tire passes over the transducer. In addition, the transducer should deflect under load the same amount as the road surface. If the transducer is stiffer than the pavement, the net effect will be like that of the wheel running up on a bump. Conversely, if the transducer deflects more than the road surface under load, the wheel will be affected as if it runs into a shallow hole. The transducer should deflect a small amount under load in order to behave like the surrounding road surface (Lee & Ferguson, 1983).
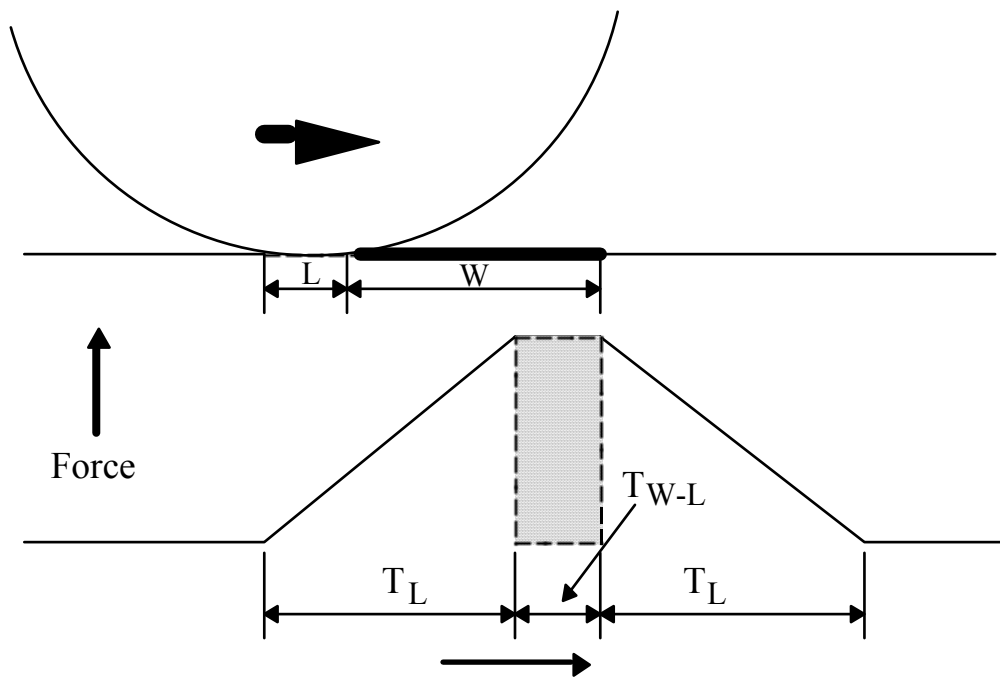
Figure 3.1. Force vs. Time Signal from a Wheel Force Transducer (Lee & Ferguson, 1983).

Another requirement of the wheel force transducer is its mass, which must be relatively small if dynamic forces of a few thousand pounds applied for a few milliseconds are to be measured accurately by sensing the displacement of the elastic element of the transducer. The inertia of the transducer mass affects its displacement with respect to time under an applied unbalanced force. Furthermore, the elastic transducer mass that is displaced downwards by an applied force will rebound when the force is removed and move upwards under the spring force of the elastic body until the force of gravity in the opposite direction reverses the movement, thus creating an oscillating motion. The oscillating motion of the transducer will continue until some form of damping dissipates the energy stored in the elastic system. Typically, the greater the mass, the slower the period of oscillation and the more the energy required for damping. An effective wheel force transducer must be at rest when the wheel force to be measured is applied. A low mass transducer tends to oscillate at high frequency and damp to a rest position relatively quickly, thus a low mass, critically damped transducer is preferred (Lee & Ferguson, 1983).

Another requirement of the transducer or sensor in a WIM system is its capacity to handle the wheel loads that will occur in practice. Wheel force transducers or sensors operate in an extremely harsh environment of impact loading, vibration, climatic extremes, and sometimes-intentional abuse, thus wear and tear is expected.

Following is a summary of some of the desirable features of wheel load transducers or sensors that have been discussed in this section:

1. Insensitive to: tire contact area (single/dual), tire stiffness, tire inflation pressure, tire position (edge-to-edge), temperature, moisture;
2. Installed even with the roadway surface;
3. Signal directly proportional to applied vertical force;
4. Small deflection under load;
5. Low mass/high compliance;
6. High natural frequency/critical damping;
7. Capacity;
8. Durability; and
9. Maintainability.

This partial list may be useful for assessing the adequacy of the transducer design and the potential performance of this integral part of a WIM system.

WIM Signal Processing Equipment

In typical WIM systems, analog signals from the wheel force transducers must be interpreted and recorded by appropriate electronic instruments to yield samples of dynamic wheel forces that serve as estimates of wheel, axle, and gross vehicle weight. Analog-to-digital conversion of signals is routine, thus WIM systems are based around digital data processors. The description of this part of the typical WIM system will not be presented in this paper due to the highly vendor-specific nature of this component. However, for the fiber optic WIM system this part of the WIM system is in the early developmental stages and will be discussed in detail in Chapter 5.

Bridge WIM Concept

The concept of obtaining the weight of vehicles in motion by instrumenting single span bridges was demonstrated in different studies dating back to the early nineteen seventies. The theory behind the bridge Weigh-in-Motion (WIM) concept was to instrument a single span bridge with strain gauges and sum the electrical outputs which would result in a total strain output bearing a direct linear relationship to the total stress. The total stress would in turn have a direct relationship to the load and consequently to the weight of the vehicle causing the stress on the bridge.

In 1983 the Materials and Research Division of the Maine Department of Transportation conducted a study to test whether applying the bridge WIM concept would supply vehicle weight data rapidly and at a low cost (WIM Conference Proceedings, 1983). The bridge selected for instrumentation to carry out this study was a new simple span bridge 125 feet long and 58 feet wide and constructed with nine I-beams. A total of eight of the nine I-beams were equipped with four single weldable strain gauges made by Hitec Corporation. The gauges were placed transverse to the traffic flow at the midpoint of the bridge. The gauges were wired in a four arm Wheatstone bridge, thus stresses would all result in a resistive unbalance of all the arms of the strain gauge bridge such that the changes would be additive and the maximum electrical output would be maximized. The bulk of the heavy traffic for the selected bridge was southbound. Therefore, the bridge had two southbound lanes and one northbound lane.

In addition, since short and long wheel base vehicles of the same weight cause different strain on the gauge system, a co-ax sensor, set up to detect and record axle counts was installed on the transverse center line of the bridge directly over the gauges and covering the two southbound lanes. Also, since, as was mentioned previously, the heaviest loaded truck travel is southbound on the selected bridge, all the data was taken and calibration completed for this direction only.

The results of the study found the following:

- It was not possible to obtain separate axle weight as the bridge was under stress from the moment the vehicle enters the span;
- Maximum strain did occur when the heavier load carrying section of the vehicle was spanning the gauge line;

- Different vehicle axle spacings stressed the bridge differently so that calibrations must be done for each type of vehicle;

- It was obvious that loads in the northbound lane would reflect strains to the southbound lanes, a potential source of error;

- Further detailed studies showed that for automobiles northbound, reflected strain would be well within the error of the system when dealing with vehicle in the 80,000 to 120,000 pounds range;

- It was observed that a different output was produced depending on where in the two southbound lanes the vehicle traveled. However, the error was smallest when outputs from beams 2, 3, 4, 5, and 6 were summed;

- Since strain gauge output is a function not only of the weight of the vehicle but also a function of the axle spacing, calibration lines for the several major types of vehicles were deemed necessary;

- Off-center or unbalanced drive wheels or bogies were suspected of causing large variations in the degree of excitation of bridge oscillation; and

- The estimated error for calculating weights using this bridge WIM system was approximately $\pm5\%$ or a total of 10% maximum.

In conclusion, the results of this study showed that vehicle weight data could be obtained from measured strain data on a simple span bridge with the previously mentioned constraints.

Another series of studies that demonstrated the bridge WIM concept were the studies dealing with FHWA's "Weigh-in-Motion (WIM) and Response" system or WIM+R system. Case Western Reserve University developed the WIM system for the FHWA WIM study (FHWA/RD-86/045, 1987). This system was portable and utilized an existing bridge to serve as an equivalent static weight scale to obtain gross vehicle weights (GVW), axle weights and spacings, and speed. The system was redesigned and used to obtain simultaneous load and response data. The redesigned system was designated the WIM+RESPONSE system or WIM+R. This improved WIM system allowed the research team to calculate GVW's, axle weights, and axle spacings of 27,513 trucks crossing 33 bridges in Arkansas, Texas, California, Illinois, Georgia, New York, and Ohio (FHWA-RD-92-046, 1992). This study showed that during low average daily traffic episodes and short span bridges increased the probability that only one truck crossed the bridge at a time, thus a higher percentage of trucks from the traffic stream were weighed and classified. Therefore, the WIM+R system could only weigh and classify vehicles when only one truck at a time crossed the bridge.

The basic principle used in WIM calculations with a 2-D idealization of the bridge is that the internal moment must be equal to the external moment at a given section. The internal moment is expressed in terms of measured strain and the external moment in terms of loads, with the use of an influence line. The flow of calculations involves the following seven steps (FHWA-RD-92-046, 1992):

- Calculate truck velocity from tapeswitch times;
- Calculate axle spacings from tapeswitch times, knowing the velocity;
- Calculate the axle position on the bridge at each strain scan, knowing the velocity and axle spacings;
- Express the external moment in terms of axle weights and calculated influence line coefficients, knowing the axle positions at each scan;
- Express the internal moment in terms of strain data and cross-sectional properties of girders;
- For a test truck of known axle weights and spacings, solve the moment equilibrium equation for the "system" calibration factor; and
- Knowing the calibration factor, solve the moment equilibrium equation for the axle weights of other trucks crossing the bridge.

For a more detailed description of the previous method, please refer to FHWA-RD-92-045. This document also includes variants to the method as proposed by other researchers.

Application and Uses

WIM data is used for highway planning purposes, pavement and structural design, and traffic forecasts and weight enforcement programs. WIM systems have become an essential part of state weight enforcement and highway planning programs in the US simply due to the sheer volume of truck traffic on our highways that must be weighed to ensure public safety and highway infrastructure longevity. Specifically, large commercial trucks currently haul 8 million tons of goods each year and traveled an estimated 170 billion miles in 1997 (ORNL, 2001). Weighing trucks using slow and cumbersome static scales is not a viable option any longer. It takes too much time, requires too many people, and often requires more space than is available.

Pavement Issues

The most important step in pavement design is determining the amount of traffic loadings the pavement will have to withstand over the course of its life. Therefore, truck weight data is required by FHWA as a basic element for most States' pavement design process. Typically, this process requires estimation of future year Equivalent Single Axle Loadings (ESALs), which in turn requires a State to maintain data on axle loadings by vehicle types as well as estimates of trends on how various types of trucks will be represented in the future year traffic stream (FHWA, 1990). ESALs provide a relative measure of road life consumption that can be attributed to individual axle loads and trucks and is a major component of the pavement design equation for determining pavement thickness.

The importance of using future year ESALs in the pavement design process was demonstrated by the American Association of State Highway Transportation Officials' (AASHTO) road test of the 1960's. The findings of this road test showed that increases in pavement damage did not proceed in a simple linear fashion with increases in axle weights, but, rather, increased with a fourth power relationship relative to the increase in weight (FHWA, 1990). Consequently, AASHTO developed the factor known as the ESAL, which converted axle weights into a damage factor (1 ESAL is defined as the amount of damage done by a single 18,000-pound axle). Using this definition, vehicle weights could be converted into total ESALs. ESALs are a function of axle weight and configuration, pavement type being impacted, and the terminal serviceability (minimum level of acceptable performance) of the pavement (Stein, 1988). However, the most important characteristic is the weight and configuration of axles.

ESAL factors are assigned to each axle weight category for each type of axle (single, tandem, tridem) and pavement characteristics, flexible (asphalt) or rigid (Portland cement). The equations for the calculation of ESAL factors or Load Equivalency Factors (LEFs) were developed by AASHTO and are presented in the AASHTO Guide for Design of Pavement Structures (AASHTO, 1993). Currently, there are two sets of equations for calculating LEFs. One set is for the calculation of LEFs for flexible pavements and one set is for the calculation of LEFs for rigid pavements.

13

Bridge Issues

Bridges control both the overall traffic volume that a highway facility can carry as well as limit the size of individual vehicle and axle loadings. Bridge design is controlled to a large degree by the following site specifics (FHWA-DP-90-076-002, 1990):

- Vertical clearance required under the bridge,
- Horizontal distance to be spanned,
- Environmental effect to be met,
- Type of materials for construction,
- Expected design life, and
- Allowable maintenance.

However, while each of the previously mentioned factors affect the bridge design process particular attention to the truck loadings on the structure must be given. Design considerations must distinguish between the weight of the structure itself (dead load) as compared to the weights of the vehicles that are to be carried (live load). From a design viewpoint, short-span bridges are more directly affected by truck loadings than are long-span bridges due to the higher live to dead load ratio. Specifically, in short-span bridges approximately 70 percent of the bridge dimension is to hold up the traffic or live loads and only 30 percent is to hold up the weight of the bridge itself. For a long-span bridge (e.g. suspension bridge) only about 25 percent of the cross section of the cables and the main members is to hold up traffic for live loads, and 75 percent is to hold up the bridge itself.

Bridge engineers use a design vehicle that is considered to be representative of all vehicles that will use a bridge during its service life for bridge design purposes. This design vehicle is a HS20-44 truck, which is defined as a "heavy semi" or "highway semi" with a 20-ton tractor and the umbrella vehicle developed in 1944. The design vehicle will be referred to HS20 from now on in this report.

Bridge design is particularly sensitive to the points at which loadings can expect to be placed on the structure. For a truck, these points of load application are the axles. Specifically, given the same load and number of axles, a short vehicle will induce more stress than will a truck with a longer wheelbase. For example, for bridges up to 140 feet in length, the HS20 truck represents a loading of 72,000 pounds on three individual axles: the steering axle of 8,000 pounds followed at

14 feet by a drive axle of 32,000 pounds occurring between 14 and 30 feet behind the driving axle depending on the span under consideration. For bridges over 140 feet in length, the load is assumed to be uniform at 640 pounds per linear foot of lane, together with a concentrated load to simulate the effect of one heavier truck (FHWA-DP-90-076-002, 1990).

Once the live load is considered in design, the fatigue it will cause must be considered. Steel bridge components and the steel reinforcing bars in concrete bridges can wear out after repeated cycles of being loaded and unloaded as trucks roll across the bridge. During the bridge design process fatigue or load repetitions are considered after the bridge components have been sized for the HS loading. The total load, as well as the individual axle loads, must be considered in the fatigue analysis. The bridge components do not bend enough to be permanently deformed rather the materials they are made of get tired, in effect, after so many cycles of being loaded and unloaded. Fatigue becomes critical with an increase in the number of cycles and with an increase in the load. Also, since the live or traffic load portion of the total load increases as span length decreases, fatigue is a more important consideration in the design of short-span bridges.

Vehicles whose load exceeds the design or umbrella vehicle load are considered "overloaded vehicles" and are often allowed to use bridges under overload permit procedures by the States.

The maximum permissible stress level to which a steel bridge or the steel reinforcing bars in concrete bridges can be safely loaded without the danger of permanently deforming the bridge members is 75 percent of the yield strength. This load level is 36 percent higher than the design load and is tolerable for a limited number of truck passes over the bridge. Therefore, overloaded vehicles reduce the life of bridges. Specifically, there is a significant reduction of fatigue life of bridge components caused by overloaded vehicles operation without passage restrictions on bridges designed to HS20 loadings. For example, for a 100-foot steel bridge, the lost life is 78.6 percent if designed for HS20 loading when overstressed 36 percent (FHWA-DP-90-076-002, 1990).

The Bridge Formula was created to create a method of control to protect the life of the Nation's bridges and insure that the "umbrella loading" used for design remains representative of trucks

using the highways. The Formula was made a part of U.S. Title 23 in 1974 to assure that the allowable weight of heavy trucks was correlated with the spacing of axles to prevent overloading of highway bridges. The Bridge Formula is:

$$W = 500\{ [LN/(N-1)] + 12N + 36 \} \qquad (1)$$

Where,

W = the maximum weight in pounds that can be carried on a group of two or more axles

To the nearest 500 pounds,

L = spacing in feet between the outer axles of any two or more consecutive axles,

N = number of axles being considered.

The loadings that can have a potential negative impact on bridges include both gross and axle specific values as well as axle sets such as tandems, tridems and quadrems. Therefore, bridge loading data are necessary for revisions of design codes and the evaluation of existing structures.

Gross weight accuracy is typically more important than individual axle loads because bridges are usually long relative to the spacing of axles. In addition, information about truck spacings (headways) on bridges is important, since maximum loading will occur when several heavy trucks are on the same span.

Furthermore, the range of loadings on bridges is necessary for probabilistic design procedures. This approach requires more detailed weight information than classic procedures that simply made use of a "standard" vehicle or loading.

Using WIM for Fatigue Determination

As mentioned previously, steel bridge components and the steel reinforcing bars in concrete bridges can wear out after repeated cycles of being loaded and unloaded as trucks roll across the bridge, a phenomenon referred to as fatigue. Fatigue shows up in the form of cracks on certain steel members of the bridge. The determination of live load spectra is a key step in the accurate determination of fatigue on highway bridges.

Typically, fatigue determination for new and existing bridges is carried out using estimated values for truck weights and number of trucks crossing the bridge. Specifically, steel bridges on

major highways are designed for fatigue using an average daily truck traffic (ADTT) of 2,500 and either 2,000,000 cycles of HS20 truck loading on multiple lanes or over 2,000,000 cycles of HS20 truck loading on a single lane. However, according to the "Guide Specifications for Fatigue Design of Steel Bridges," an HS15 fatigue truck loading should be used, which includes the effect of overloaded trucks as well as the actual number of trucks crossing the bridge whenever possible (AASHTO, 1989).

The FHWA's WIM+R system mentioned previously was used to evaluate the fatigue life of four existing bridges using live load spectra. Four steel girder bridges were instrumented to obtain strain data at fatigue critical details and at sections of maximum strain. The fatigue life evaluated with the WIM+R system was then compared to the fatigue life computed by the AASHTO simplified approaches. The load parameters or WIM data used for the evaluation of fatigue life were gross vehicle weight (GVW), axle weights, axle spacings, and average daily truck traffic (ADTT). The fatigue life was estimated according to the AASHTO guide specifications, which suggest four alternatives; all four based on the evaluation of equivalent stress ranges at critical fatigue details. These four alternatives are as follows: 1) field measurement of individual stress ranges, 2) use of GVW's from a nearby weigh station, 3) use of GVW's computed with WIM data, and 4) use of HS15 fatigue truck. Reliability factors are assigned to each option so that the theoretical resulting stress ranges are equal. The fatigue life of each bridge was computed for all but the second alternative. The effect of impact and secondary cycles were quantified by introducing equivalent impact and secondary cycle factors of fatigue. Estimates of the impact and secondary cycle factors were computed from the measured data. Please refer to Daniels et al and Gagarine and Albrecht for details on calculations for impact and secondary cycle factors for fatigue.

The AASHTO specifications state that the fatigue life is infinite if the equivalent stress range multiplied by the reliability factor is less than the limiting stress range for the detail. However, to compare the alternatives the fatigue lives were computed even if the limiting stress was not exceeded. For alternative one mentioned previously, the fatigue life was computed for the equivalent stress ranges corresponding to the primary dynamic cycle and primary dynamic plus

secondary cycles. For the other two alternatives, the stress ranges were computed using equivalent GVW's. Equation 2 was used to estimate the fatigue life of the four bridges:

$$Y = fK(10^6)/T_aC(R_sf_{re})^3 \qquad (2)$$

Where

R$_s$ = reliability factor
f$_{re}$ = equivalent stress range
T$_a$ = estimated lifetime average daily truck traffic (ADTT) in the right lane
C = stress cycles per truck passage = 1 for bridges longer than 40 ft
K = detail constant
f = 1.0 for safe life, 2.0 for mean life
Y = fatigue life in years

For alternative one, the equivalent stress range was calculated as the difference between the maximum and minimum stresses measured during a truck event. For the other two alternatives, the WIM GVW's and WIM stress ranges of all truck events were presented as histograms for all transducers on the four bridges. The equivalent stress ranges and equivalent GVW's were computed and the safe fatigue life of the four bridges was computed with the alternative methods recommended in the AASHTO fatigue guide (AASHTO, 1990). Please refer to Daniels et al and Gagarine and Albrecht for additional details on the calculations using equation 2.

The results of the study of using the WIM+R system for the prediction of fatigue life of highway bridges showed that fatigue lives computed with alternatives three and four were shorter than those obtained with the field measurements. Therefore, one of the conclusions made from the study was to first estimate the fatigue life of a bridge-using alternative 4 of the 1989 Guide Specifications for Fatigue Evaluation of Existing Steel Bridges, which would give a conservative estimate. If the safe life was found to be shorter than the desired service life, the fatigue analysis described as alternative 1 should be performed using actual measured stress ranges.

Conventional Equipment

There are four typical technologies used in highway WIM system weight measurement, which include bending plate, piezoelectric, load cell, and capacitance mat. All of these types of systems can also be used successfully on bridges provided all user requirements are met. Considerable amounts of information exists on these conventional WIM systems, thus this report will only cover the accuracy of these systems for comparison with fiber optic WIM systems.

Accuracy

Table 3.2 shows the accuracy specifications of typical bending plate and load WIM scales. From Table 3.2 it can be seen that as the speed increases to highway speeds the accuracy of the bending plate and load cell WIM systems decrease slightly.

Table 3.3 gives typical values for the inherent variance component of the system accuracy (for a ±1 standard deviation confidence interval) for piezoelectric, bending plate, and single load cell systems. The table shows that it is common for WIM systems to be less accurate when weighing individual axle groups than when measuring gross vehicle weight. Time out factors are sometimes programmed into WIM systems to assist in separating the weight of one vehicle from another. Capacitance mat WIM systems are not as accurate as load cell and bending plate WIM systems for estimating weights.

Table 3.2. Accuracy specifications for bending plate and load cell WIM scales[a]
(1 standard deviation confidence interval).

Speed	Application	Load type	Bending Plate Accuracy	Load Cell Accuracy[b]
2 to 10 mi/h (3.2 to 16 km/h)	Low speed/slow roll just prior to static scales	Single axle Tandem axle Gross weight	± 3% of applied ± 3% of applied ± 2% of applied	± 2% of applied ± 1.5% of applied ± 1% of applied
11 to 25 mi/h (18 to 40 km/h)	Low speed ramp	Single axle Tandem axle Gross weight	± 4% of applied ± 4% of applied ± 3% of applied	± 4% of applied ± 3% of applied ± 2% of applied
26 to 45 mi/h (42 to 72 km/h)	Medium speed ramp	Single axle Tandem axle Gross weight	± 6% of applied ± 6% of applied ± 4% of applied	± 5% of applied ± 4% of applied ± 3% of applied
46 and above mi/h (74 and above km/h)	High speed ramp or mainline	Single axle Tandem axle Gross weight	± 8% of applied ± 8% of applied ± 5% of applied	± 6% of applied ± 5% of applied ± 4% of applied

[a] From IRD Bending Plate and Load Cell Weigh-in Motion Scales Technical Specifications
[b] Normally single load cell scales are calibrated for one of the speed ranges. If site conditions require more than one speed range, the system is calibrated for the range agreed to by the vendor and user.

**Table 3.3. Inherent variance component of system accuracy [a]
(1 standard deviation confidence interval).**

WIM System Technology	Axle Group WIM Accuracy (%)	GVW[b] WIM Accuracy (%)
Piezoelectric cable[c]	12	10
Bending plate	3	2
Single load cell	2	1

[a] *Source*: Bergan, A.T., C.F. Berthelot, and B. Taylor, "Effect of Weigh in Motion Accuracy on Weight Enforcement Accuracy," *Proc. of 7th Annual Meeting*, ITS-America, Washington, D.C., 1997 and IRD Bending Plate and Load Cell Weigh-in Motion Scales Technical Specifications, Aug. 1997 and Jan. 1998.

[b] Gross vehicle weight

[c] By comparison, the Kistler piezoelectric quartz sensor specification for wheel load measurement accuracy is approx. ±3 percent.

Chapter 4 – Background on Fiber Optic Sensors

Using light for communications is as old as the human use of fire. With the advent of the mirror, human beings began to use the sun as the light source for signals directed to people some distance away that duly noted the message conveyed. These ideas continued to be refined over the centuries, including the notable effort by Alexander Graham Bell with the photophone that was used to convey a message via a light beam over 200 meters (Udd, 1991). These early methods were severely limited by the lack of a good light source and a low-loss, reliable transmission medium. However, in 1962, the laser was invented, which dramatically altered this situation by supplying a coherent light source that could be directed over hundreds of thousands of miles in free space to a distant receiver.

The lack of a suitable transmission medium, however, continued to impede the progress of optical communication until Kapron et al. demonstrated that the attenuation of light in fused silica fiber was low enough that long transmission links were possible (Udd, 1991). Using long lengths of hair-like fiber, the possibility of fiber links of miles in length allowed the transmission of laser-modulated light signals. To explain how these fibers conduct light consider a swimmer at the bottom of a pool; if he or she looks to the surface of the water at a shallow enough angle, the bottom of the pool is perfectly mirrored by the water-air interface. Light is conducted down the length of the fiber by similar but multiple internal reflections. In fibers, light is internally reflected from the lower index material, the cladding, back into the core. In this manner it continues to propagate forward, through continual reflection (Udd, 1991).

Fiber Optic Sensor Key Components

The following sections will describe the functions of the key components of fiber optic sensors. The key components include: optical fiber, light source, optical detector, and optical modulator. The theory of operation of each of the key components will not be described in this report. The reader should refer to the publications referenced in these sections for more details on theory of operation.

Optical Fibers

Optical fibers are used to sense environmental effects in two distinct ways. One method is typically referred to as extrinsic and the other as intrinsic. Figure 4.1 illustrates the case of an extrinsic fiber optic sensor that is sometimes also called a hybrid fiber optic sensor.
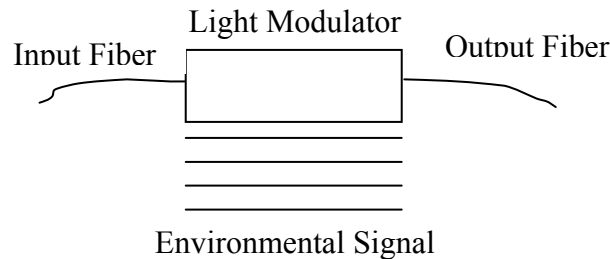
Figure 4.1. Extrinsic fiber optic sensor (BRR, 2000).

In this case an optical fiber leads up to a "black box" which impresses information onto the light beam in response to an environmental effect. The information could be impressed in terms of intensity, phase, frequency, polarization, spectral content, or other methods. An optical fiber then carries the light with the environmentally impressed information back to an optical and/or electronic processor (BRR, 2000). Figure 4.2 shows a series of representative examples of extrinsic sensors and the types of environmental effects they are used to sense.

The intrinsic or all fiber sensor is shown in Figure 4.3. This type of sensor uses an optical fiber to carry the light beam and the environmental effect impresses information onto the light beam while it is in the fiber.

Intrinsic fiber optic sensors can be more sensitive since the environmental signal is directly impressing information onto the light beam. However, intrinsic fiber optic sensors used in WIM system applications are more susceptible to damage caused by the forces impacted on it by the weight of the vehicles passing over the fiber. Therefore, great emphasis needs to be placed on the installation procedures to insure the fiber will be

protected and yet be sensitive enough to provide accurate readings. Figure 4.4 shows a series of representative examples of intrinsic sensors and the types of environmental effects they are used to sense. An important subclass of intrinsic fiber optic sensors is the interferometric sensors, which often exhibit high sensitivity.

| Encoder Plates/Disks | | | | |

-Linear and angular position

-Pressure
-Flow
-Damage

-Liquid level
-Pressure

-Pressure
-Acoustics
-Vibration

-Temperature
-Viscosity
-Chemical analysis

-Temperature
-Strain

-Flow measurement

-Temperature

-Pressure
-Acceleration
-Vibration
-Rotary position

-Temperature
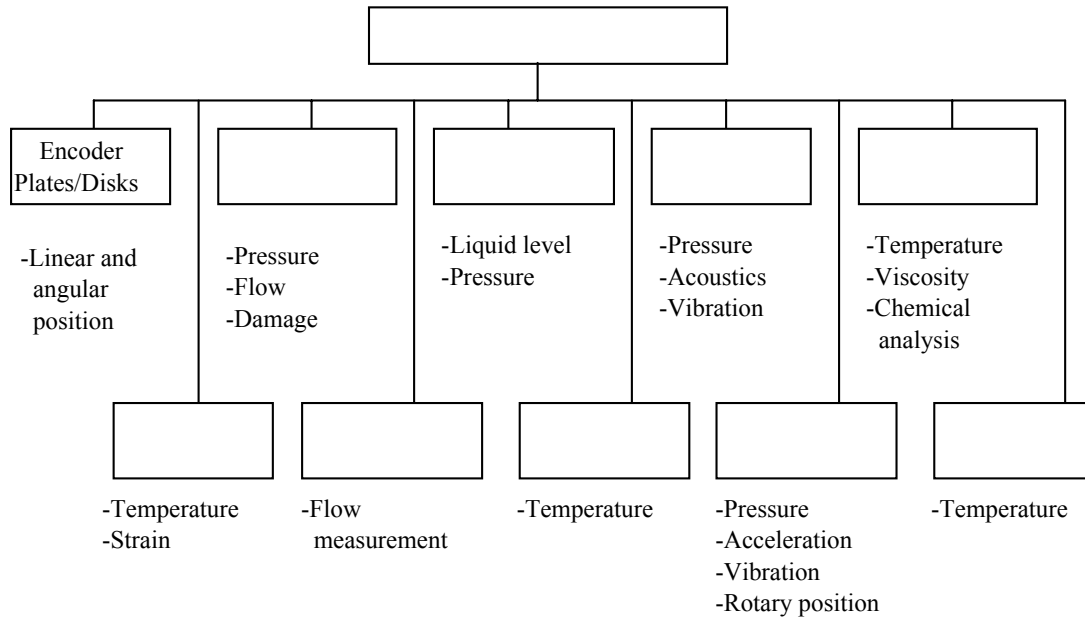
Figure 4.2. Extrinsic fiber optic sensor applications (Udd, 1995).

Optical Fiber

Environmental Signal
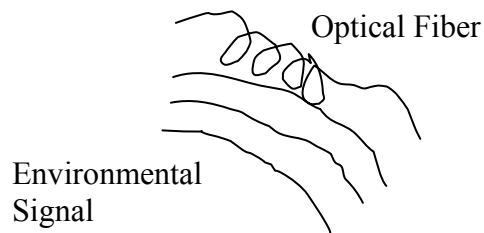
Figure 4.3. Intrinsic fiber optic sensor (BRR, 2000).

```
                    ┌─────────────────┐
                    │                 │
                    └────┬──────┬──────┘
          ┌──────────────┼──────────────┬──────────────┐
     ┌────┴────┐    ┌────┴────┐    ┌────┴────┐    ┌────┴────┐
     │         │    │         │    │         │    │         │
     └─────────┘    └────┬────┘    └─────────┘    └─────────┘

-Strain                        -Temperature
-Pressure
-Vibration




                        ┌──────────┬──────────┬──────────┐
                   ┌────┴────┐ ┌────┴────┐ ┌────┴────┐ ┌────┴────┐
                   │         │ │         │ │         │ │         │
                   └─────────┘ └─────────┘ └─────────┘ └─────────┘
```

-Strain   -Temperature   -Strain   -Acoustic
-Temperature   -Pressure   -Acceleration
-External   -Temperature   -Strain
  refractive   -Magnetic field
  index   -Temperature
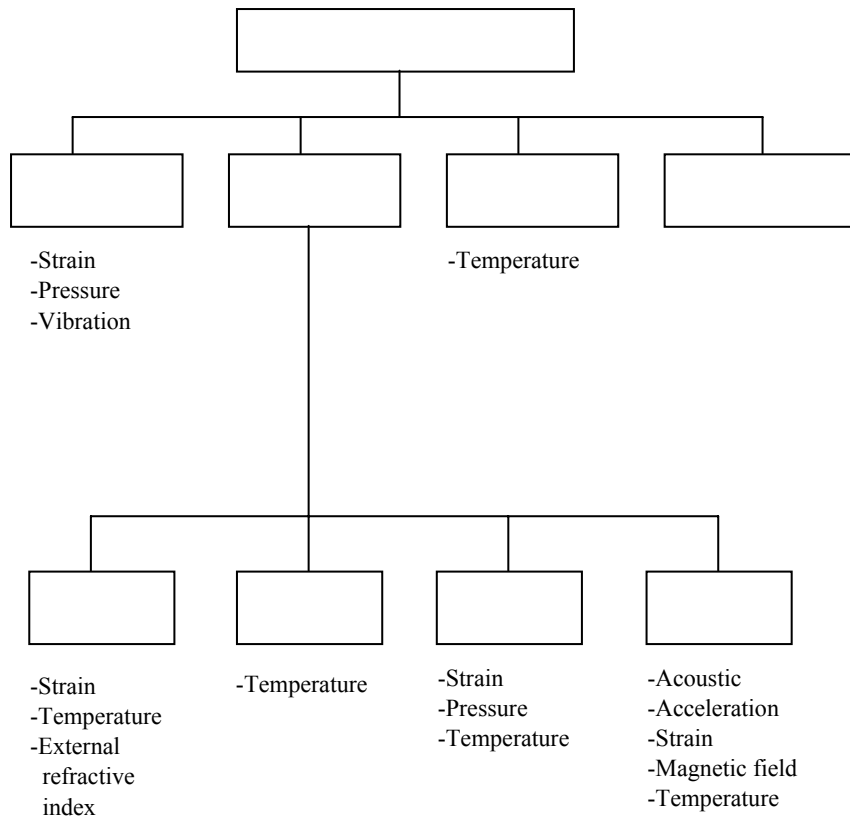
Figure 4.4. Intrinsic fiber sensor applications (Udd, 1995).

Light Source

Light sources used to support fiber optic sensors produce light that is often dominated by
either spontaneous or stimulated emission. An intermediate case that is also important
for some classes of fiber optic sensors is based on superradiance, which is a combination
of spontaneous and stimulated emission (Udd, 1991). Typically, when a light source is
activated, energy, which may be in the form of heat, chemical reactions, electrical
current, or a pumping light source, is used to create excited states in a material from
which light may be emitted. For example, for a gas laser this may involve the excitation
of an electronic state in an atom as in the case of a helium-neon or argon laser. The
energy necessary in gas lasers to cause the higher electronic state in the atoms to be
attained could be achieved by causing electrons to flow across a potential induced in the
gas. The necessary energy is then delivered by the subsequent collisions of the electrons
with the atoms or molecules in the gas (Udd, 1991).

When a light source is activated, higher-energy states of the active source media are populated. In the absence of external perturbations of these energy states, the first light emitted will be due to spontaneous emission (Udd, 1991). Devices dominated by spontaneous emission have important advantages for fiber optic sensors. For example, the devices are "low noise" and are relatively immune to optical feedback effects. The low circulating optical power in their active area contributes to extremely high reliability.

If the flux of photons past an excited state is sufficiently high, the threshold condition, there is a high probability that the excited state will be "stimulated" to radiate by the passing photon. Furthermore, the newly created photon will have the same phase and wavelength as the stimulating photon, which results in a coherent light beam. Stimulated emission becomes dominant as the photon flux is sufficient for the release of a photon by stimulated emission becomes more probable than the absorption of the photon. To operate the device in a continuous mode with predominantly stimulated emission output, the losses due to emission of the light and absorption must be balanced by the generation of new photons (Udd, 1991).

Semiconductor Light Sources

Semiconductor-based light sources offer advantages for most fiber optic sensors in power consumption, reliability, size, and cost that often preclude the selection of alternative light sources. This section will introduce two of the most commonly used semiconductor light sources for fiber optic sensor applications, which are the light-emitting diodes and the laser diodes.

Light-Emitting Diodes (LEDs) are commonly used as a light source for fiber optic sensors. There are two basic types of LEDs used; the surface-emitting diode and the edge-emitting diode. The surface-emitting diode radiates in an isotropic fashion, and butt coupling a fiber in close proximity to the emitting surface captures light. These devices are commonly used in association with large-core multimode fibers and couple a few percent of the light emitted. The edge-emitting diode confines light to a waveguided region. By structuring the diode with a recombination region sandwiched between layers

of material with higher bandgaps and lower indices of refraction, the light can be confined to a plane. This approach results in what is referred to as a double heterostructure and when electrodes are deposited to confine current flow to only a portion of the recombination region, the light-emitting region can be confined to a small area (Udd, 1991).

Another type of semiconductor-based light source is the laser diode. A laser diode is formed when a semiconductor is arranged so that light is confined to a waveguiding region so that the light level in the diode exceeds that necessary for stimulated emission. One of the issues associated with the operation of laser diodes is that their output is often highly susceptible to feedback. This can be understood in part by examining the laser diode output power versus current drive characteristics. At very low currents the output from the laser diode is dominated by spontaneous emission. As the current level is increased, the threshold condition is passed and light emission is due in large part to stimulated emission. Unlike the light-emitting diode, in the stimulated emission regime, the output light level of the laser diode rises very steeply with increasing current (Udd, 1991). When light is back-reflected into a laser diode operating at or above threshold, the effective photon flux in the cavity is changed depending on the relative phase and degree of coherence of the back-reflected light to light circulating in the cavity. The net result is that the output of the light source is modulated by the back-reflected light (Udd, 1991).

Optical Detector

The process of optical detection involves the conversion of optical energy in the form of photons into an electrical signal in the form of electrons that can be processed by conventional signal processing electronics. Semiconductor photodiodes and avalanche photodiodes are the most commonly used optical detectors for fiber optic sensors. These types of detectors are generally used (in the final analysis) to monitor power returned from the sensor (Udd, 1991). These detectors can also be used to detect the intensity of discrete spectral components when they are used in conjunction with appropriate optical components such as gratings or filters. To detect spectral distribution, as is important for wavelength encoding sensors or certain multiplexing schemes, a photodetector array

combined with a diffraction grating is commonly used. This section will provide a qualitative overview of optical detection and will include the following subsections: basic principles of semiconductors, semiconductor photodiodes, avalanche photodiodes, and spectral detection.

Basic Principles of Semiconductors

The term semiconductor refers to a class of material whose ability to conduct electricity lies somewhere between insulators (such as glass) and conductors (such as copper or silver). Semiconductors can have either an excess of electron carriers (*n*-type material) or an excess of "hole" carriers (*p*-type material), where a hole is the absence of an electron in an allowed energy region. The electrons in semiconductors have allowed energy levels that are closely spaced together in bands with forbidden energy gaps between them. The lower-energy bands are occupied first with the result that only the highest-energy unfilled bands determine the electrical properties of the solid. The two most energetic bands, the valence band and the conduction band, are very important in this regard, as is the forbidden energy region between them called the energy gap, E_g. The valence band represents the highest-energy bound states within the material. The conduction band represents the lowest-energy states in which the electrons may move freely throughout the semiconductor lattice (Udd, 1991).

Semiconductor Photodiodes

A photodiode consists of a *p-n* semiconductor junction. When a *p-n* semiconductor junction is formed, a region of high internal electric field exists between the two types of material (Udd, 1991). Within this region, electrons and holes created by photon absorption are "swept out" by the field, leaving a volume of depleted charge. This type of junction can therefore serve as optical detector when it is physically configured so that input optical power impinges on the depletion region, where it is converted to electron-hole pairs that are then swept out, thus creating a charge separation and buildup. This charge buildup can be detected in two ways, depending on how the junction region is electrically connected. If the junction is treated as an open circuit, the voltage across the junction is measured in photovoltaic mode. On the other hand, if the junction is shorted

(or even reverse biased), a current flows externally, completing a circuit between the regions. In this configuration, the current is measured in the photoconductive mode (Udd, 1991).

For fiber optic applications in general, *p-n* junction diodes in the form commonly used for photovoltaic powering are not used for detection. Instead, three-layered devices are used in which an intrinsic layer of high-resistivity material is present between the *p-* and *n*-type layers. A schematic diagram of such a PIN photodiode is shown in Figure 4.5. This device configuration is used in order to have as many of the incident photons absorbed in the depletion region as possible. This is desired because the electric field
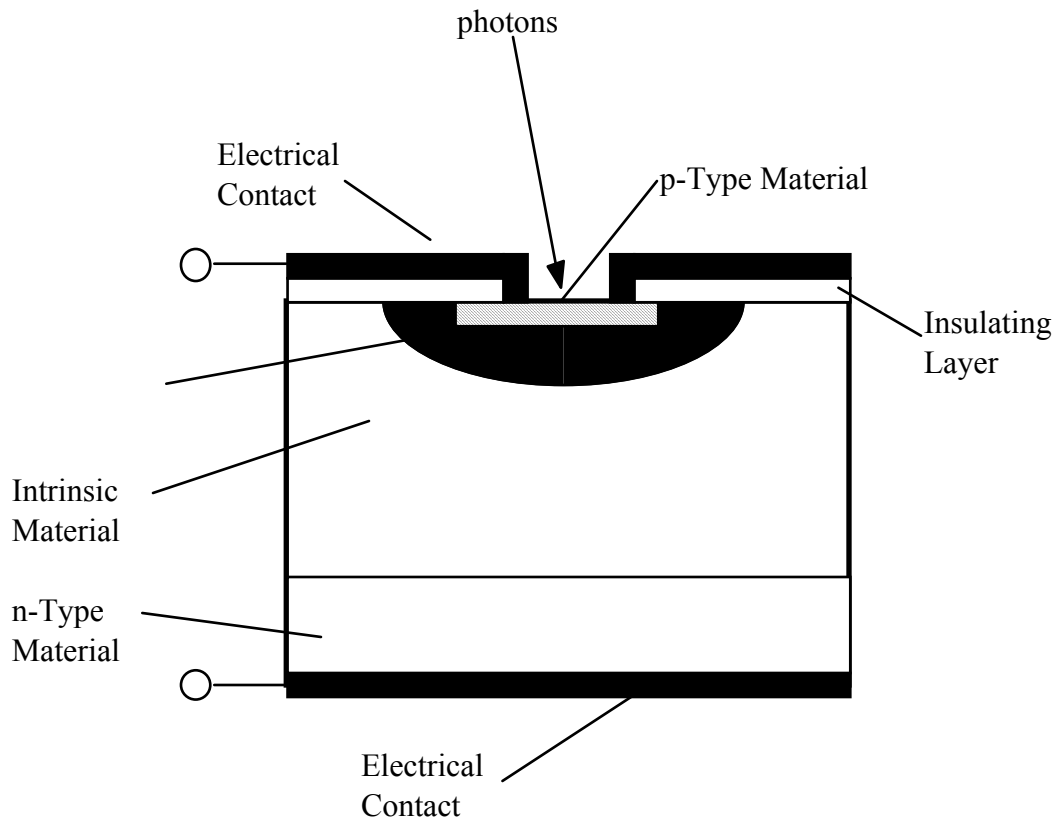
Figure 4.5. Schematic diagram of a PIN photodiode (Udd, 1991).

distribution is greater in that region and therefore produces the maximum charge separation (Udd, 1991). The field in the depletion region is significantly higher than in the *p*- and *n*-type regions on either side of it. Therefore, if photons are absorbed outside of this region, charge separation is less likely to occur, which results in electron-hole recombination.

Avalanche Photodiodes

The requirement for high-speed operation dictates the use of small values of load resistance. However, this produces very small signal voltages. Consequently, photodiode detectors are often combined with high-speed preamplifiers in a single package in order to achieve acceptable signal levels. Another method exists for providing signal amplification without sacrificing high-speed operation. The resulting device is called an avalanche photodiode (APD).

In an avalanche photodiode the p-n junction is operated under very high values of reverse bias, which causes the optically generated carriers to be accelerated to very high energies due to the field. These carriers have enough energy to excite additional carriers from the valence to the conduction band. The initial carriers retain enough energy to remain in the conduction band. The current produced by a single optical absorption is then multiplied through an "avalanche" process, thus the term for the device (Udd, 1991).

For many applications APDs offer an attractive solution to the problem of high-speed detection of very small optical signals. However, these devices are highly susceptible to drift in signal gain due to fluctuations in temperature and bias voltage. Therefore, they require both thermal stabilization and a very well regulated bias voltage for high-accuracy use.

Spectral Detection

Wavelength encoding fiber optic sensors require the detection of the spectral components, such as the optical intensity of the optical signal returned to the signal processing location. There are a number of ways in which optical intensities at different

wavelengths can be determined. The simplest method is shown in Figure 4.6 where a narrowband optical transmission filter is interposed between the return signal and the photodetector. If the photodetector has a response rate of $S(\lambda)$ amperes/watt, knowledge of the detected power and the filter bandpass wavelength will allow the intensity of the return signal component at wavelength λ to be determined (Udd, 1991).
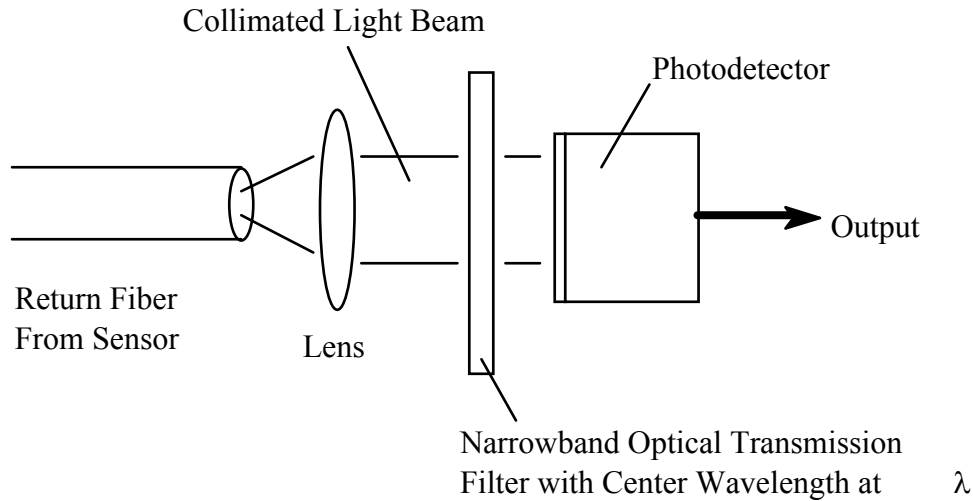
Figure 4.6. Simple detection of a single spectral component (Udd, 1991).

A number of techniques have been used for real-time approximation of many or all spectral components in a signal. Only two will be mentioned here. In the first, a detection scheme similar to that shown in Figure 4.6 is used. However, in this case, an adaptive optical filter whose bandpass wavelength can be modulated by an electrical signal replaces the fixed-wavelength optical filter. The main drawbacks of such detection systems are their cost and limited wavelength range. Also, they are basically mechanical in nature and may have limited lifetimes if used continuously in operating fiber optic sensor systems (Udd, 1991).

However, the most commonly used method of detecting the spectral distribution of optical signals is shown in Figure 4.7. In this case, the collimated return signal is spectrally dispersed in angle by an optical component such as a diffraction grating. The different spectral components are then detected individually by a photodetector array

such as a charge-coupled-device (CCD) camera. Highly sensitive two-dimensional
arrays of this type are available that have thousands of individual sensing elements,
thereby making possible high-resolution wavelength encoding sensors (Udd, 1991).
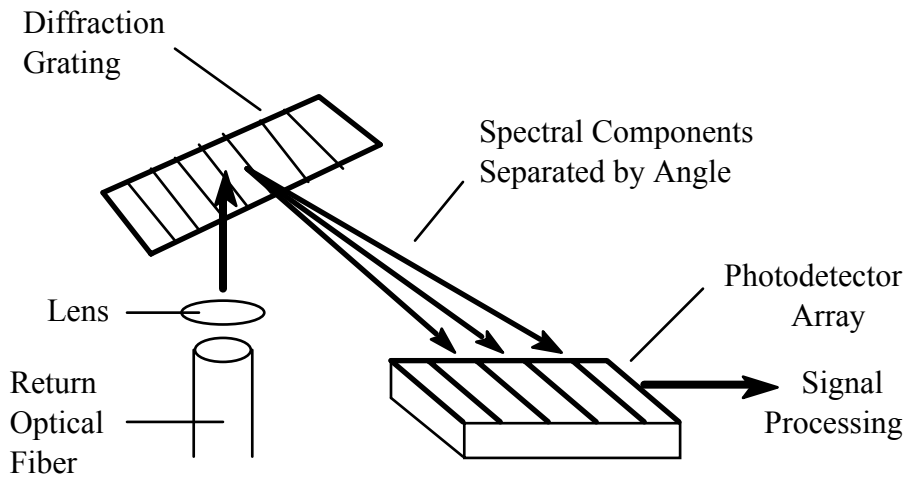
**Figure 4.7. Measurement of fiber signal output spectrum using a diffraction grating
and photodector array (Udd, 1991).**

Optical Modulators

Optical modulators are a key component of optical fiber systems, performing a variety of
functions such as amplitude (intensity), phase, frequency, and polarization modulation.
Optical modulators are mostly implemented as solid-state devices in which light is
modulated by varying the optical properties of the device material using an electrical
control signal. The control signal is linked to the material properties by an electro-optic,
acousto-optic, or magneto-optic mechanism.

There are three basic types of solid-state optical modulators and these include bulk,
integrated-optical and all fiber devices. These three types of optical modulators will be
discussed briefly in this section. For more detailed information on these optical
modulators, please refer to the references given in the text.

Bulk Modulators

In bulk modulators, which have been available commercially for years, the signal propagates through a uniform block of material. Bulk modulators, however, lack waveguiding and require high electrical drive power and external optics to couple light in and out of optical fibers. The majority of the bulk modulator devices used in fiber-sensor applications are based on the electro-optic and acousto-optic effect mechanisms.

In a bulk electro-optic phase modulator, optical phase modulation is achieved by varying the refractive index of the crystal by applying an electric field across the crystal. The electro-optic refractive index is linearly proportional to this applied electric field (Udd, 1991). Lithium niobate (LiNbO$_3$) is one of the most widely used materials for electro-optic devices. It is a dielectric crystal with large electro-optic coefficients and is transparent over a wavelength of 0.4 to 4.5 μm. In the absence of an applied electric field, it is birefringent (two rays propagating at different velocities).

The behavior of electro-optic modulators in electrical systems can usually by analyzed by simple equivalent-circuit models. For example, the modulator can be modeled as a parallel-plate capacitor with capacitance C given by the following equation:

$$C = \varepsilon LW/d$$

where ε is the permittivity of the modulator crystal, L is the device length, W is the crystal width and d is the crystal thickness (Udd, 1991).

A bulk electro-optic intensity modulator can be easily realized by taking advantage of the polarization dependence of the phase modulator. A simple implementation of an intensity modulator in LiNbO$_3$ consists of a polarization-dependent modulator inserted between crossed polarizers. By changing the phase modulator voltage, the polarization of the beam incident on the output polarizer is varied, which in turn leads to the modulation of intensity (Udd, 1991).

Bulk acousto-optic devices in fiber-sensor applications are used most often as optical frequency shifters. In acousto-optic modulators, an optical beam propagating through a

crystal interacts with a traveling-wave index perturbation generated by an acoustic wave. The perturbation results from a photoelastic effect whereby a mechanical strain produces a linear variation in refractive index (Udd, 1991).

Acousto-optic devices are often made of materials such as $LiNbO_3$ and quartz, since the waves can be launched efficiently in these crystals over a frequency range from tens of megahertz to several gigahertz (GHz). The acoustic velocity in $LiNbO_3$ is about 6 x 10^3 m/s, thus a 1-GHz acoustic wave has a wavelength of about 6 μm, which is comparable to optical wavelengths. The amplitude of the associated index perturbation is proportional to the square root of the acoustic intensity (Udd, 1991)

Integrated-Optical Modulators

Integrated-optical devices are formed from optical waveguides fabricated on the surface of an appropriate substrate. Since these devices are not subject to optical diffraction limitations, it is possible to realize modulators with very low drive requirements, wide bandwidth, small size, and optical-fiber compatibility (Udd, 1991). Integrated-optical devices used for fiber-sensor applications include phase modulators, intensity modulators, and optical frequency shifters. In addition, multiple components can be combined on a single chip, which simplifies packaging.

A simple integrated-optical phase modulator consists of a single-mode waveguide and two electrodes of length L with separation d. A field applied between the two electrodes overlaps the optical field and induces an index change, which results in phase modulation. A key advantage of guided-wave phase modulators is that a low electrode voltage can result in substantial phase modulation.

All-Fiber Optical Modulators

Modulation of an optical signal within an optical fiber is an extremely attractive concept for fiber-sensor applications, since it would eliminate the need for fiber coupling, which in turn would reduce the optical insertion loss as well as simplify packaging. All-fiber devices are challenging to implement because the most common fiber material is glass,

34

which is noncrystalline, preventing a direct link between an applied electric field and the refractive index. Therefore, mechanical means such as squeezing the fiber are required to obtain an index change (Udd, 1991). The performance of all-fiber modulators is still weak and relatively slow compared with discrete devices. However, they are of considerable interest and are being actively developed. All-fiber phase modulators and frequency shifters will be described in this section.

Phase modulation in all-fiber devices is achieved by either stretching or squeezing the fiber by some external means, which is expressed mathematically as follows:

$$\phi(t) = 2\pi/\lambda[L\Delta n(t) + n\Delta L(t)]$$

where $\Delta n(t)$ and $\Delta L(t)$ are variations of the refractive index and the device length, respectively. Compared with bulk and integrated-optical devices, in which the effect of length variation is negligible, even a small fractional change of length of the long fibers in all-fiber modulators can lead to significant phase modulation.

All-fiber frequency shifters are based on traveling-wave coupling using a fiber that supports two guided modes with a difference in propagation constant $\Delta\beta$. An acoustic wave of frequency ω_a launched into the fiber perturbs the index profile resulting in mode coupling, which causes a frequency shift of $\pm\,\omega_a$. The phase-matched interaction required for efficient power transfer is obtained by setting

$$\Delta\beta = 2\pi/\Lambda_a$$

where Λ_a is the acoustic wavelength (Udd, 1991). This technique has been demonstrated with fiber supporting two spatial modes and also with high-birefringence fiber that supports two polarization modes.

For additional information on the three types of modulators introduced in this section please refer to "Fiber Optic Sensors – An Introduction for Engineers and Scientists" edited by Eric Udd, 1991 or other appropriate references.

Chapter 5 – Results of State-of-the-Art Study

As described in the Methods and Approach chapter a State-of-the-Art study for the use of fiber optic sensors in Weigh-in-Motion System applications was conducted using three techniques: 1) literature search and review, 2) attend pertinent conferences, trade shows, etc., and 3) visit field sites where this technology was being used for WIM. The literature search and review was conducted to determine what types of studies or programs had been formally documented where the use of fiber optic sensors had been implemented to determine dynamic loads on bridges caused by moving vehicles and their performance criteria (precision, accuracy and durability). The conference and trade show information was used to determine whether this technology was available in part or as a whole system. The site visits of the field sites where this type of technology was being used were to determine the potential of this technology in a real life situation rather than a laboratory or controlled setting installation.

This chapter describes the studies and their results based on the three techniques used by the research team to conduct the state-of-the-art study for the use of fiber optic sensors in WIM system applications. The results of the state-of-the-art study are presented in this section and are organized by the entity that conducted the study.

New Mexico State University / Naval Research Laboratory (NRL)

Project Background
This research project, completed in August of 1998, was a landmark in the use of a distributed fiber optic based sensor system to monitor the structural health of a civil structure. The structure in question is an in-service two-span, continuous, non-composite multi-girder steel bridge. Throughout the structure are 120 Fiber Bragg grating (FBG) fiber optic sensors, more than any other steel bridge in the world at that time. This project was part of a multiphase research project co-funded by the National Science Foundation and the Federal Highway Administration Turner-Fairbanks Highway Research Center (TFHRC).

The first phase of this program was an interagency collaboration between FHWA and the Optical Sciences Division of the Naval Research Laboratory (NRL). This included tests performed at TFHRC of a prototype sensor multiplexing system designed by NRL with Bragg grating sensors embedded in concrete beams and deck panels as shown in Figure 5.1. The concrete beams and deck panels contained 35 FBG sensors and were loaded to failure. The demonstration proved that FBG sensors could survive such an installation; were functional even beyond the failure of the host material; and showed strain sensitivities superior to conventional strain gages.

The next phase involved the design, fabrication, and installation of a 32-channel sensor system. The objective of this research project was the development and implementation of a bridge monitoring and evaluation system that can be used to:

- Assess the traffic loading on the bridge,

- Define a baseline behavior for the structure,

- Evaluate the effects of damage on the capacity and performance,

- Assess the effectiveness of repairs and maintenance programs,

- Check the performance compared to the design assumption, and

- Remotely monitor critical structures, and provide a warning when abnormal conditions occur.

A secondary objective was the development of guidelines for the installation of Bragg grating fiber optic sensors on existing bridges to investigate practical issues in the full-scale application and regular operation of fiber optics by civil engineers rather than optical scientists.
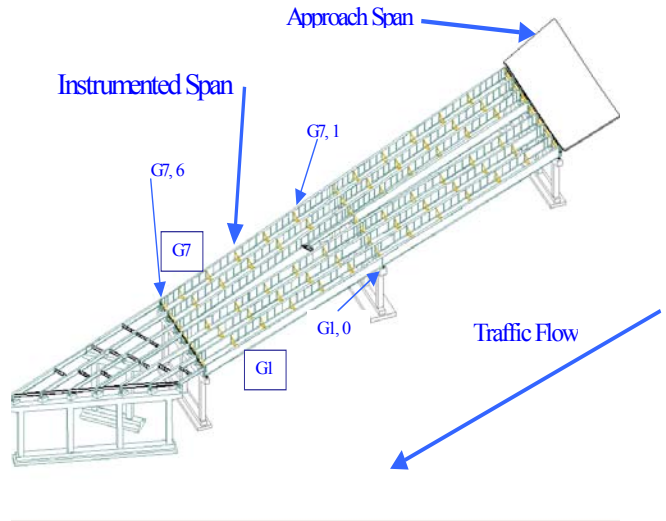
Figure 5.1. I-10 Overpass Over University Avenue, Las Cruces, NM.

Equipment Used

The core technology for this project is the Fiber Bragg grating (FBG). Commercial grade off the shelf single mode optical fiber typically consists of fused silica with a germanium dope. It was discovered years ago that the germanium in the core of this optical fiber was sensitive to ultraviolet (UV) light (with a wavelength around 248 nm). If the core of the optical fiber is exposed to coherent UV light, a perturbation is created in the index of refraction. If the core is exposed to two interfering beams of UV light at an angle θ, an interference pattern is induced holographically onto the fiber core, thus creating a Bragg grating. Figure 5.2 depicts this process.
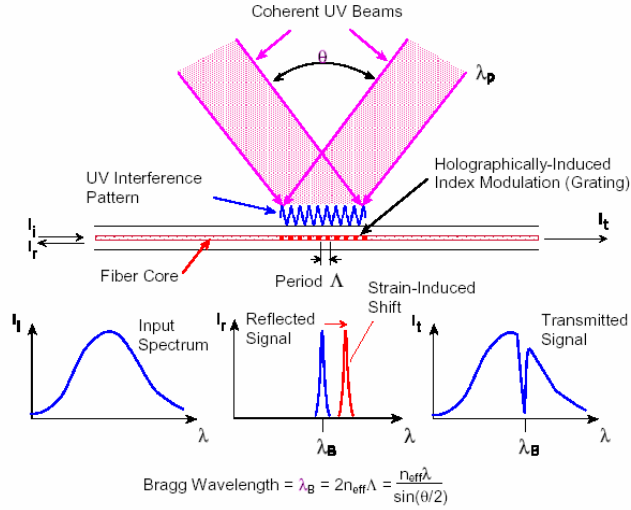
Figure 5.2. Fiber Bragg Grating Creation.

If a broad spectrum (white light) source of light travels down the core of the fiber, the light transmitted shows absorption at a certain wavelength. There is also light reflection back towards the light source at this same wavelength. This wavelength is a function of the period of the UV beam interference pattern and can be controlled by modifying the angle between the two coherent UV beams. This wavelength is the Bragg wavelength. If the fiber is then subjected to a mechanical strain, the period of the interference pattern is increased or decreased and the Bragg wavelength changes.

This physical phenomenon can be exploited. The change in Bragg wavelength is directly proportional to the change in mechanical strain. Multiple Bragg gratings formed at different central wavelengths can be created on the same fiber. These multiple gratings may then be interrogated using several different wavelength multiplexing techniques.

39
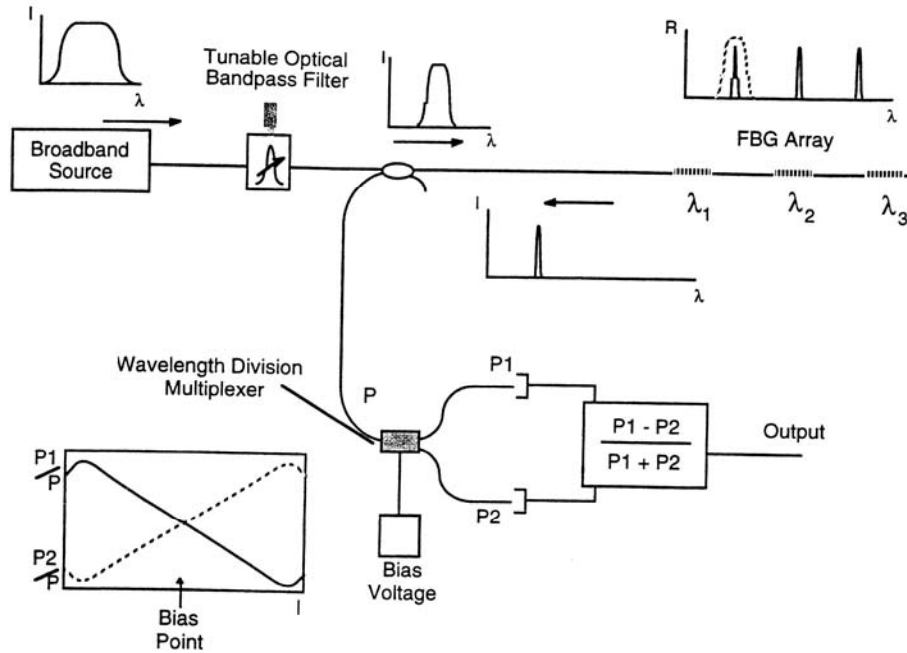
Figure 5.3. Schematic Diagram.

The schematic diagram of the instrumentation is shown in Figure 5.3. This interrogation technique relies on the use of a wavelength division multiplexer (WDM) to determine the shifts in the FBG reflected wavelength. A light source (ELED) provides the broadband spectrum, which is filtered by an adjustable band pass optical filter (Fabry Perot Etalon), which permits the illumination of a single FBG at a time. The bandwidth of the Fabry Perot filter is considerably wider than the reflected FBG spectrum (~2 nm compared to .2 nm). The reflected component from the FBG sensor is then directed into the WDM. This device is basically a 1x2 port device, which directs the input optical power between the two output ports depending on the wavelength of the incoming light. The type of transfer function of such a device is shown in the inset of Figure 5.3. A bias voltage is used to set the device such that initially the input power is equally divided between the two output ports for the nominal (no strain) reflected component of the FBG sensor. As the FBG sensor is strained and the reflected wavelength shifts, the WDM will split the input optical power, P, unequally between the ports P1 and P2, depending upon the wavelength shift. By detecting the power at each output port and taking the difference over the sum of P1 and P2, to normalize for overall intensity variations, a voltage is obtained which is directly proportional to the FBG wavelength shift. If the WDM is operated in its linear

40

range, there will be a simple linear dependence between the voltage and the strain. The
tunable Fabry Perot optical filter permits multiple FBG sensors on a single optical fiber.
There is a limit however due to the limited spectral range of the Fabry Perot filter and the
bandwidth of each FBG. Figure 5.4 shows the picture of the demodulation system
underneath a notebook computer.

Figure 5.4. FBG Interrogation System in Use.

The instrumentation system was designed and fabricated by NRL specifically for this
experiment based on previous designs, which were limited to a smaller number of total
FBG sensors.

Experiment Details

FBG sensors were installed on the top flange, web, and bottom flange of the 7 steel
girders at several locations on the east and west piers. The FBG sensors were mounted to
the structure in much the same manner as conventional resistance strain gages. Figure
5.5 shows the layout of the sensors and a close-up of the installation.
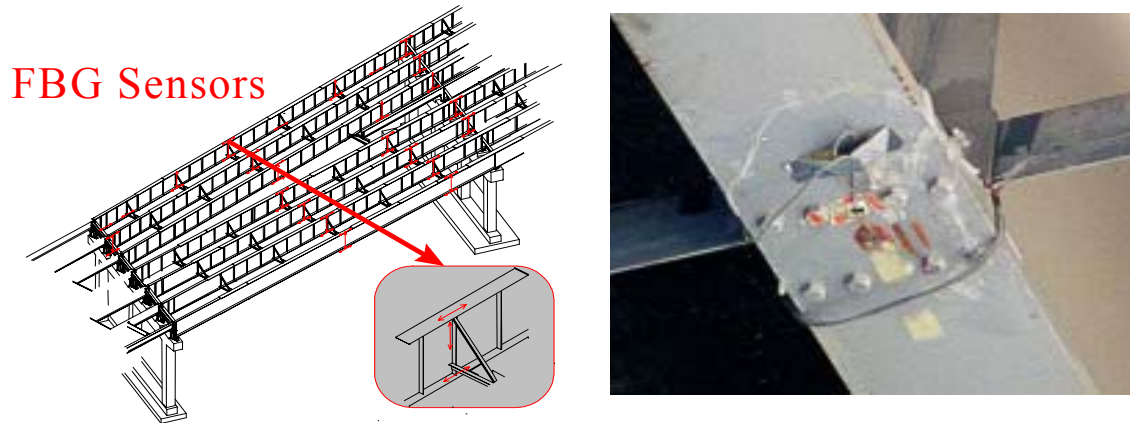
Figure 5.5. Sensor Layout and Close-up.

The surface was prepared by grinding off the layer of paint and polishing the surface of the steel. The optical fiber section containing the FBG sensor was then adhered to the steel surface using MBOND 200, from The Measurements Group, Vishay. This is the same cyano-acrylate adhesive that is used for conventional strain gages. The adhesive has a short curing time, which allows for prompt installation.

Data was acquired from normal traffic to check the system operation. It was immediately apparent that it might be possible to discern relative vehicle weights from the strain responses. Figure 5.6 shows a typical response showing two vehicles of differing weights and axle configurations.
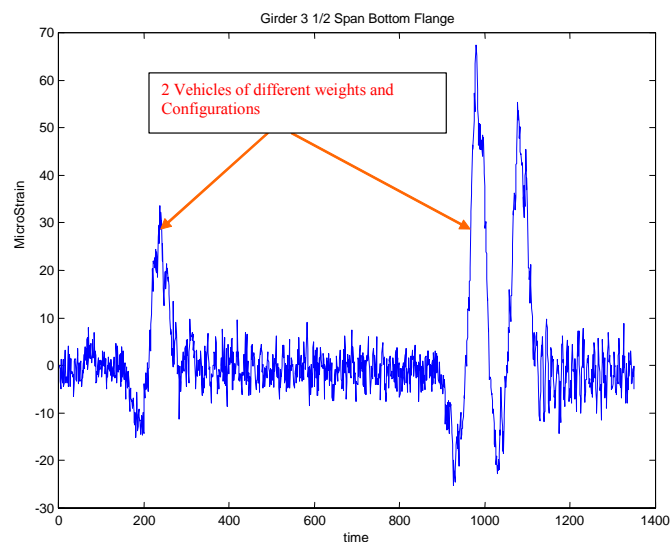
Figure 5.6. Typical Data from Normal Traffic.

42

A truck with a known weight was scheduled to cross the bridge in an empty, half full, and full condition. Figure 5.7 shows a sketch of the test vehicle. The truck was scheduled to cross the bridge at different speeds. The test runs were repeated 3 times at each speed. The Gross Vehicle Weight (GVW) was obtained for each configuration at a local truck scale. The tests were performed at night between midnight and sunrise. This was done to insure a greater chance of having only the test vehicle on the bridge and to reduce the effects of thermal gradients on the results.
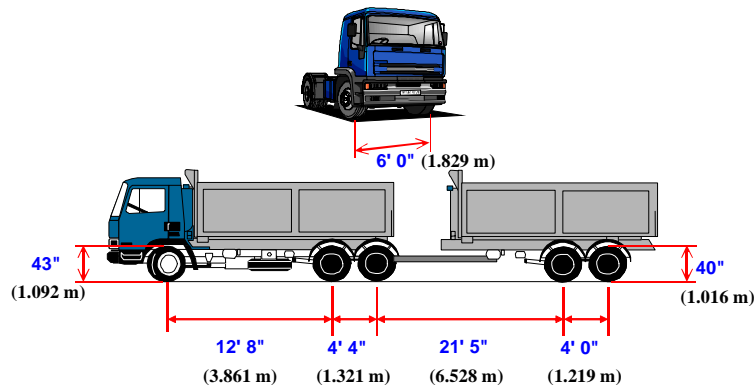
Figure 5.7. Test Truck.

The data showed that in several locations, the resolution of the data acquisition system was such that responses were measured down below 2 microstrain. The system was much more sensitive and had a better signal to noise ratio than a conventional strain gage system. The responses were compared to a finite element model of the structure and were found to be very close to the expected response values.

It was determined that it would be possible to calibrate the system and arrive at a gross vehicle weight for this particular vehicle configuration, however, a different vehicle with the same gross vehicle weight but different axle configuration and traversing a different lane of the bridge would yield different strain values.

Data was collected every 5 minutes, 24 hours a day, for 72 days to determine the long term performance of the system and collect statistical information on vehicle traffic. It

was discovered that by processing the signals form the FBG sensors it was possible to determine the location of the vehicle on the structure as well as the speed. The 72 days of data acquisition provided a wealth of information related to the traffic patterns on this section of Interstate 10. Figures 5.8 and 5.9 show some of the statistical data acquired from typical traffic observed over the 72-day period.
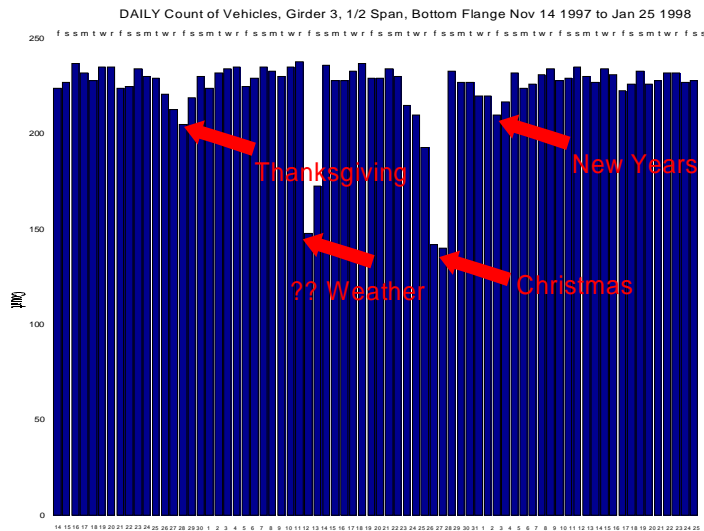
Figure 5.8. Distribution of Daily Vehicle Count.
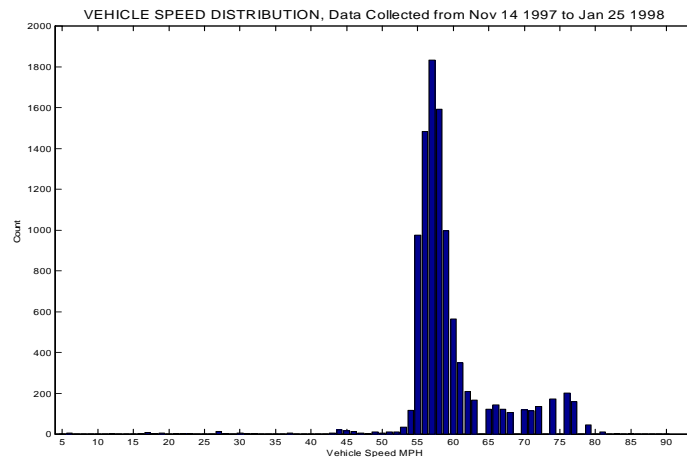
Figure 5.9. Distribution of Vehicle Speeds.

<u>**Summary**</u>

The fiber optic demodulation system developed by NRL allowed for the use of multiple FBG sensors on one optical fiber. This allowed as many as 120 locations on the structure to be monitored. The system was limited in sampling frequency at the time to about 45

Hz. It was determined that the sample rate would need to be increased to about 1000 Hz to provide discreet data on strains imparted by individual vehicle axles and measure the vibration modes of the structure.

The system shows great promise in the areas of structural health monitoring. The data observed showed the possibility of using the entire bridge structure as some type of vehicle classification system whereas providing data on individual axle loads would need further development.

Status to-date

Currently, there are no plans to pursue the use of this system for traffic monitoring purposes such as vehicle classification, and Weigh-in-Motion (WIM). As mentioned previously, additional modifications and field testing would be necessary to optimize this system for WIM system applications.

Blue Road Research (BRR)

Project Background

Blue Road Research (BRR) has been developing Fiber Bragg Grating (FBG) based spectral demodulation systems the past five years and has actively pursued using FBG sensors in the area of civil structures with projects funded by the Oregon Department of Transportation (ODOT). The advantages of FBG sensors over conventional electric strain gages such as greatly reduced size, electromagnetic interference resistance, and higher temperature capability make them ideal choices for smart structure applications. BRR has recently installed a FBG sensor system into an asphalt and highway concrete pad to study the use of FBG sensors for vehicle weigh in motion.

The research on using FBG sensors for weigh-in-motion was a carry-over from results of testing on the Horsetail Falls bridge in the Columbia River Gorge National Scenic Area in September of 1998 with 28 FBG sensors. Figure 5.10 shows a picture of the bridge. The tests initially performed on the Horsetail Falls bridge were made with a portable

optical spectrum analyzer that had a resolution of about 5 microstrain. In order to perform more comprehensive testing, the ODOT wanted sub-microstrain resolution and ideally, a response of at least 100 Hz. With improved light sources, fiber grating filters, and receivers BRR developed a spectral demodulation system, which achieved a resolution of .1 microstrain at a frequency response of 2000 Hz.


Figure 5.10. Horsetail Falls Bridge.

<u>**Equipment Used**</u>

For many applications a low-cost, high-speed demodulation system is required. BRR investigated a series of approaches including overcoupled couplers, a miniature Mach-Zehnder interferometer, and chirped fiber gratings. Trade offs were made between these three designs and the chirped fiber grating approach was selected on the basis of temperature stability, sensitivity, and overall cost. The design allows sensing speeds only limited by the speed of the detection circuit.

Figure 5.11 shown is the optical diagram for the demodulation system. An Edge Light Emitting Diode (ELED) couples light into a single mode fiber and through a 50% beam splitter. Half of the light is guided out the FC port on the front of the box to a Bragg grating sensor. The sensor acts as a strain or temperature transducer and reflects a very small spectral band (or peak) back towards the box but allows most of the optical power to pass through. This reflected peak travels back into the box, and through two beam splitters. Half of the power at the second beam splitter is collected by a photo detector while the other half first goes through a chirped fiber grating filter and then is detected by

a matched detector. The chirped grating truncates the signal in such a way that the ratio of the two output signals is linearly proportional to the strain or change in temperature.
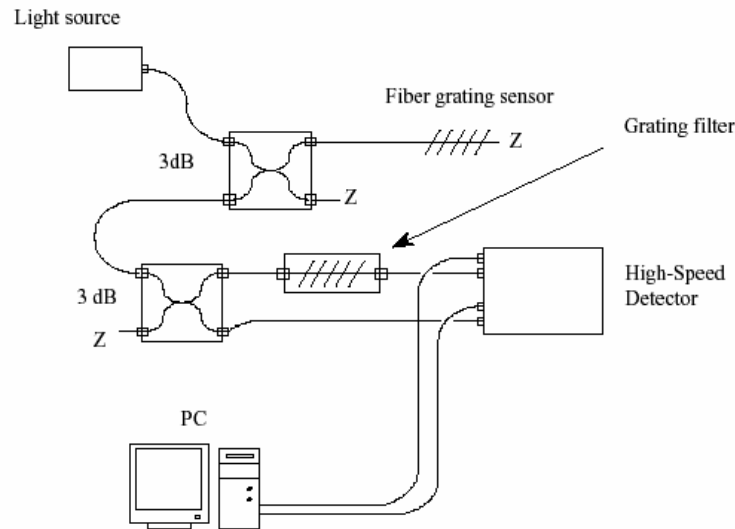
Figure 5.11. Optical Schematic of Blue Road Research Demodulation System.

In its basic form, a typical Bragg grating has a gage of approximately 5mm. For most civil structure applications this gage length is too short, so a method of effectively increasing the gage length was developed. In order to increase the gage length of the Bragg grating to provide a more macroscopic strain value useful in civil structure applications, the grating is packaged in a tube with the tie points defining the effective gage length. Figure 5.12 shows a long gage sensor with optional brackets for surface mounting. This package design provides a gage range from 2.5 to 100 cm. The maximum diameter of the grating package is less than 7 mm, making it non-obtrusive and ideal for embedding into composites, placing into grooves in concrete, etc.   The design also provides excellent protection to the optical fiber itself. The optical fiber has excellent tensile properties but is prone to failure when kinked or scratched.

Several variations of the sensor design were used in this experiment. Smartec, SA in Grancia, Switzerland, which is collaborating with BRR on its dynamic fiber grating sensor system, manufactured several of the sensors.
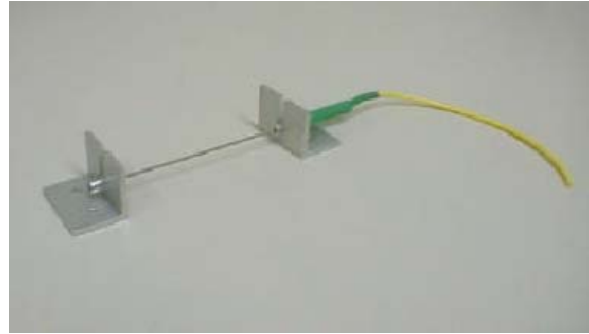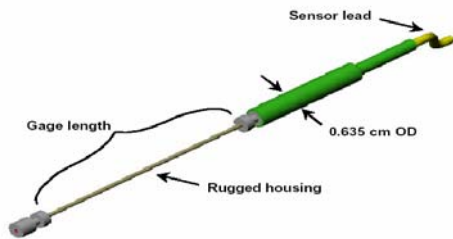
Figure 5.12. Long Gage Housing for Fiber Bragg Grating Sensor.

<u>Experiment Details</u>

This section describes the experiment details for testing of Fiber Bragg Grating sensors developed by BRR. The first part of this section describes testing performed on the Horsetail Falls Bridge. The second part of this section describes testing performed on an asphalt and concrete pad that was built at the BRR facility. The third and final part of this section describes testing performed on the I-84 freeway.

       Horsetail Falls Bridge

Tests were initially performed in support of health monitoring of the fiber reinforced polymer upgrade to the Horsetail Falls bridge. However, it became readily apparent that system could monitor vehicle traffic. Several centrally located sensors were selected for additional tests. Figure 5.13 shows a plot from one of these sensors.
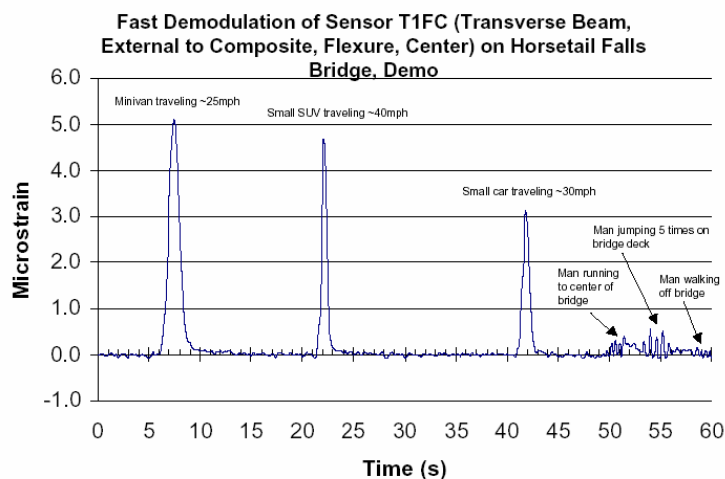
Figure 5.13. Typical Response from a Centrally Located Sensor.

In Figure 5.13, three vehicles are show: a minivan, an SUV, and a small car. The measured strains are proportional to the vehicle weight. The sensitivity of the system is demonstrated by the signals generated by a 180 lb man running and jumping on the bridge. The sensitivity levels are approximately .2 microstrain for the responses shown.

Asphalt and Concrete Pad

As mentioned previously, a second set of tests were performed on an asphalt and concrete pad that was built at the BRR facility. The objectives were to improve the sensor traffic monitoring performance and evaluate different sensor housing designs. Each pad was 3m X 3m X 10cm and was placed on a 10cm gravel bed.

Figure 5.14 shows a slot being prepared to receive the sensor in asphalt. When the mechanical preparation was finished, the slot was cleaned and dried. A thin layer of epoxy was placed in the slot. Next, the sensor was installed and the slot was filled with epoxy. After the epoxy had cured, the optical connections were made to the laboratory close by to make sure they survived the installation. This was followed by a series of tests that are still ongoing.

Figure 5.14. Installation of the Long Gage FBG Sensors.

Figure 5.15 shows the response of the 3500 lb car as it pulled onto the concrete pad and then reversed its direction. The response from the two axles is apparent. The difference in magnitude is due to the fact that the wheels did not follow the same path in both directions.
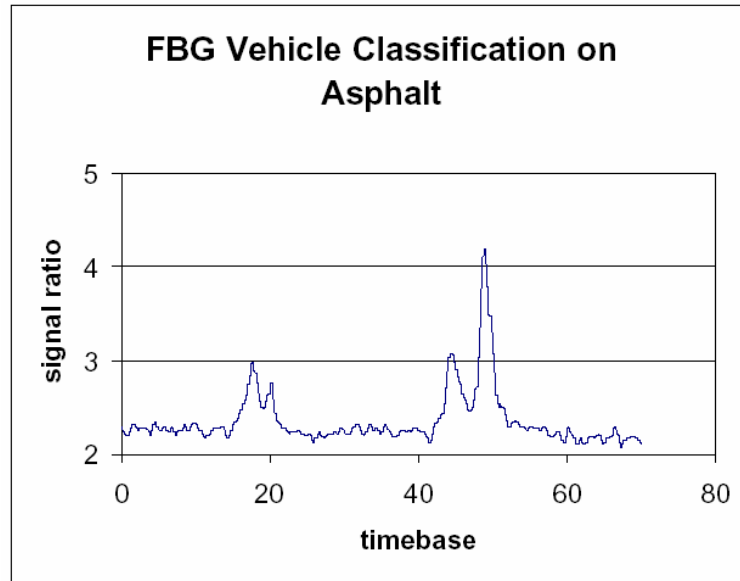
Figure 5.15. Response from a 3500 lb Car.

Additional testing is ongoing with the laboratory test pad as well as a section of highway pavement adjacent to the facility. Additional work is planned to evaluate the design and durability of the sensor, the method of installation, and to make it insensitive to wheel position.

I-84 Freeway

Blue Road Research and the Oregon DOT installed fiber Bragg grating (FBG) vehicle classification sensors into the I-84 freeway during August of 2001 and August of 2002. Two of the four original sensors installed in August 2001 failed shortly after installation, likely due to overstrain. The other two sensors have been operational without a failure since that time. Four improved, second-generation sensors were installed in August 2002 and have also been in operation since that time. Each sensor was installed with the objective of traffic axle and vehicle classification, rather than weigh-in-motion. However, data collected highly supports weigh-in-motion (WIM) as an add-on capability, since the technical approach proposed for WIM builds heavily on lessons learned from these earlier installations.

Due to some variable drift in the baseline of the system and mechanical detachment of the original sensors installed in 2001, BRR redesigned the sensors and later placed four

additional sensors online in the I-84 freeway during August 2002. Each separate sensor design yields varying responses to traffic, based on its type or design, but all sensors produce peaks corresponding to traffic crossing over. Figure 5.16 shows a composite beam attached inside a long-gage traffic sensor. This is one of three new second-generation designs placed into the freeway during 2002.
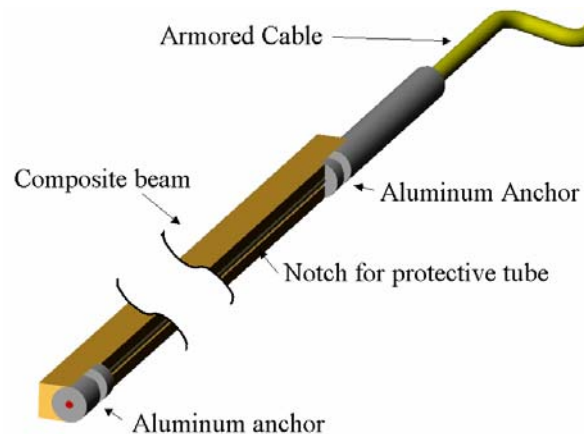
Figure 5.16. A composite beam encloses a long-gage traffic sensor.

The advantage of enclosure into a composite encasing is that the casing serves to protect the tubing and grating from extremely high strain forces as well as shock. Two of the sensors installed during 2002 were manufactured in this long-gage composite (LGC) configuration with a length of 48 inches by 1/4 inch.

An additional sensor was manufactured as an enhanced-strength long gage sensor (LGE), similar to the originally installed traffic sensors. Enhancements made include additional splice protection (reinforced steel pin) and crimped anchor support, enhancing the housing strength by as much as a factor of 10.

A third design (UNC) uses a polyamide optical fiber epoxied directly into a groove machined into a 24 inch by 1/4 inch composite beam. It uses a composite beam to reinforce the fiber, but encloses the fiber only inside of the composite and not inside tubing. An unsleeved fiber grating allows the strain from traffic to be directly transferred to the grating area without length integration as the composite beam flexes due to traffic.

It provides a simplified manufacturing method, reducing cost and manufacture time, but is sensitive to tire position and width.

All four of these sensors were embedded into the freeway with a groove depth of approximately 3 inches below the surface. This unique depth advantage over other experimental optical WIM systems allows for a protective environment that may contribute to added life span and continued use after repaving. Figure 5.17 shows a top-view of the layout of the second-generation sensors in the I-84 freeway.
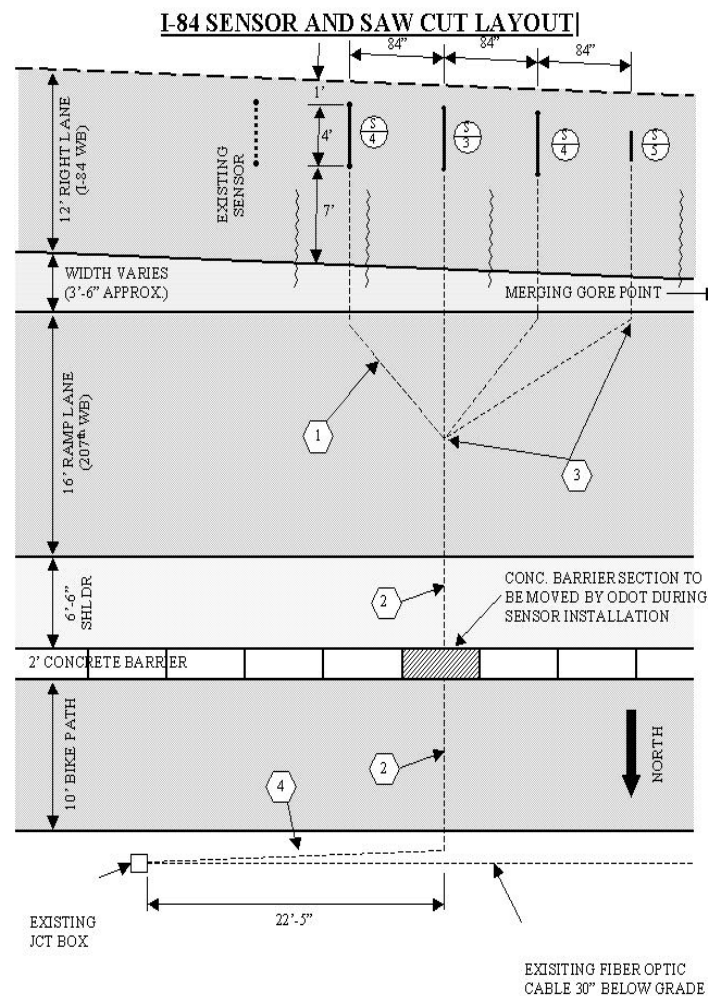
Figure 5.17. Sensor layout and placement for second installation into I-84 (BRR, 2003).

All four of the sensors installed on August 20, 2002 have no indication of wavelength offsets differing from those set or measured during manufacture. Figures 5.18 and 5.19

show preliminary data on reactions (relative amplitude vs. time) of the second-generation sensors. There are still some unresolved issues as to the performance of the sensors, although repeatability seems to have improved with the second-generation sensors. There is still some time-dependent drift based on the road heating and cooling, but this is very slow and can be corrected by temperature compensation.
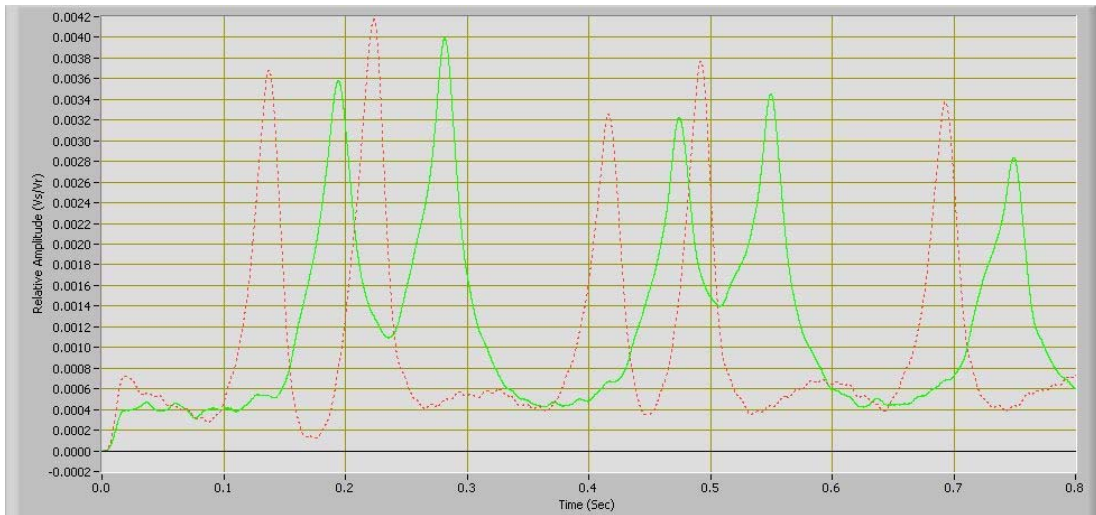
Figure 5.18. The LGE (first peak/dotted line) and LGC sensors, respectively, react to a 5-axle vehicle (BRR, 2003).
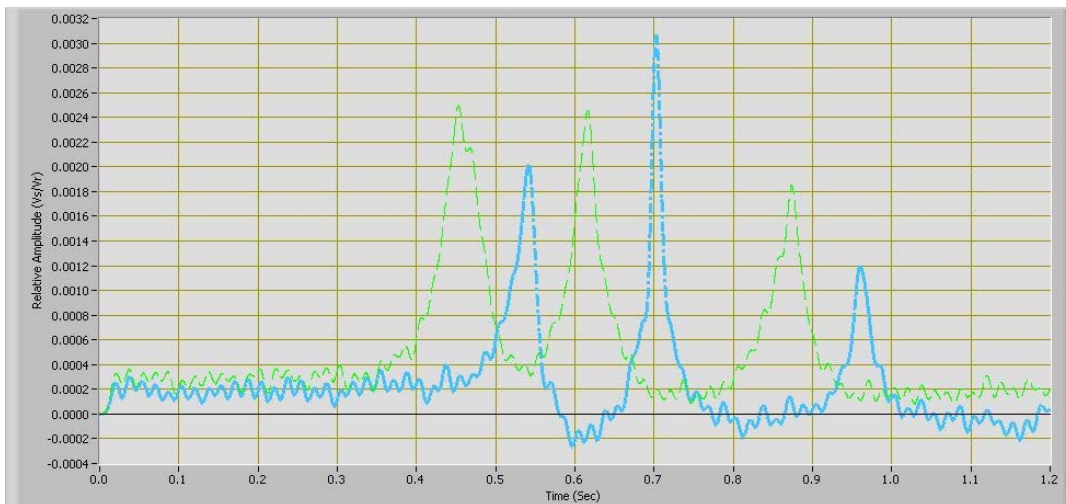
Figure 5.19. The LGC (dashed) and the UNC sensor react to traffic passing over (BRR, 2003).

The relative height of the peaks corresponding to individual axles tends to vary more so in the composite beam sensors. Although this may not be an ideal lead into weigh-in-motion applications, it is logical that sensitivity may be a function of several factors. It is anticipated that these variations may be corrected by understanding more about the sensor position in the roadway, tire position, embedment techniques, and sensor types, as applied to weigh-in-motion. For vehicle axle counting or classification, this is not necessary.

If the FBG sensors are used in traffic detection, compatibility with existing roadway classifiers is valuable. For this reason, it was important to study the feasibility of interfacing the fiber traffic sensors with standard, off-the-shelf traffic classification equipment. Using Diamond Traffic's Phoenix traffic classifier, laboratory data was signal-processed to match the amplitude-triggering requirements of this traffic classifier. Live data from the traffic sensors was stored on the computer as analog voltage measurements. Later, this data was exported as a scaled voltage into the piezo inputs on the classifier box.

Blue Road Research loaned an optical demodulation unit for the data acquisition and electronics to convert the optical signal to an electrical voltage compatible with vehicle classifier boxes. One potential capability of this device is for WIM use. To further investigate this product, an analysis of FBG WIM capabilities will be completed.

Summary

The system developed by BRR has proven to provide data that has high sensitivity (less than 0.2 micro-strain) at high sample rates (>5000 Hz). The system is ideally suited for structural health monitoring. While civil structure demonstrations using the system have been limited to one fiber grating sensor operating at high speed per fiber, BRR has delivered systems operating 4 and 8 fiber grating sensors operating at high speed (10 kHz) to the Navy as part of a Phase II SBIR project. BRR has utilized these systems on bridges, concrete and asphalt test pads and most recently the I-84 freeway. Both the

bridge and I-84 systems have shown the ability to detect a wide range of traffic and significant potential for weigh in motion.

Status to-date

Future work may include modifying and improving the second-generation fiber grating strain sensors and packaging to establish capabilities for WIM by studying same-vehicle repeatability, vehicle calibration, and axle response/stability. A further effort with interface requirements between the optical demodulation and the traffic classifier should also occur; as an optimal interface for retrofitting with existing equipment would be hardware-convertible and not require the use of a computer.

To advance this technology forward for WIM capabilities, these sensors will be characterized to determine any position-dependant effects related to the tire(s) crossing over the sensor. This may potentially be accomplished by offsetting sensors in the roadway to determine tire position. Further, a study of the optimal installation depth, speed-related effects, and materials and procedures for installation, will be examined. As this is a leading-edge technology, no database or library of information exists to determine how these factors influence measurement data.

Oak Ridge National Laboratories (ORNL)

Project Background

This research project described the development of a first-generation prototype portable fiber-optic weigh-in-motion system. The Applied Technology Division of the Oak Ridge National Laboratory for the U.S. Department of Energy conducted the research and development program, during the fiscal years 1990-1991.

The overall objective of this project was to develop, demonstrate, and deliver a first-generation prototype system with the following target system characteristics.

Operational Characteristics

The operational characteristics of the system were to be as follows:

- Accurate to ±1% of calibrated static vehicle weight
- Summed vehicle axle weights to acquire gross weight
- Operated with vehicle speeds up to 5.0 km/h
- Alarm when invalid measurements occur
- Used portable 80386-exportable computer technology
- Operated over a temperature range of –20 to 100°F
- Yielded reproducible results in multiple events/passes
- Accurate field calibration

Packaging Characteristics

The packaging characteristics for the equipment were to be as follows:

- 5 packages – 50 lb per package,
- packages to be compatible for hand loading on aircraft, and
- packages to survive moderate vibration during transport.

Vehicle Characteristics

The vehicle characteristics for the study were to be as follows:

- Vehicle width – 3m maximum
- Tire tread widths – 0.75m maximum
- Tire diameters – 0.5m to 2.0m
- Axle track widths – 1.0m to 3.5m
- 0.1 tons to 30.0 tons per axle
- 12 axles maximum

Operational Site Characteristics

- Flat and level concrete surface such that roadway parameters are not variable

Equipment Used

The system was comprised of four components: transducer, contact switch, optoelectronics, and computer interface. The transducer and contact switch hardware was designed to physically position in the roadway during field measurements. This equipment consisted of two specially designed transducers that utilize fiber optic sensors and eight specially configured contact switches positioned in strategic locations. The main purpose of this hardware is to acquire pertinent data on each passing vehicle. These measurements include applied dynamic load, velocity, tire position, and tire contact length/width. The hardware was also required to measure other parameters associated with passing vehicles, such as acceleration, to distinguish valid from invalid measurements. Figure 5.20 shows a diagram of the fiber optic weigh-in-motion system.

The transducer's base and pressure plates were fabricated using semi-rigid hardened tool steel. The high rigidity of the design insured that vehicles having abrupt or course tread patterns could be measured with more repeatability than with a totally flexible system. The base plate was fabricated with two grooves 48 in. x 1 in. x 1/4 in. in length, width, and height, respectively. These grooves protect and house the sensors. Each traducer contains two fiber-optic sensor assemblies. The purpose of two sensors is to increase system sensitivity over an extended dynamic weight range. In each transducer one sensor was designed for lighter vehicle and the other for heavier vehicle measurements.
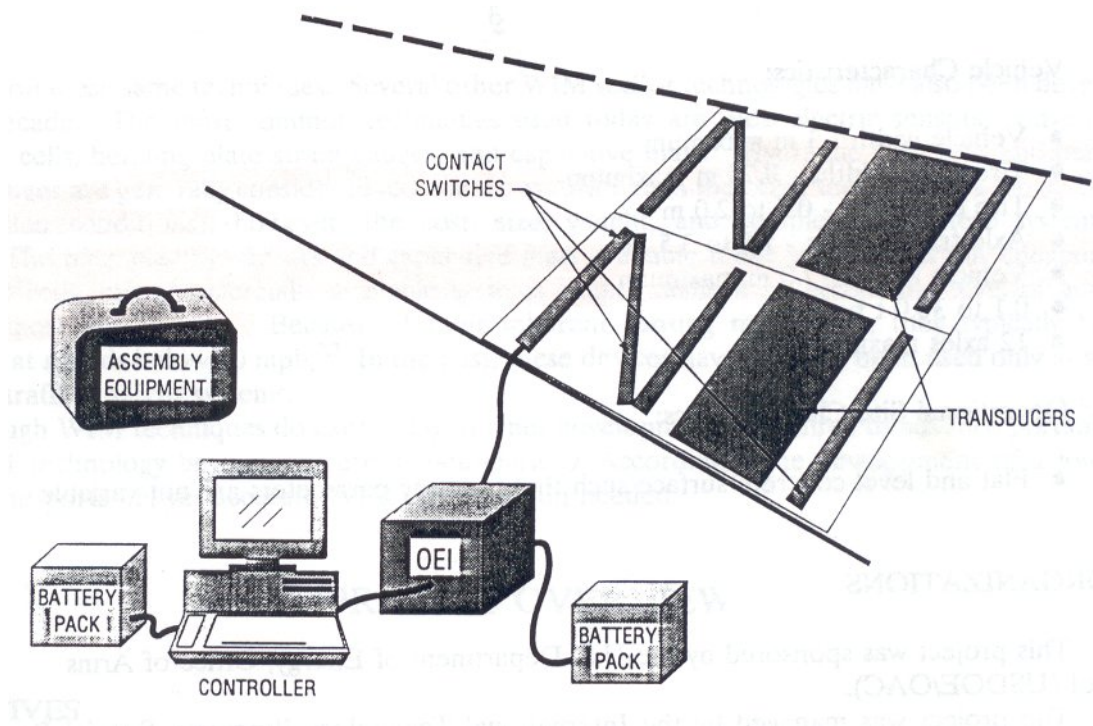
Figure 5.20. Diagram of portable fiber optic weigh-in-motion system (Muhs et al., 1991).

The optical fiber used to fabricate the sensor for this project was made from transparent silicone rubber. It was chosen because of its durability, compression repeatability, temperature response, sensitivity to applied weight, and overall simplicity. The basis for this type of sensor is that as a dynamic force is applied by a vehicle, the amplitude of light traveling through the optical fiber decreases with an increasing force. This phenomenon occurs as the optical fiber is compressed from its original circular shape into an ellipse having a smaller cross-sectional area. Since the amount of light traveling through the fiber is directly proportional to its cross-sectional area, less light is confined to the optical fiber as it is compressed.

The fiber-optic assemblies were encased in an injection-molded polyether polyurethane material, prior to installation in the transducer. This process improved the performance of the sensor during varying temperature and humidity environments.

The sensitivity of each sensor is determined by the contact pressure grid configuration used with each sensor. By varying the configuration the transmission loss-vs.-applied – load relationship for each sensor can be matched to the desired dynamic weight ranges. An example of a contact pressure grid configuration and its effect on the sensitivity of the sensor is shown in Figures 5.21 and 5.22.
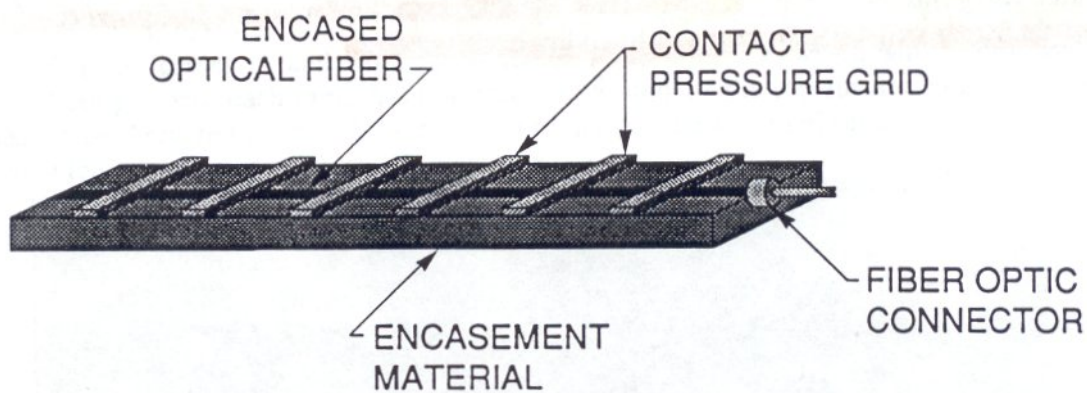
Figure 5.21. Illustration of a contact pressure grid configuration (Muhs et al., 1991).

Each sensor has a differing contact pressure grid and subsequent sensitivity. When a dynamic load is applied uniformly, each sensor behaves independently as shown in Figure 5.22.
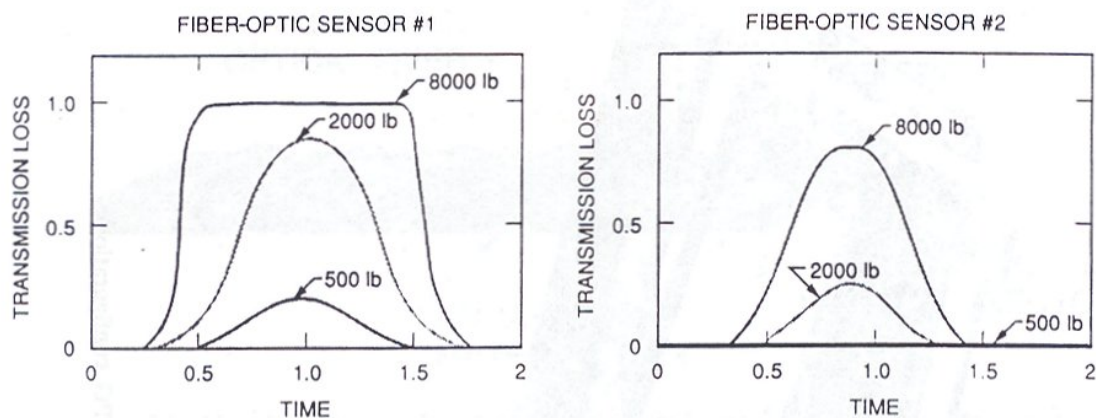

Figure 5.22. Comparison between two fiber optic sensors subjected to identical dynamic loads (Muhs et al., 1991).

The contact switches were used to acquire axle velocity, tire position and tire footprint. Since the velocity measurement was a required portion of the algorithm used to determine weight the switches were positioned on the ramps of the transducer to allow a near-instantaneous velocity to be measured as the tires crossed the transducer. An acceleration measurement was obtained on each axle to determine if the vehicle had abruptly accelerated or decelerated. This measurement was required to ensure repeatable and accurate weight measurements. The reader is referred to the final report (Muhs et al., 1991) documenting this study for more information on the algorithm theory.

The optoelectronics consisted of three major subsystems: on-board electronics (electronics housed in the transducers), optoelectronic interface, and battery pack. Figures 5.23 and 5.24 show the optoelectronic interface and battery pack used for the prototype fiber optic WIM system.
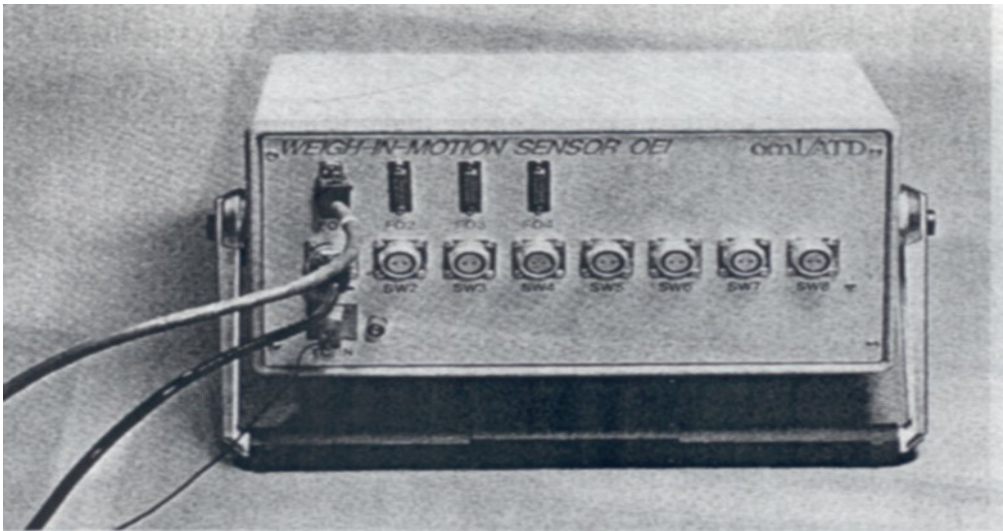
**Figure 5.23. Prototype optoelectronic interface (Muhs et al., 1991).**
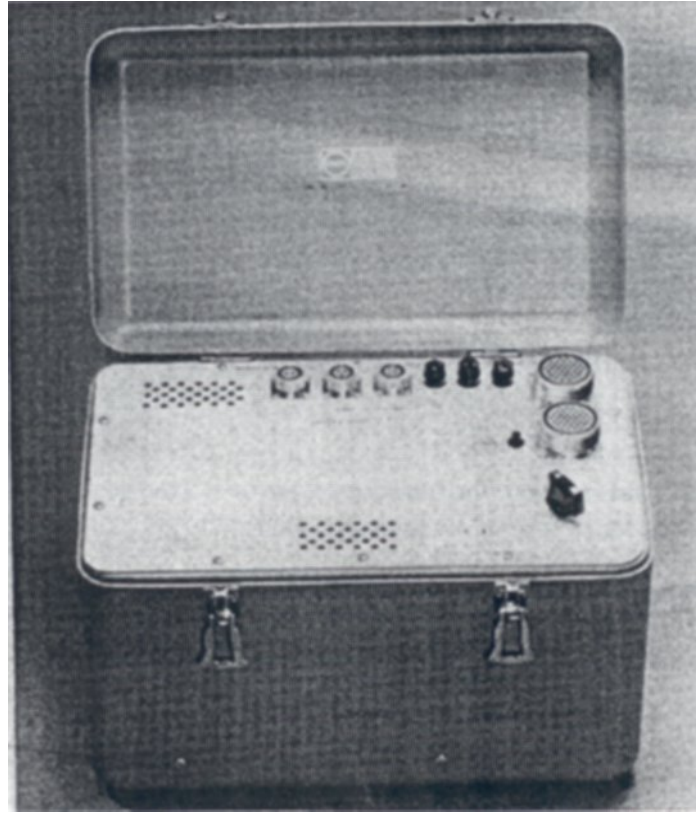
Figure 5.24. Prototype battery pack (Muhs et al., 1991).

The purpose of the on-board electronics was to 1) house the remotely located light emitting diode (LED) used as the fiber-optic-sensor light source, 2) detect, convert into electrical signals, and amplify the light signals, and 3) obtain temperature information within the transducers. On each transducer, two photodetector preamplifiers were packaged on polyethylene-encased silicone-rubber optical fibers from the adjoining LED, because of the need for two contact switch channels connected to the optoelectronic interface.

The optoelectronic interface had five functions: 1) condition and interface the received sensor signals with the computer data acquisition system (DAS), 2) supply the LED with a constant temperature-compensated current, 3) interface the computer calibrate/measure control signal to the LED, 4) interface multiple contact switch signals to the computer DAS, and 5) interface the temperature channel with the computer.

Experiment Details

Laboratory evaluations and calibration of the system was accomplished by using a hydraulic press to simulate various dynamically applied loads. The press included a calibrated load cell, which was used as a standard weight measurement device form which comparisons to the fiber-optic-sensors were made. The evaluations were made by comparing the sensor transmission deflections to the load cell response as a load was applied. Figure 5.25 shows the hydraulic press used to evaluate the fiber optic WIM system during the laboratory evaluations. Figure 5.26 shows an example of the hydraulic press load cell response compared to the fiber optic sensor response.
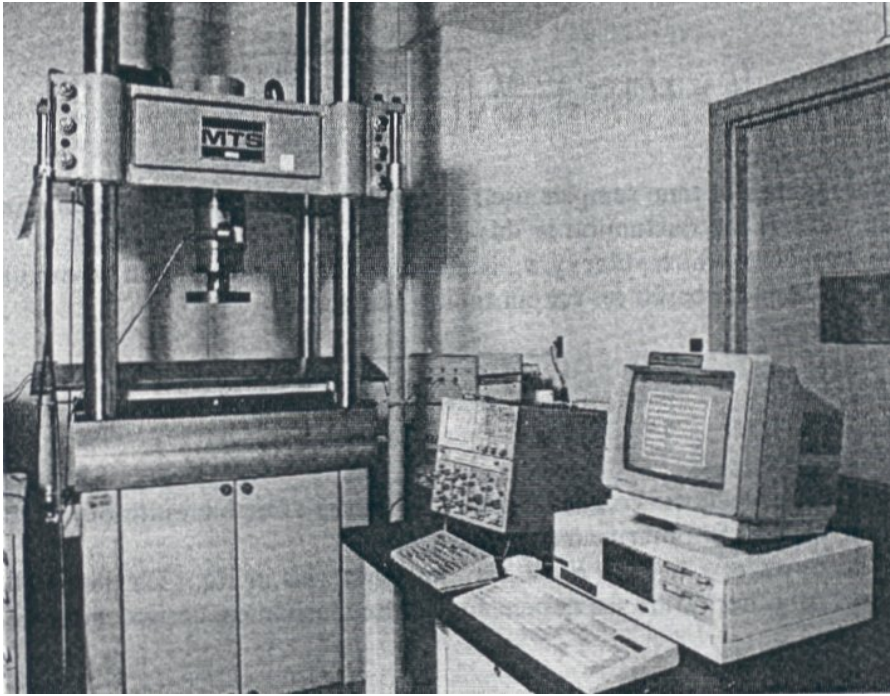
Figure 5.25. Hydraulic press used to evaluate the fiber optic WIM system (Muhs et al., 1991).
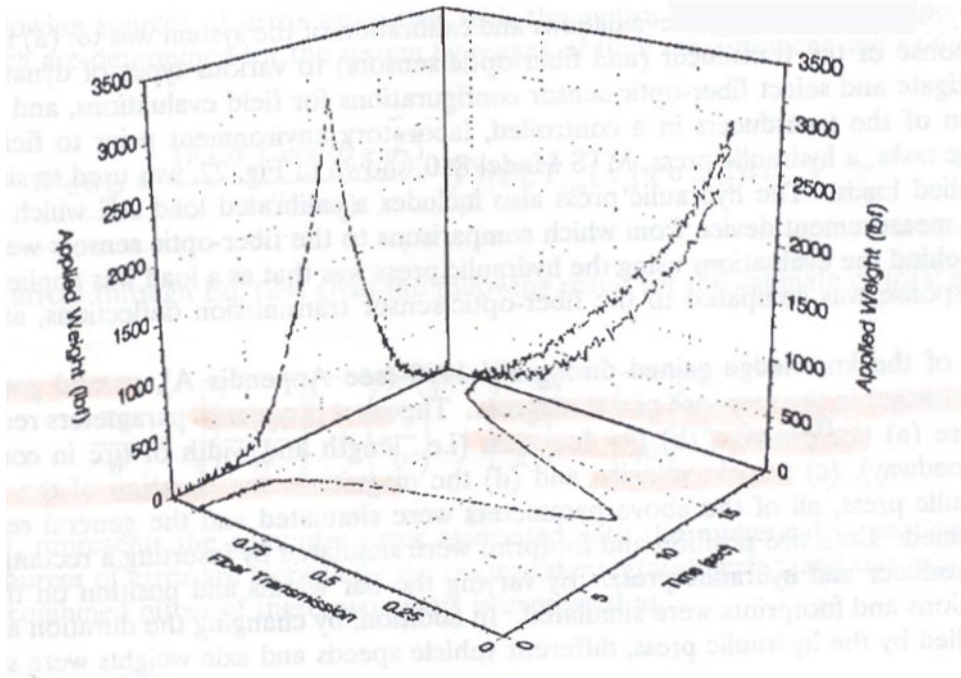
Figure 5.26. Example of hydraulic press load cell response compared to the fiber optic sensor response (Muhs et al., 1991).

Using the hydraulic press parameters known to cause changes in the response of a transducer tire position, footprint, vehicle velocity, magnitude and duration of load were simulated and the general response of the sensors was obtained. Tire position and footprints were both simulated by inserting a rectangular steel bar between the transducer and hydraulic press. By varying the bar widths and position on the transducer, tire positions and footprints were simulated. In addition, by changing the duration and magnitude of the force applied by the hydraulic press, different vehicle speeds and axle weights were simulated.

The roadway used during field evaluations was a section of relatively flat 6-8 inch concrete that exhibited very few cracks, joints, or other vertical protrusions. The four vehicles listed in Table 5.1 were selected because their respective weight ranges, tire sizes, tread patterns, and suspension systems are comparable to vehicles used in actual scenarios.

Table 5.1. Vehicle Characteristics for Field Evaluations.

Vehicle	No. of axles	Ave. weight/axle	Tire configuration
Lightweight van	2	1 ton	Singles
Utility truck	2	2 ton	Singles and duals
Tractor-trailer	5	3-5 ton	Singles and duals
Crane	4	10-20 ton	Singles and duals

To handle the data being acquired during field evaluations, the computer's control program generated a data file for each pass of every vehicle. The data transferred to the data file was:

- Left and right side static weights of each axle (W)
- Velocity of each axle (v)
- Measured response of sensors for each axle (Σ)
- Left and right side tire positions
- Left and right tire widths
- Temperature
- Time of measurement

Each vehicle was driven over the system 15 times, 5 passes at 3 different speeds ranging between 2 and 5 km/h, and a calibration curve was generated for each sensor. Each calibration curve compared the actual static weight of each axle of every vehicle with the total area under the transmission loss-vs.-time curve ($v\Sigma$) as shown in Figure 5.27.
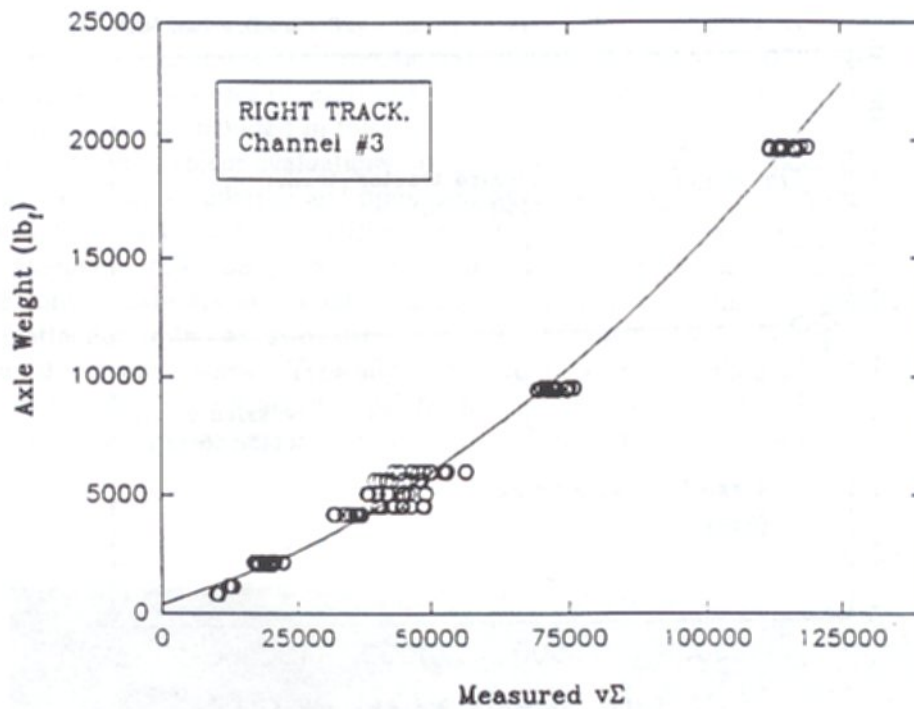
Figure 5.27. Initial fiber optic WIM calibration curves using multiple vehicles (Muhs et al., 1991).

The calibration curves were then included in the computer's control program, and the four vehicles were again driven over the system approximately 15 times to determine the first-order approximation of system accuracy. Figure 5.28 shows a summary of the fiber optic WIM system response over a weight range of 3,979 to 116,555 lb_f. During the field test, it was observed that the measured sensor response, $v\Sigma$ varied with velocity by an average of 2.5%.
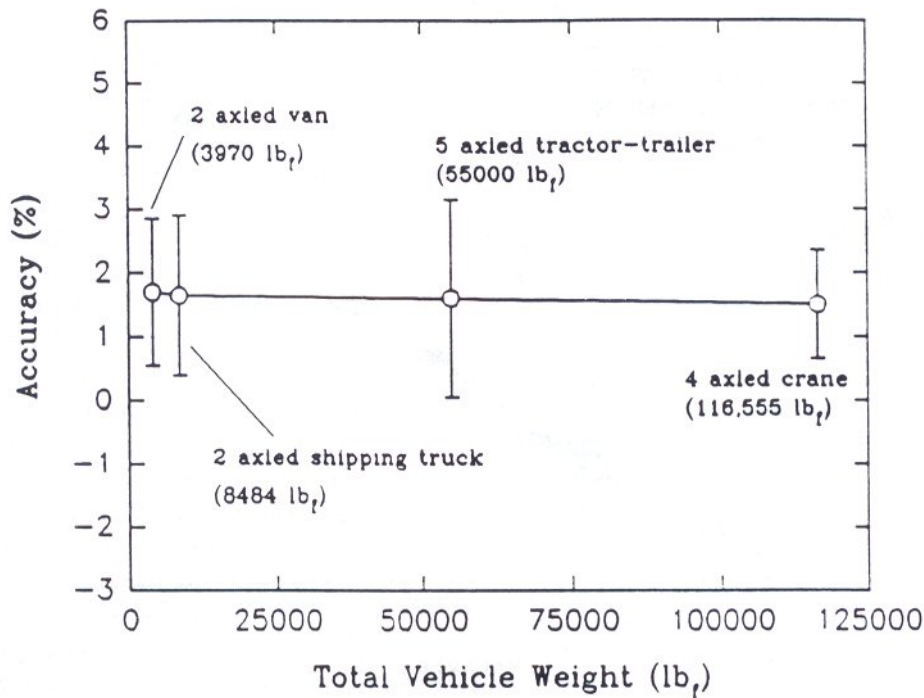
Figure 5.28. Summary of system response tested over a weight range of 3,979 lb$_f$ to 116,555 lb$_f$ (Muhs et al., 1991).

Summary

The aim of this research project performed by the Oak Ridge National Laboratory (ORNL) was to develop and demonstrate a portable fiber optic weighing system for potential application by the U.S. Department of Energy's Office of Arms Control On-Site Inspection Agency during treaty weighing operations. As a result of ORNL's 1991 development efforts, a first generation, portable, fiber optic WIM system was successfully produced and demonstrated. The prototype consisted of two custom-built transducers (containing two fiber-optic sensors each), eight contact switches, one custom-built optoelectronic interface, one custom-designed computer/controller, and one battery pack. The system weighed approximately 350 lb distributed among six transportation cases. It was capable of measuring individual axle loads ranging from 0.1 tons to 30 tons at a speed of 5 km/h and automatically summed individual axle weights to obtain the total gross vehicle weight. Under controlled environmental and site conditions, the system demonstrated accuracy ranging form ±0.5% to ±3.0% from a known static gross vehicle weight.

The prototype fiber optic WIM system was designed and fabricated with the capabilities of acquiring, digitizing, and measuring dynamic loads ranging between 0-10 tons with a standard deviation of 8 percent at low speeds. The transducer was designed such that its dynamic range could be modified form 0-1 tons to 0-10 tons by altering the hardness of the polyethylene housing surrounding the optical fiber. To insure environmental stability, the optical fiber was subjected to a series of environmental durability evaluations including compression repeatability, temperature/compression cycling, and humidity cycling with no evidence of detrimental performance degradation.

Status to-date

The 1991 study by ORNL produced a portable prototype WIM system that utilized fiber optic sensors. As with many research projects, once the funding for this particular study was gone, the development of this type of technology was postponed until additional funding was secured. Currently, there are no immediate plans to continue the development of the portable WIM system prototype produced by ORNL that utilized fiber optic sensors made with transparent silicone optical fibers.

New Jersey Institute of Technology (NJIT)

Project Background

Professor F. Ansari and Research Assistant J. Wang of the New Jersey Institute of Technology conducted research on the response of highly birefringent polarimetric sensors, when subjected to dynamic compressive loads of varying magnitudes, and loading rates. The researchers believed that the results of their research were fundamental to the application of this type of fiber optic sensor for the measurement of weights of vehicles in motion.

### Equipment Used

This research project was based on the findings of previous studies that indicated the suitability of high birefringent (Hi-Bi) polarization maintaining optical fibers for the measurement of pressure. An understanding of the behavior of polarimetric sensors

under compressive states of stress was developed from these studies. A polarimetric sensor is defined as a sensor in which the environmental signal alters the polarization of a light wave in an optical fiber (Udd et al., 1998). Highly birefringent optical fibers have been developed for polarization dependent devices and coherent transmission in order to eliminate the influence of external perturbations in unstable environments. Maintenance of the polarization state in these fibers is attributed to the stress anisotropy in the core, which is generated by the stress applying elements in the cladding. The break up of the cylindrical symmetry in a fiber results in two distinct modes of polarization. Consequently, polarimetric Hi-Bi optical fibers are able to maintain the linear polarization state of light entering them along the planes parallel to their principal axes. Furthermore, when these fibers are compressed or a load is imparted on any place along the length of the fiber the polarization is no longer linear and is at an angle. Therefore, such fibers serve as an appropriate choice for applications in dynamic loading environments, where the stability of the polarization state would lead to the stability of a sensor's response (Ansari & Wang, 1996).

The experimental setup for this study consisted of polarizing optics and a servo-hydraulic loading system. Circularly polarized monochromatic light was launched into a fibercore HB600 Bow-Tie fiber. A 30 mW polarized helium-neon laser operating at 632.8 nm was employed as the light source. The relatively high output power of the laser eliminated the need for signal modulation. A schematic of the experimental setup is shown in Figure 5.29.
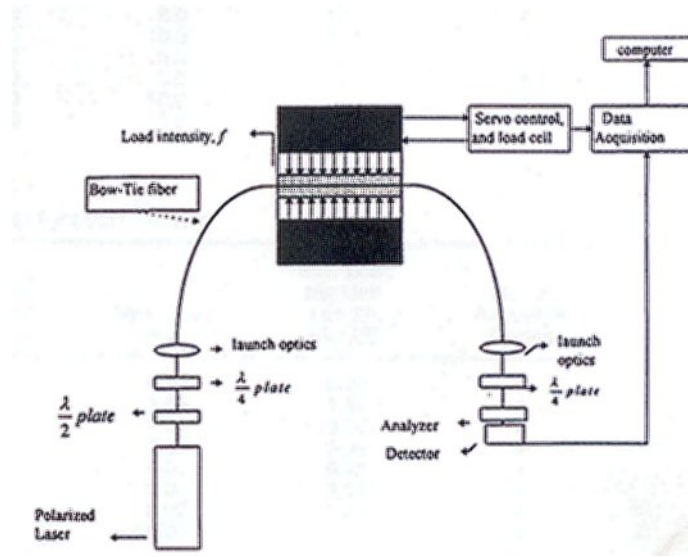
Figure 5.29. Experimental setup (Ansari & Wang, 1996).

The loading component consisted of a closed loop servo-hydraulic testing machine, capable of applying up to 100 Kips of tensile or compressive loads.

Experiment Details

Two different loading programs, a ramp and a step function, were chosen for applying time dependent compressive loads to the fiber. Ramp loads were applied at two different frequencies. For calibration and control, two of the experiments involved applying slow, quasi-static loads. Loads were cycled for at least four times for repeatability. A fixed length of fiber was employed with all sensors. The effect of sensor length on the dynamic response was not investigated.

Tables 5.2 and 5.3 depict the experimental program for the ramp, and step function loading. Varying the frequency and the value of targeted maximum load amplitudes controlled loading velocities. For ramp function experiments, two frequencies of 0.5 and 1 Hertz were employed in reaching similar maximum loads. In Tables 5.2 and 5.3, loading rate or velocity is defined as the slope of the applied load versus time relationship. Theoretically, for the step function this slope is infinite. However, from the practical standpoint, the slope of the step function possesses a finite value, and it can be calculated in a similar manner as to the procedure employed with the ramp function

loading. In some cases, there was a slight difference between the targeted program load, and the actual applied load by the testing machine. These differences are depicted in columns 4 and 5 of Tables 5.2 and 5.4, respectively. A 250-micron diameter fiber was sandwiched between two one-inch thick stiff rubber pads prior to load applications. A pre-load of 9 Kips was applied to ensure instantaneous transfer of load from the machine to the optical fiber. Rubber pads are necessary both in the field and in the laboratory for the protection of the fiber from damage. The magnitude of the pre-load was chosen by testing and measuring the stiffness of the testing frame assembly. The pre-load was not included in Tables 5.2 and 5.3 since it was not applied in a dynamic manner.

Table 5.2. Ramp Function & Quasi-static Loading (Ansari & Wang, 1996).

Loading Rate (Kip/ft-sec)	Time to Max load (sec)	Targeted Max Load (Kip)	Targeted Max Load per Unit length (Kip/ft)	No. of Repetitive Cycles
0.15	20.0	2.0	3.0	4
3.0	1.00	2.0	3.0	4
6.0	0.50	2.0	3.0	4
6.0	1.00	4.0	6.0	4
9.0	1.00	6.0	9.0	4
12.0	0.50	4.0	6.0	4
12.0	1.00	8.0	12.0	4
15.0	1.00	10.0	15.0	4
18.0	0.50	6.0	9.0	4
24.0	0.50	8.0	12.0	4
30.0	0.50	10.0	15.0	4
0.15	100.00	10.0	15.0	4

Table 5.3. Step Function Loading (Ansari & Wang, 1996).

Loading Rate (Kip/ft)	Time to Max Load (Sec)	Max Load (Kip)	Max Load Per Unit Length (Kip/ft)	No. of Repetitive Cycles
45.80	0.068	0.63	0.95	4
67.70	0.068	1.04	1.56	4
111.70	0.076	2.05	3.08	4
86.40	0.076	2.06	3.09	4
213.30	0.076	4.08	6.12	4
304.00	0.076	6.02	9.03	4
402.00	0.076	8.02	12.03	4
460.50	0.076	10.05	15.08	4

Table 5.4. Comparison of Predicted Load Intensities (Ansari & Wang, 1996).

No. of Fringes to Max load	Max Applied Load Intensity (Kip/ft)	Computed Load Intensity (Kip/ft) Calibration Factor (0.74 Kip/ft/fringe)	Computed Load Intensity (Kip/ft) Calibration Factor (0.82 Kip/ft/fringe	Computed Load Intensity based on Regression (Kip/ft)
3.90	3.23	2.89	3.20	3.22
3.55	2.99	2.63	2.91	2.96
3.43	2.90	2.54	2.81	2.88
7.34	5.85	5.43	6.02	5.70
11.35	8.75	8.40	9.31	8.59
7.08	5.67	5.24	5.81	5.51
15.05	11.64	11.47	12.71	11.59
19.09	14.56	14.73	16.32	14.77
10.97	8.48	8.12	9.0	8.32
15.00	11.31	11.10	12.30	11.23
19.28	14.14	14.27	15.81	14.32
19.99	14.89	14.79	16.39	14.84

Experiments were performed at a quasi-static rate differing only the amplitude of the maximum load. This yielded two different calibration factors, which were used with linear regression for computation of applied loads. Results presented in table 5.2 show accuracy is dependent on the amplitude of the calibration load.

Summary

Results of this project clearly indicated that it was possible to accurately measure the magnitude of dynamic compressive loads with the proposed sensor. The sensor response was a function of the amplitude as well as the velocity of applied loading. Calibration of this sensor, for the desired velocities, should be achieved through regression analysis. Regression parameters pertaining to particular sensor characteristics of fiber length and loading velocities should be determined through a set of experiments covering the entire anticipated spectrum of loading rates and amplitudes.

Status to-date

No additional documentation was found to indicate continuation of this research.

University of Connecticut (UCONN)

Project Background

This was a research and development project conducted by Ramesh B. Malla, Ph. D. (Principal Investigator), Norman W. Garrick (Co-Principal Investigator), and several graduate students at the University of Connecticut. The objective of this project was to present a new fiber technique for direct measurement of the wheel loads of vehicles in motion by using the Dual Core Forward Time Division Multiplexing (FTDM) fiber. The experiments confirm the sensing fiber's ability to measure the magnitude as well as location of the load acting on it. It also has the advantage of providing an output signal with a much higher intensity than obtained from other techniques, thus allowing easier detection and measurement.

The main advantage of this fiber-optic system is that it is envisioned to measure wheel loads of many vehicles moving at the same time in multiple lanes, and still measure simultaneously several other important parameters, such as vehicle speed, inter-axle distance, distance between the left and right tires. All measurements can be taken with a simple system using a single continuous fiber, a single light source and a single photo-detector and associated electronics. Optical signals from different points along the fiber do not interfere with each other, even if these points are each under different vehicles at the same time.

Equipment Used

The research work on this fiber optic WIM sensor has been conducted in the Department of Civil & Environmental Engineering at the University of Connecticut since 1997 (Principal Investigator: Ramesh B. Malla, Ph. D.). The research work was initiated with a NCHRP IDEA funding in 1997 (Malla and Garrick, 2000). The WIM system that was developed during this research work consisted of four main parts, the Forward Time Division Multiplexing (FTDM) fiber, load-transmitting device, optical set-up, and data acquisition setup.

Special Optical Fiber Used

The FTDM fiber used for this research had two light-guiding regions of different refractive index. The fiber comprises a small single mode inner core having an index of refraction n1, an inner cladding around the core having an index of refraction n2 lower than n1, a second light guiding region around inner cladding, having a graded multi-mode near parabolic refractive index, the highest value of which n3 is substantially higher than n1, and an outer cladding having an index of refraction n4, substantially lower than n2. Figure 5.30 shows a cross section and a typical refractive index profile of the test fiber.

Tests were conducted with two separate custom-made spools of the fiber. One spool contained the fiber having outer diameter equal to 140 micrometers and the other fiber having the outer diameter of 125 micrometers. The first series of tests were done using the fiber of 140 micrometers outer diameter (Malla et al., 1998; Sen, 1999). The second

series of tests were conducted using the fiber having outer diameter of 125 micrometers (Lin, 2000; Malla and Lin, 2001). The principle by which the fiber acts as a force sensor is described in the following paragraphs.
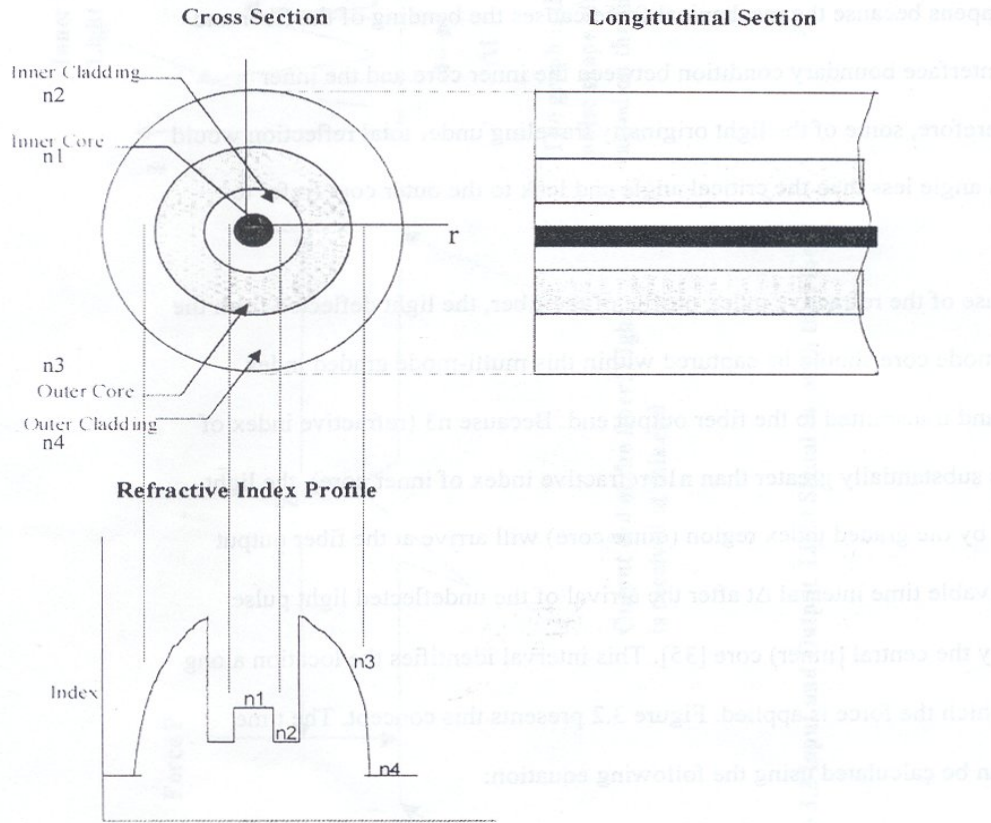
**Figure 5.30. Typical cross section and refractive index profile of the test fiber (Malla et al., 1998).**

A train of light pulses with a width of the order of sub-nanosecond or shorter is injected into the inner core of the fiber at one end. When a mechanical force is applied at any point along the fiber, the fiber will bend and a fraction of the light pulses along the inner core are deflected into the outer core. These deflected light signals propagate along the outer core and reach the other end of the fiber some time after the arrival of the undeflected light pulses as the effective refractive index, n3, of this region is higher than the refractive index, n1, of the inner core. This time difference between the two light pulses gives the location along the fiber where the force was applied (Malla et al., 1998).

74

As some of the light escapes into the outer core there is a loss in the intensity of the light traveling in the inner core. Therefore, new light pulses are observed in the outer core. The magnitude of the force can be determined from the relative intensities of these two light signals or from the decrease of inner core light and increase in the outer core light. This separation of the signals in time is called Forward Time Division Multiplexing (FTDM). These special characteristics of the fiber, i.e. its ability to measure magnitude and location of a load, were verified by laboratory experiments in a custom fabricated 140 micrometer outer diameter FTDM dual core fiber by introducing bending in the fiber by hand (Malla et al., 1998).

Load Transmitting Device (Transducer)

The laboratory prototype load transmitting device main components consisted of a top plate, spring, pins and base plate. On vehicle wheel loading, the springs compress causing the pins to push down on the fiber. After the vehicle has passed, the springs would return to their original position. The pins were designed to have adjustable height. Lowering the pins from the top curved plate will provide a small amount of initial bend to the fiber before loading. This will facilitate measuring the effects of the smaller loads. Larger loads can be measured by raising the pin to create a gap between the pin and the fiber. Contentious revisions were made to the device to get wider ranges of response and better accuracy from the fiber. Figure 5.31 shows the basic components of the preliminary load transmitting device without the revisions. The device was designed to be placed underground with the top just above the road surface. As shown in Figure 5.31, the top plate is curved to prevent it from being an obstruction on the road.
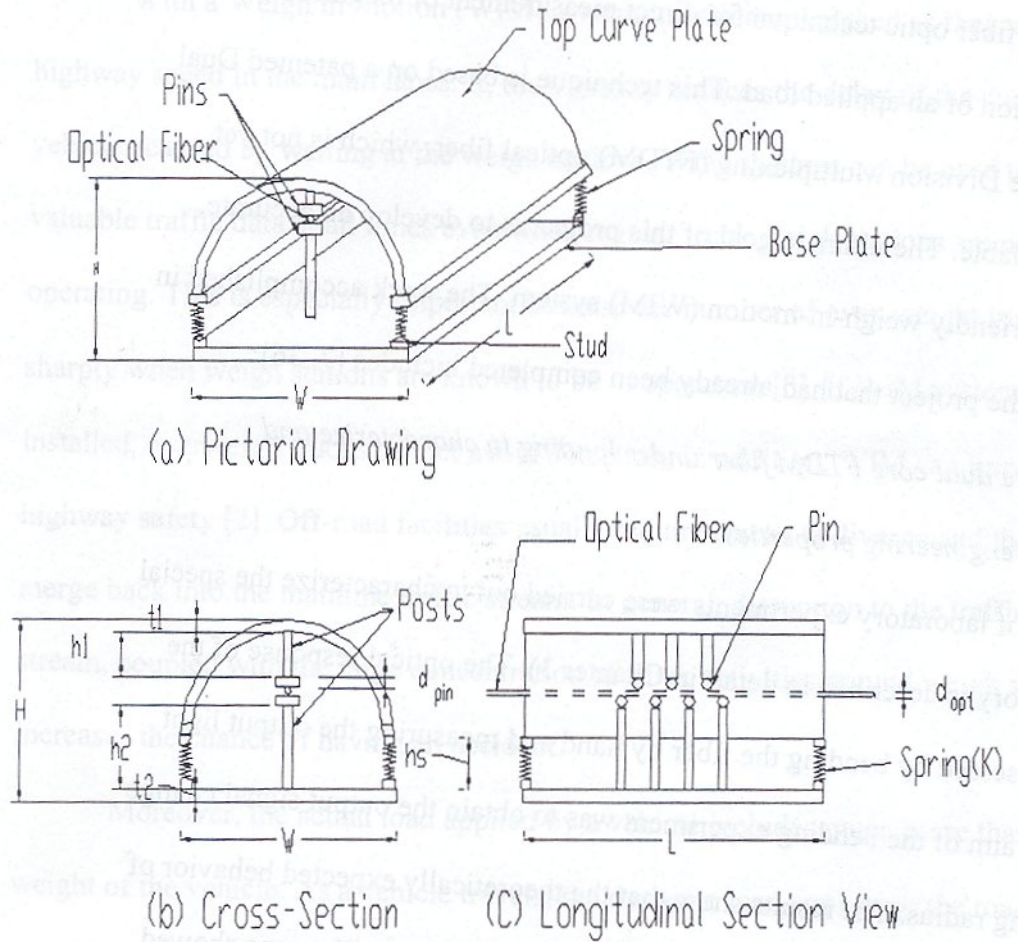
Figure 5.31. Sketch of preliminary load transmitting device (Sen, 1999; Lin, 2000).

A series of laboratory tests were conducted on the preliminary WIM device with the 140 micrometer special FTDM dual core optical fiber. The device was loaded by a universal loading machine and a passenger vehicle wheel (Sen, 1999; Malla and Garrick, 2000). The test results essentially verified the expected principle behind the fiber as described previously. The machine load tests showed a good relationship between the magnitude of the applied load and the change in the optical signal intensity of the inner core light. The results also showed a good relationship between the location of the applied load on the fiber and the delay time of arrival of the two light guiding region pulses at the output end. The results obtained from testing under a car wheel were quite similar to those obtained for the load machines. Based on these results, the fiber and the prototype load transmitting device showed good potential for determining the magnitude and location of vehicular loads. However, the tests also revealed certain deficiencies in the fiber and the

76

preliminary load transmitting device, and a need for further detailed studies of the WIM system in the subsequent study (Lin, 2000; Malla and Lin, 2001). Some of the revisions to the load transmitting device included the following (see Figure 5.32 for details; Lin, 2000):

- The length of the device was increased to 12 inches from 8 inches to accommodate most of the tire width on the road;

- Four more studs fitted with springs were added on both the base plate and the top curved plate for increased mechanical support which in turn allows the measurement of a larger range of vehicle loads;

- Two "alligator" springs were attached, one at each end of the device along the length of the device to provide small tension to the fiber so that the fiber can revert back to its original position immediately after each wheel load; and

- A rigid frame was fabricated for the pin and post assembly to offer better stability and still provide the option of removing, raising and lowering the pins/post assembly.


Furthermore, one of the desirable objectives of the load transmitting device was to get a wider range of response and better accuracy from the fiber. During the experiments, the researchers observed that the previously selected pin diameter was too large for the inner core light to leak out. Therefore, the U-shape bend on the middle pin on the top plate was changed to a V-shape bend to allow for more inner core light to leak out.
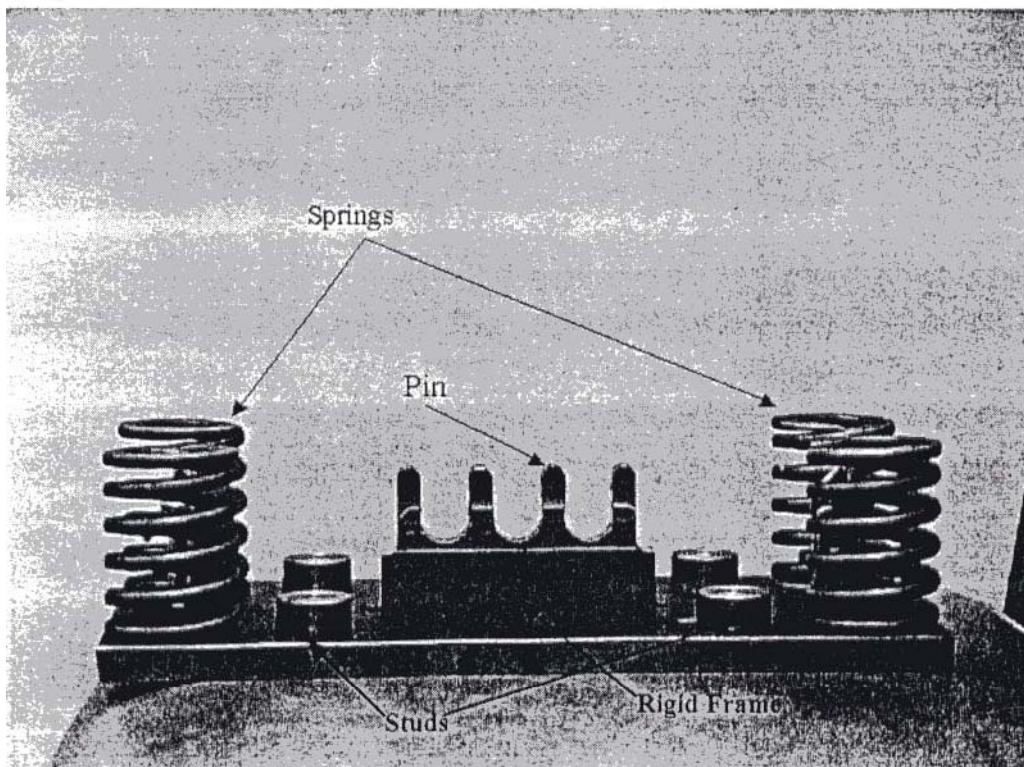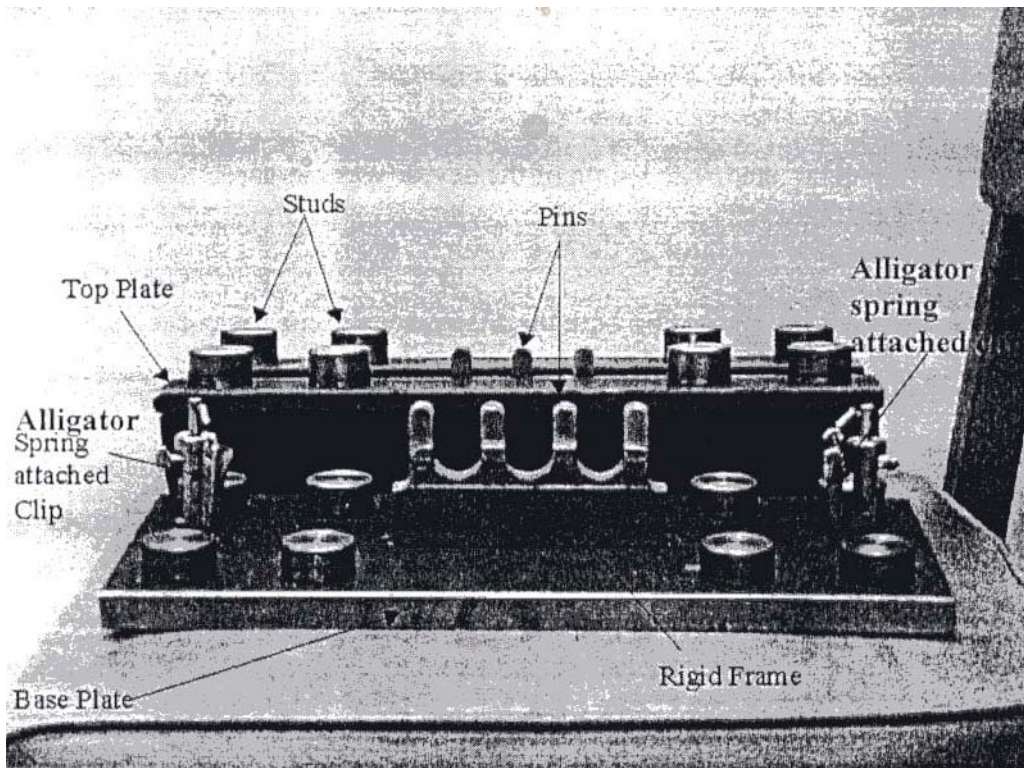
Figure 5.32. Revised load transmitting device (Lin, 2000).

Optical Experimental Setup

A micro-block positioner made by Melles Griot was used to focus the light beam into the fiber. It can achieve a sensitivity of $0.1\mu m$. A FUJIKURA 3-step cleaver was used to cleave the fiber, since a clear-cut cross-section is one of the most important factors affecting the launching of light into the fiber. With the cleaver, a consistent quality end surface was obtained. Figure 5.33 shows a diagram of the optical experimental setup.
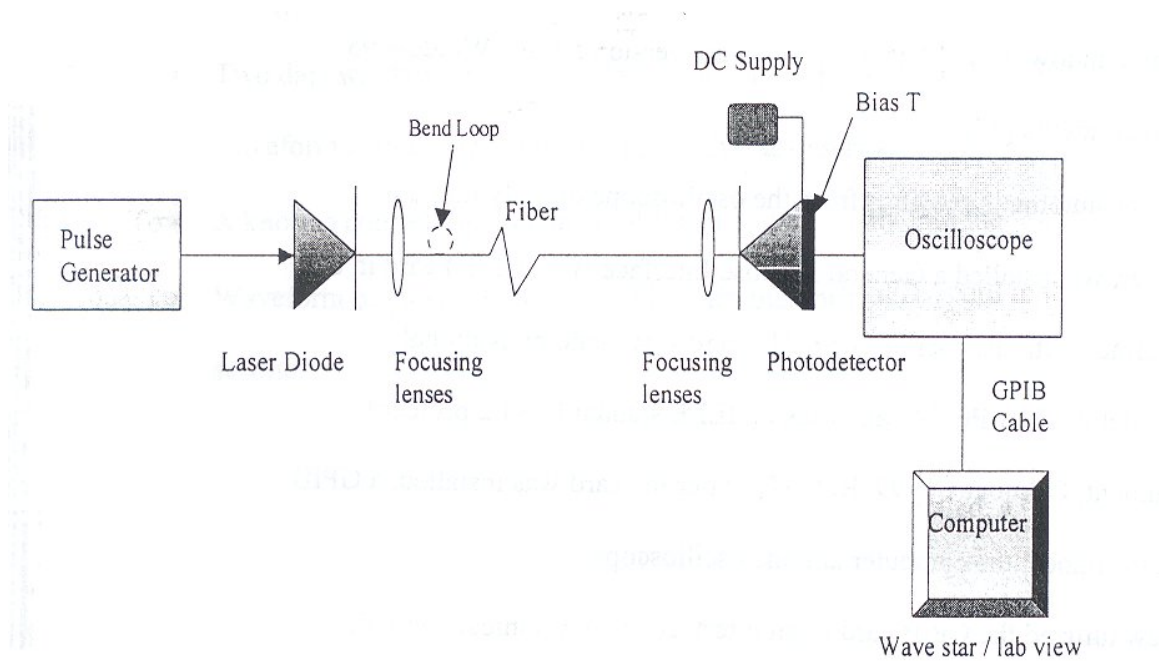
Figure 5.33. Optical experimental setup (Lin, 2000).

An AVTECH pulse generator was used to modulate the laser diode to generate the light pulse signal. The pulsed light beam from the laser diode was then focused with a lens system into the fiber. A micro-block positioner was used to position the input end of the fiber. At the output end, a second lens system was used to focus the light to a photodetector, which converted the light into electric signal and transmitted it to the oscilloscope. A General Purpose Interface Bus (GPIB) cable connected the oscilloscope to a personal computer for data acquisition.

**Data Acquisition Experimental Setup**

The data acquisition system setup consisted of the following components: A Tektronix oscilloscope with sampling head and Time base, a Pentium 166 computer with operating system Windows® 95, and Lab View software version 5.0 from National Instruments. Lab View uses a General Purpose Interface Bus (GPIB) card as an interface to communicate with the oscilloscope. Lab View is then programmed to simulate the functions of the oscilloscope and execute a series of commands from the computer to control the oscilloscope. These commands function exactly like the buttons on the front panel of the oscilloscope. This set-up is called a Virtual Instrument.

Experiment Details

This WIM system was tested and evaluated under vehicle wheel loads in the laboratory to determine if the test results would be similar to results obtained from previous loading machine tests. Vehicles were driven on the wooden track with one wheel passing over the load transmitting device. Three most commonly seen types of vehicles (passenger car, van, pick-up truck) with known weight were tested.

The test setup consisted of two long wooden tracks spaced approximately 4 to 5 feet apart. The spacing between the tracks was varied to accommodate different vehicle width. The tracks were built using wooden planks, which were combined to provide a 16-inch wide, 6 inch high and 32-foot long track on each side. Figure 5.34 shows a sketch of the wooden track test setup.
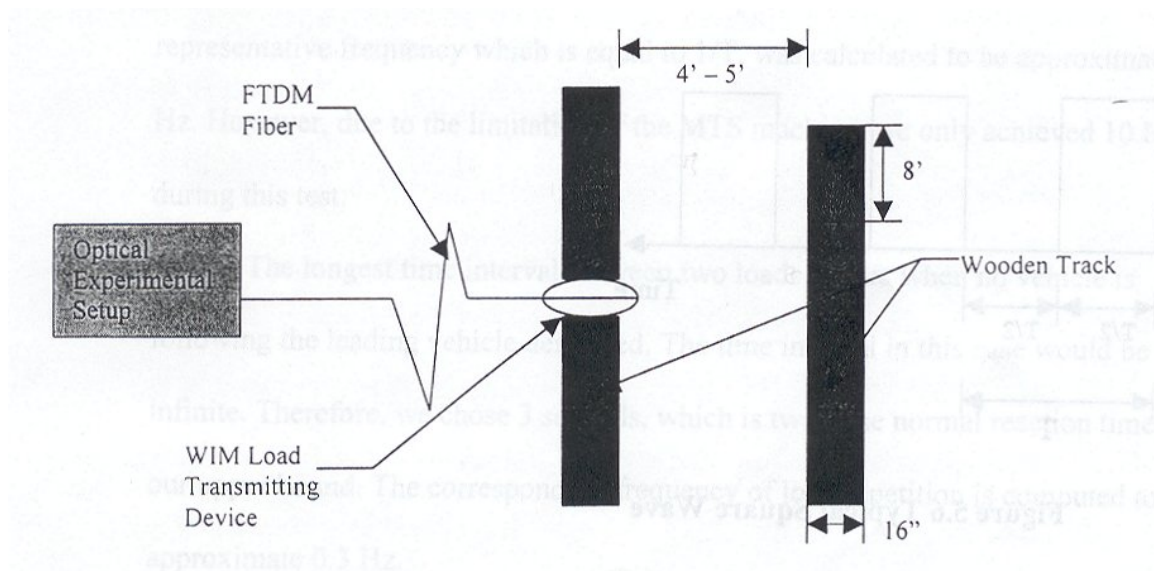
Figure 5.34. Sketch of the wooden track test setup (Sen, 1999; Lin, 2000).

The load transmitting device was placed in the center of one track with only 1 inch of the top curve plate exposed over the surface. Figure 5.35 shows pictures of the wooden track (top) and the placement of the load transmitting device (bottom). A gauge for measuring the displacement was attached to the top edge of the device.

The test for vertical displacement using the WIM device under the vehicle wheels produced readings from both the oscilloscope and the displacement gage. As vehicles ran over the load transmitting device, the vertical deflection of the top curve plate and the light intensity from the oscilloscope were recorded. Two types of data were recorded separately for each vehicle. First, the static wheel load was observed by bringing the vehicle to a full stop over the device without the wheel contacting the wooden planks, ensuring that the wheel load was completely supported by the device. Output intensity of the inner core light and the vertical displacement of the device were recorded. Second, the vehicles were driven at slow speeds (5 mph) over the load transmitting device to record the minimum light intensity and maximum deflection simultaneously. Each test was repeated 4 times to minimize data recording error. A 3-pin assembly in the WIM device was used to create bending in the fiber for the experiments reported herein. The tests were done using the 125 micrometers outer diameter FTDM fiber in the load transmitting device.
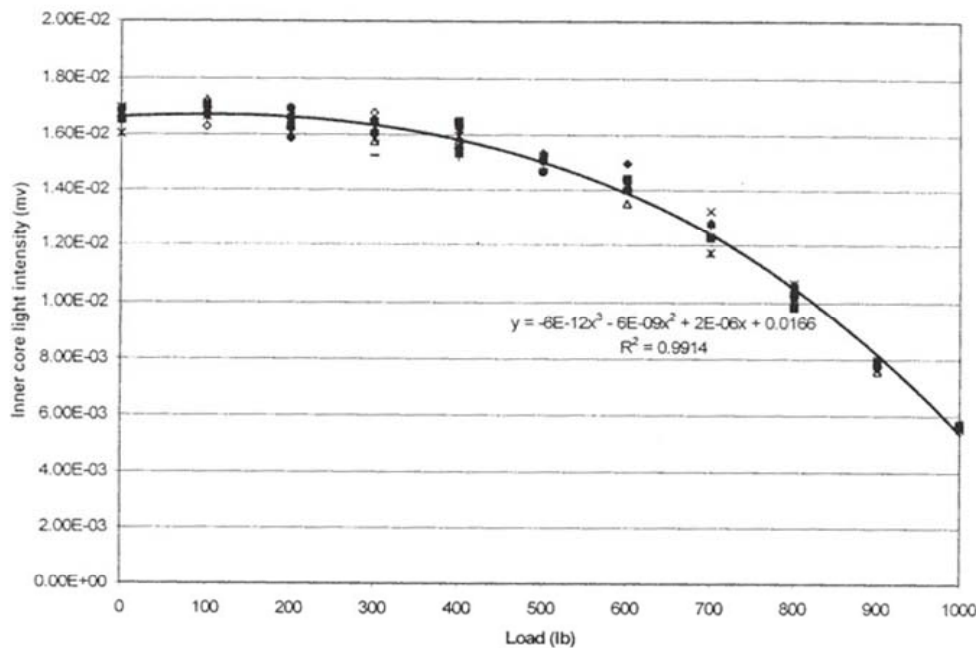
81
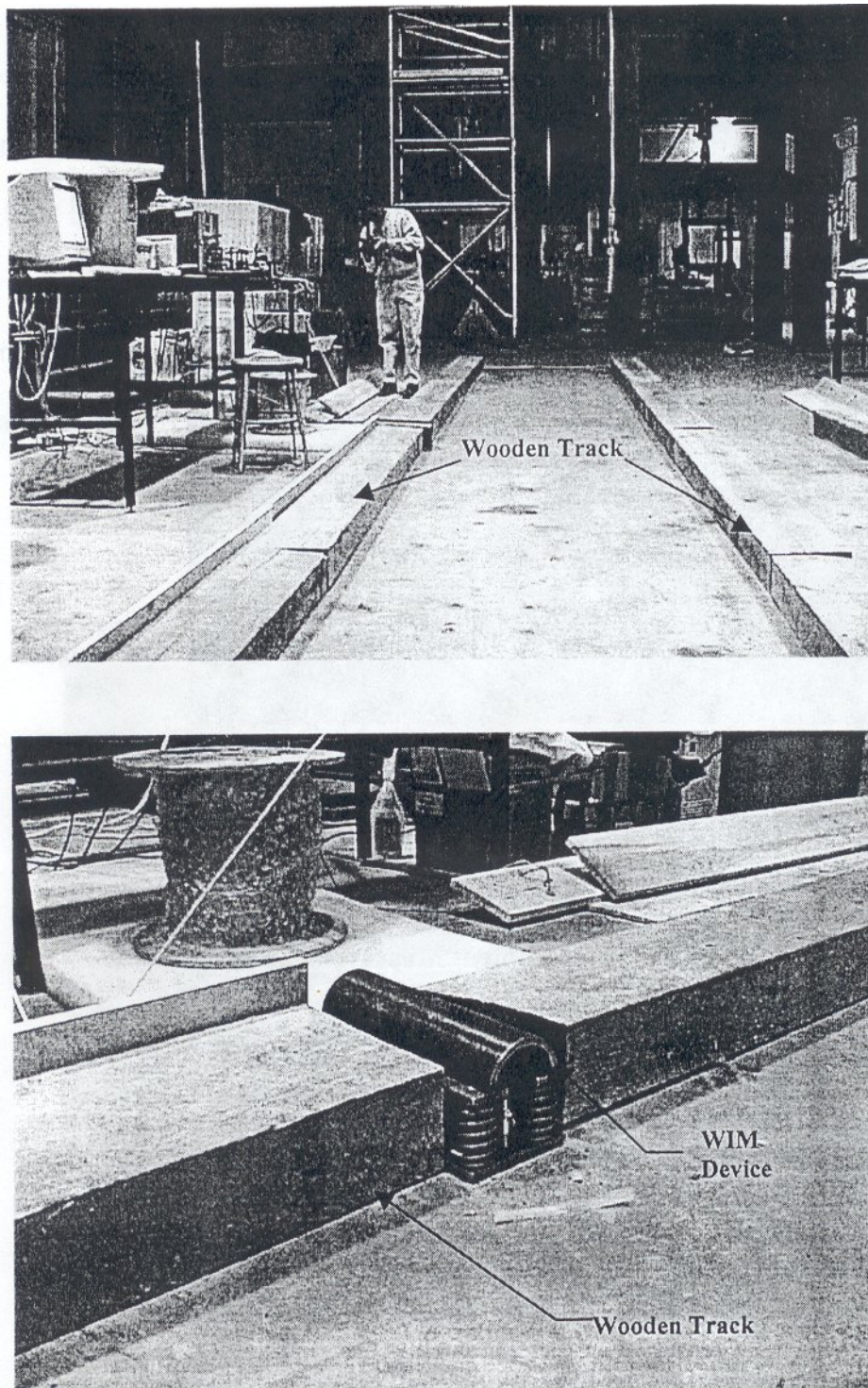
**Figure 5.35. Wooden track (top) and placement of the load transmitting device
(bottom) (Lin, 2000).**

Testing under vehicle wheels, showed no significant differences between readings taken
at static and slow moving (5 mph) wheel situations. The inner core light intensity change

82

results from vehicle wheel load tests were compared with those obtained from static vehicle wheel load tests. The inner core light intensity change represents the intensity change from the reference intensity (output inner core intensity when no load is applied). The researchers made the decision to use the intensity change rather than just the intensity due to the observed fluctuations (noise) in the output signal. Therefore, it was difficult to directly use the inner core light intensity value as the indicator for measuring the applied load. By using the difference between the inner core light intensities before and after the load application, the difficulty with the noise was greatly reduced.

Figure 5.36 shows the relation between the inner core light intensity change and the load. This figure also shows that there is a linear relationship between core light intensity change and the load after 500 lb. The researchers concluded that before the 500 lb load was achieved the bending in the fiber introduced by load less than 500 lbs was not enough to cause the inner core light to leak out.

The equation shown on the figure is:
$$y = -6E\text{-}12x^3 - 6E\text{-}09x^2 + 2E\text{-}06x + 0.0166$$
$$R^2 = 0.9914$$

Figure 5.36. Relationship between inner core light intensity change and load (Lin, 2000).

Table 5.5 shows a comparison between the wheel loads determined by the fiber optic WIM system during the laboratory test (column 4) and the wheel loads determined from the vertical dial gauge displacement reading (column 5) and wheel loads based on actual gross vehicle weight (column 7). Based on the values shown on Table 5.5, the wheel load for a passenger car determined by the fiber optic WIM system was off by about 7% (800 vs. 743 actual) and the wheel load determined by the deflection reading was off by about 12% (650 vs. 743 actual) from the wheel load calculated based on actual gross vehicle weight. Both mini-van and pick-up truck weights were underestimated approximately 6% by the WIM system and 4% by reading the gauge.

Table 5.5. Inner core light intensity change vs. deflection reading and wheel load.

	Ave. Inner Core Intensity Change (WIM) (mv)	Ave. Deflection Gauge Reading (in)	Est. Applied Wheel Load (WIM) (lb)	Est. Applied Wheel Load (Dial gauge reading) (lb)	Actual Gross Vehicle Weight* (lb)	Approx. Testing Vehicle Single Wheel Load** (lb)
Passenger Car	6.67	0.24	800	650	2822	743
Mini-van	8.2	0.33	910	930	3837	970
Pick-Up	10.92	0.37	970	1000	3998	1037

*Actual gross vehicle weight was based on vehicle specification obtained from **www.cars.com**

**Approximate testing vehicle single wheel load was based on a 150 lb driver + actual gross vehicle weight then divided by four.

The approximate single vehicle wheel load is assumed to be one quarter of the sum of vehicle gross weight and a 150 lb driver. Normally the vehicle weight is not distributed evenly between four wheels.

Summary

During this study several characteristics of the experimental fiber were discovered. Inner core light is more sensitive to macro-bending, while outer core light is more sensitive to micro-bending. Tests proved the WIM system to be successful on load sensing. The statistical analysis of data shows that the load and inner core light intensity exhibited a

linear relationship within a certain range. The repetitive loading test in the laboratory showed a very little frequency dependency of inner core output light signals for a given applied load. This implies that the response of the WIM device is independent of the vehicle speed for the range of load-frequency considered. However, it is not clear whether the laboratory experiment setup can simulate different vehicle speeds in the real world.

In addition, as stated in the objective the main advantage for using the dual core FTDM fiber was the potential of being able to determine the position of the load on the fiber as the new outer core peak occurred when bending was introduced in the fiber. This would in turn give the WIM system based on this type of fiber optic sensor the capability of determining the wheel loads of multiple vehicles crossing the sensor simultaneously. However, the test results on the behavior of the two available batches of the special optical fibers (140 and 125 micrometers outer diameter) revealed that the fibers had some deviation from the theoretically expected behavior. Especially, in the second batch of fiber (125 micrometers outer diameter fiber), it appeared that the outer core could not retain the light leaked out from the inner core and guide it to the output end, which is an essential characteristic for the determination of the location of the applied load. One of the researchers' recommendations to address this shortcoming was that a new dual core fiber should be fabricated and tested that will have a difference in the refractive indices of the outer and inner core larger than what was in the fibers that were tested for this study.

Status to-date

Work on this subject area is on going as per memorandum from Dr. Ramesh B. Malla (Malla, 2002). The test results on the experimental fiber from the studies described previously have given useful information needed to improve the design and performance of the special fiber, and to optimize the configuration, size and performance of the prototype load transmitting WIM device. Currently, research work is on going to study in detail the light retaining and mechanical bend loss characteristics of the inner and outer light guiding regions as related to several important parameters. Some of these parameters include overall fiber dimensions, thickness of the inner and outer light

guiding regions, thickness of the inner and outer claddings, wavelength of light to be used, refractive indices of various regions in the fiber, the radius of bend and the spacing between the bends. Also, the aim is to design and build an improved prototype WIM device and to conduct additional tests to fully characterize its performance. Finally, the goal is to develop a dedicated WIM fiber optic sensor system that will be rugged enough for field-testing.

Florida Institute of Technology (FL Tech)

Project Background

Researchers at the Florida Institute of Technology have been working on the development and improvement of a fiber-optic traffic sensor that could be used for traffic classification and WIM applications. The research was conducted by Paul J. Cosentino, Ph.D., P.E. (Principal Investigator), Barry G. Grossman, Ph.D. (Co-Principal Investigator), and several graduate students. The WIM system application used two fiber optic microbend sensors that were embedded in the pavement or placed on top of the road. When the vehicles passed over the sensor, a loss of light occurred that corresponded to the weight of the vehicle and the length of time the vehicle's tire made contact with the sensor. The loss was converted to a voltage and sampled by a computer that analyzed the voltage drop to determine key characteristics of the vehicle.

The research projects included the construction, installation and evaluation of the fiber optic microbend sensors in traffic monitoring applications including WIM. In addition, in a 1999 study a software application that used National Instruments DAQCard-700 for analog/digital (A/D) conversions was written specifically for the project. The application captured and analyzed analog data produced by vehicles passing over the sensors. The application determined the vehicle's velocity, classification, and weight.

Equipment Used

As stated previously, this project used a fiber optic microbend sensor that was designed for use in traffic monitoring applications including WIM. A microbend sensor consists of

a mechanical deformer, optical fiber, and light source and detector circuits. The microbend effect is caused by periodic changes in the geometry of the optical fiber causing the light guided in the core of the fiber to be coupled out of the core into the cladding (Cosentino & Grossman, 1997).

The microbend loss theory, explains how microbending losses cause the propagating light intensity to be coupled out of the core. The loss occurs when the guided, higher-order core modes are coupled to the weakly guided cladding modes (radiative modes) in multimode fibers. This mode coupling occurs when environmental effects, such as an external load, that induces physical periodic bends in the fiber change the fiber geometry. To understand the microbend effect, this mode coupling must be examined (Cosentino & Grossman, 1997). The microbend loss theory is explained in many fiber optic texts and thus will not be described further in this report.

Microbend Sensor Design

To design a fiber optic microbend sensor, the relationship between intensity loss and deformer periodicity for the optical fiber must be known. This relationship allows the optimum periodicity or the period at which the greatest intensity loss occurs to be determined. Then intensity versus load curves can be measured and used to determine sensor response to external load. The researchers from Florida Tech carried out extensive testing to find the best combinations of deformers and fibers for a microbend sensor. For details of the testing, please refer to Cosentino & Grossman, 1997 in the reference section.

The researchers at Florida Tech chose a mesh/fiber combination and constructed a long, flexible microbend sensor with a loop at one end (Figure 5.37). The results from the previous testing showed that an Acrylate coated fiber used with a single-sided polypropylene mesh deformer produced the most linear results for load vs. intensity loss. The linear range of this sensor design was from 0% to 55% loss (Shuhy, 1999). The flexible sensor was then placed into a watertight packaging. Laboratory testing of the

sensor was performed to determine sensor characteristics prior to field installation.
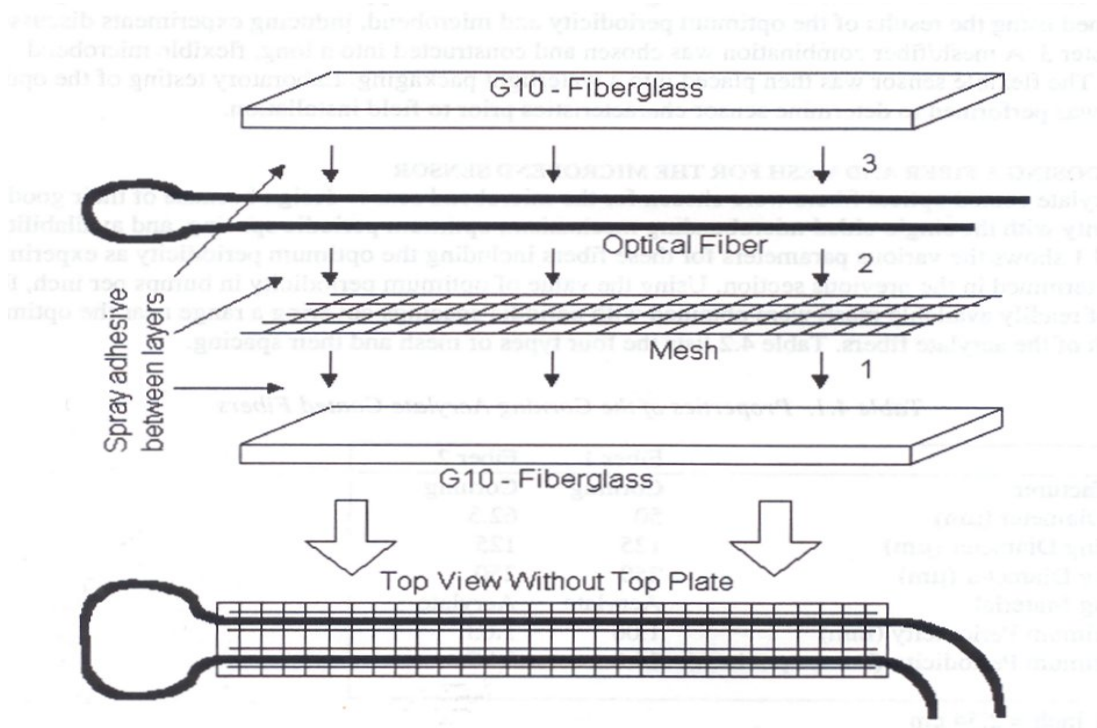

Figure 5.37. Microbend sensor construction (Cosentino & Grossman, 1997).

Opto-electronic Interface Box

A key component in the fiber-optic sensor system is the opto-electronic driver. It generates the optical signal, which is acted upon by the sensor. The output signal is proportional to the load on the sensor. In a 1997 study, a 3-channel opto-electronic interface box was designed and constructed for test purposes. The 3-channel box was used to drive the fiber optic traffic sensor (FOTS). It worked from a 12V battery and consumed approximately 100mA. The front panel (Figure 5.38) contained six ST-fiber-optic connectors, three light emitting diode's (LED), and three PIN diode receivers. The front also included an analog voltmeter to adjust the receiver voltage in the field when the automatic gain control was not in use. This ensured that calibrated measurements were taken at all times. The back panel (Figure 5.39) contained the electronic connectors for data acquisition equipment and PEEK® classification boxes. Within the right side of the interface was a small cooling fan that was used in case of high temperatures.
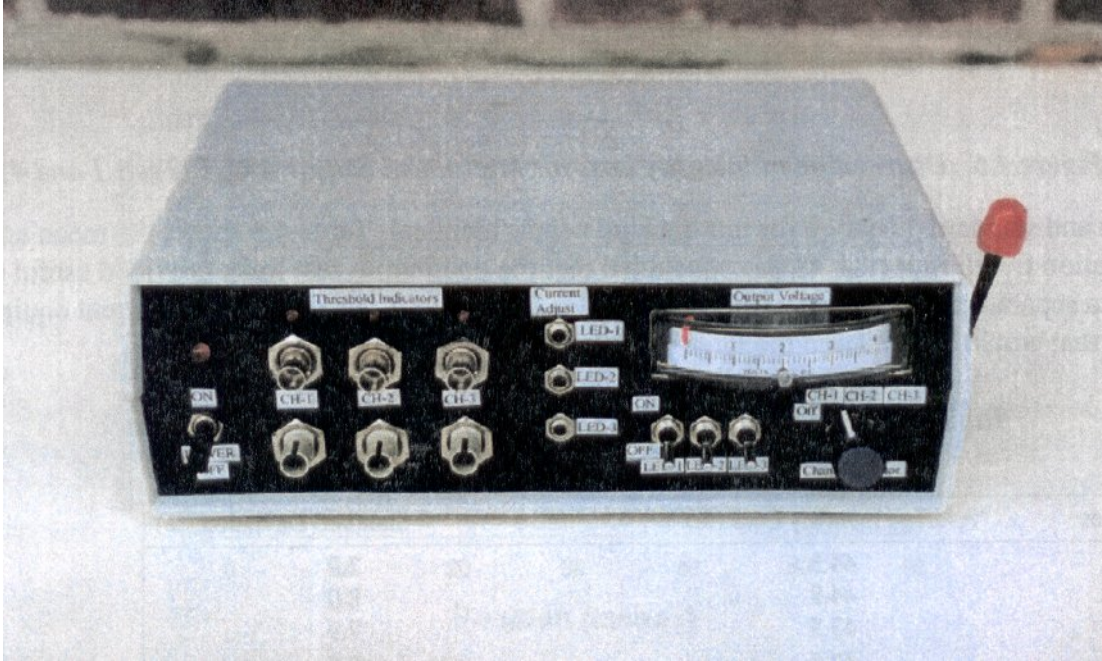
Figure 5.38. Opto-electronic Interface Box – Front Panel (Cosentino & Grossman, 1997).
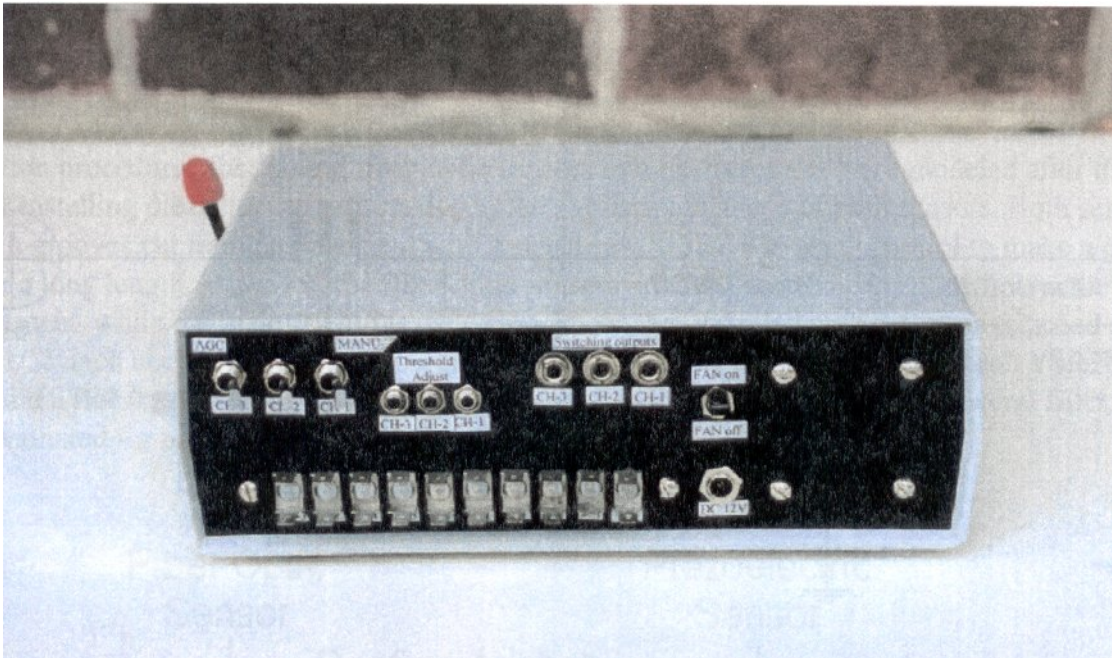
Figure 5.39. Opto-electronic Interface Box – Back Panel (Cosentino & Grossman, 1997.

The electronics of the 3-channel box consisted of one common power supply and three identical opto-electronic driver units. A voltage regulator was used to provide a constant

89

5 volts. The power supply gave two voltages, 12 and 5 volts. The three-pin voltage regulator was mounted on a heat sink. When the voltage level was below a predefined limit it triggered two LED's.

The LT1413 dual operational amplifier served as the automatic gain control and as a unity gain amplifier for the receiver. When the 10K potentiometer was adjusted to a level voltage the first op-amp drove the infrared LED. If the receiver received more or less light due to temperature differences, the voltage level at the negative input of the first op-amp changed and the amplifier provided the LED with current to bring the set-level back. The 1 micro-Farant capacitor produced the delay. All references were temperature stable due to the use of an LM399 (National Semiconductor) precision voltage reference. This microchip was a zener diode and a resistor in a one-thermal insulated cup. The resistor served as the heating element and kept the temperature of the zener constant at 60^0 C. The analog output of the receiver was monitored for the data acquisition hardware and software, which also went to a comparator (LM392). This comparator checked to see if the voltage level went below a predefined limit, and if so, it triggered two LEDs. The first was a regular red LED and the second was an encapsulated LED with a phototransistor to activate a digital input. The single analog voltmeter had a channel-selector switch to display one of the channels each time (Cosentino & Grossman, 1997).

In a 1999 study Florida Tech researchers used a fiber optic transmitter/receiver interface box to couple the light from the fiber optic light emitting diode (LED) into the microbend sensor. When no external load was placed on the sensor all light coupled from the transmitter returned to a matched photodiode detector. However, when a vehicle passed over the microbend sensors, the mesh pressed on the fiber causing a loss of light intensity. The fiber optic transmitter/receiver interface box had an analog output for each sensor that was connected to the DAQCard-700 mentioned previously. If the light loss was large enough, the photodiode circuit's output voltage would drop below the trigger level of the DAQCard-700 and the DAQCard's driver would call a function in the application that was specifically developed for the study. The application would analyze the analog data received looking for the trigger and the pulse produced by the vehicle that

passed over the sensor. The application would match pulse pairs from the two sensors, calculate the vehicle speeds, and determine vehicle weights from the pulses.

Data Acquisition System

For the 1997 study the information obtained from a fiber optic sensor for traffic classification and WIM required that the waveform resulting from passage of a tire be analyzed after it was captured and stored. A portable data acquisition system was developed for use with the fiber optic sensors. Several virtual instruments were developed using National Instruments LabVIEW software. One virtual instrument (VI) was designed to acquire waveforms (multiple waveform acquisition) and store them for future analysis while another VI was designed to open the data file created by the multiple waveform acquisition and allow the user to selectively zoom in and out on sections of each waveform and write them to an output file. For more information regarding the virtual instruments please refer to Cosentino & Grossman, 1997.

For the 1999 study the data acquisitions system consisted of the DAQCard-700 A/D card from National Instruments and a computer that ran Windows 95 operating system and had an available Type II multifunction PC Card (PCMCIA) slot. The DAQCard-700 had a 16 single-ended, 8 differential analog input channels with 12-bit resolution.

Experiment Details

In the 1997 study researchers at Florida Tech were investigating an alternative WIM sensor to the piezoelectric sensors used at the time by the Florida Department of Transportation. Figure 5.40 shows a side-by-side comparison of the installation of fiber optic sensors vs. piezoelectric sensors. The fiber optic sensors were placed in grooves cut into the pavement with a street saw. The sensors were designed for installation below the surface of the pavement. Roofing asphalt was one of several filler materials being evaluated for placement over the sensor.
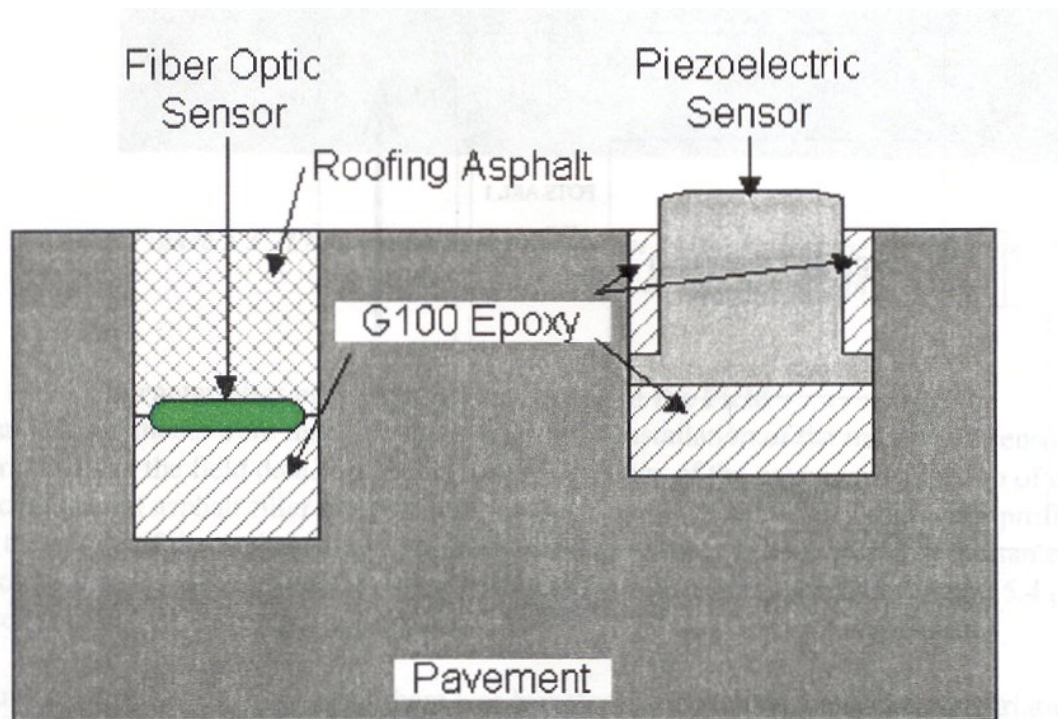
Figure 5.40. Cross-section of a Fiber Optic Sensor and a Piezoelectric Sensor in the Pavement (Cosentino & Grossman, 1997).

The fiber optic sensor was epoxied into a groove with G-100 epoxy. This material is an epoxy/sand mixture with a one-hour cure time. For the sensor, this epoxy forms a consistent, solid and level base. Type III Steep roofing asphalt was heated and poured into the groove to cover the sensor (see Figure 5.41). This material was chosen because its elastic properties allow loads to be transferred to the sensor and it can easily be cut level with the surface of the pavement after it solidifies. The roofing asphalt hardens quickly after placement allowing the reopening of the roadways.
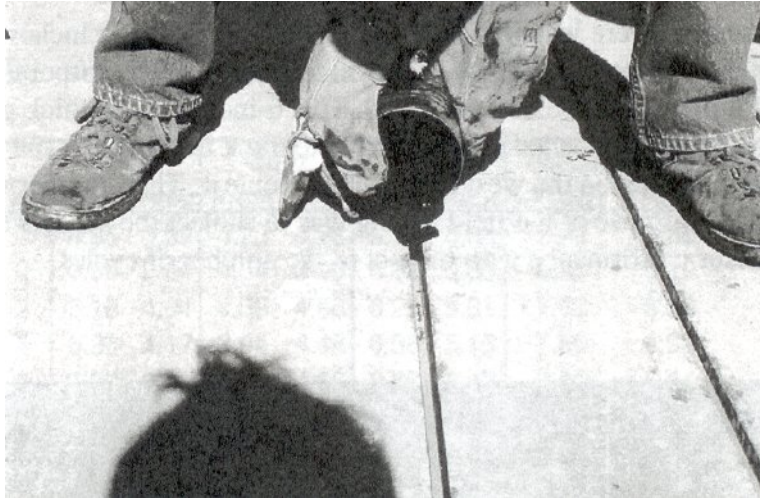
Figure 5.41. Picture Showing Sensors Being Covered with Hot Roofing Asphalt (Cosentino & Grossman, 1997).

During the course of this study, a potential problem with the roofing asphalt was observed. Namely, the roofing asphalt was cut level with the road surface while it was still warm, and it could decrease in volume while it cooled resulting in a groove in the pavement and less pressure on the sensor. Therefore, since the 1997 study several other installation materials have been tested. Various materials have been used to make the sensor more or less sensitive to vehicle weights including Bondo®, 3M 5000 Loop Sealant, and 3M 5200 Quick Cure Polyurethane Sealant. The two 3M sealants have the property of expanding while curing. Therefore, it was necessary to return after the installation site after curing to level the material with the road surface.

For the 1997 study field installations of the fiber-optic microbend sensor were conducted at Florida Tech's Applied Research Laboratory, the access road to a ready-mix concrete plant, and the access road to an asphalt plant. A total of six sensors were installed, with three placed in flexible pavement and three placed in concrete pavement. All six sensors were 6-feet long. Figure 5.42 shows a photograph of the microbend sensor installation on the pavement surface.
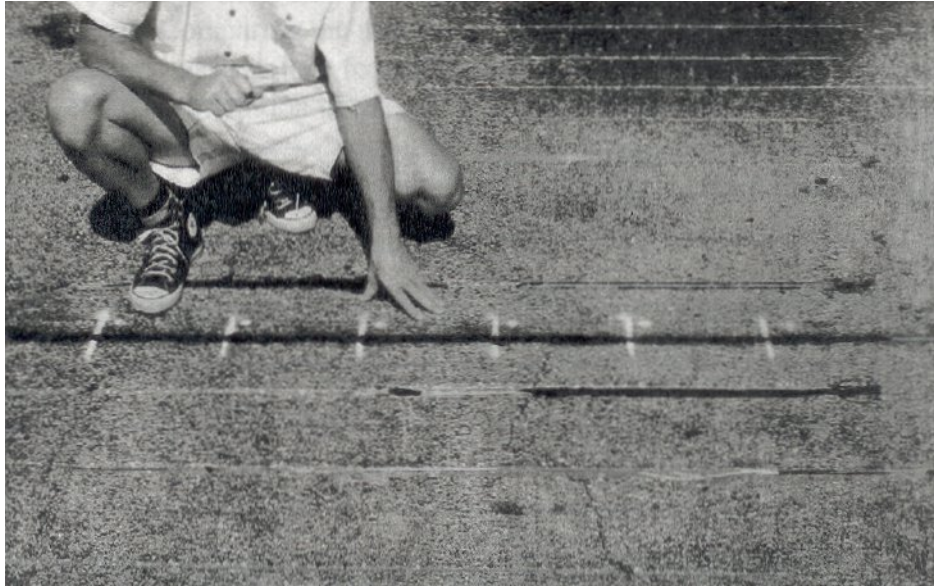
Figure 5.42. Photograph of the Pavement Surface after the Installation of Microbend Sensor at 1/4-inch Depth (Cosentino & Grossman, 1997).

A program was written in C++ to record the field waveforms from three of the sensors. The program takes the voltage signals from the opto-electronic interface and displays the signals as shown in Figure 5.43. The sensor thresholds were input for the minimum and maximum voltage changes. The minimum threshold ensured that no calculations were performed with the software until at least this change in voltage was recorded. The maximum threshold was used to ensure that the calculations performed at the peak voltage change were not being affected by a saturated signal.

These sensors were embedded in rigid pavement and the half-axle weights are shown for front and rear dual tandem axle assemblies. A negative sign in front of the weight signifies that the truck was entering the plant while a positive number signifies that the truck was leaving the plant. This was used for distinguishing between empty and loaded ready-mix trucks.

94

Threshold Setting for Sensor3

Low 10%   Hig 95%

Data Set 3

TEST	Sensor1	Sensor2	Sensor3
Front (Pounds)	-6812	-7404	-5923
Mid (Pounds)	-5331	-3850	-5035
Back (Pounds)	-3850	-4146	-5035
Weight (Pounds)	-15992	-15400	-15992
Speed (Mil/H)	-14	-14	-14

Weight(lb)	Sensor1	Sensor2	Sensor3
Basic	-15992	-15400	-15992
Current	-7	-10	-8
Intensity	-66	-114	-55

Start 1000   End 3000   High 95%   Low 5%
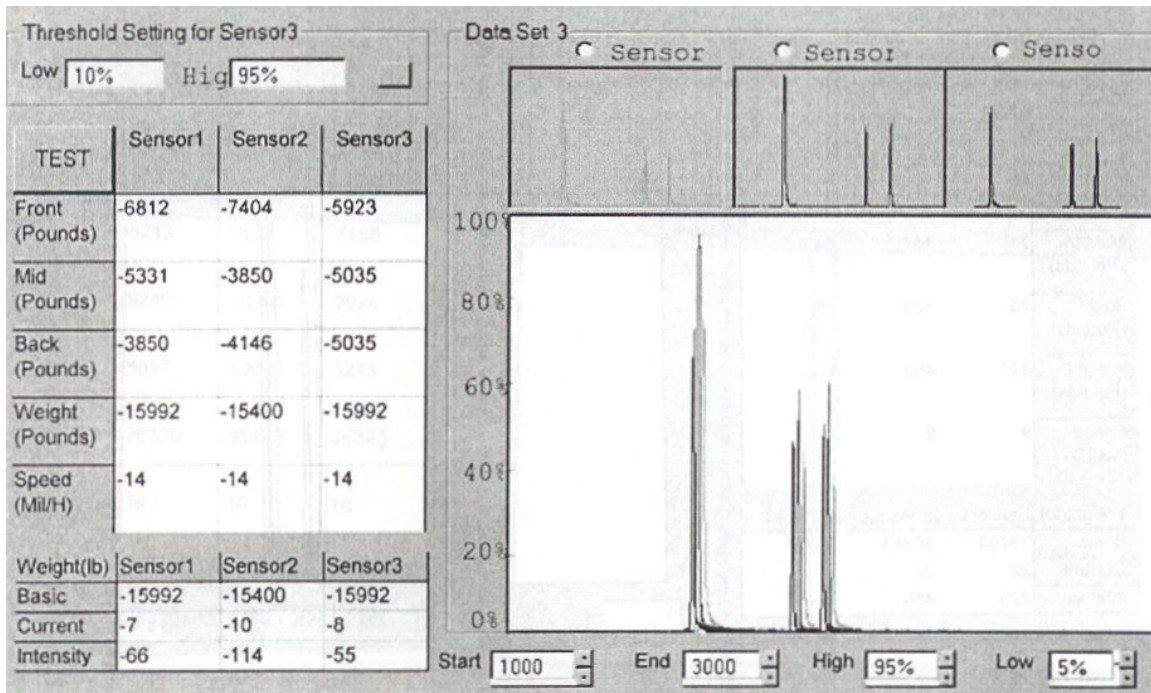
Figure 5.43. Data Acquisition Software Screen #1 Displaying Half-Axle Weights from Class 6 Ready-Mix Truck. Note: Truck Assumed Not Loaded (Cosentino & Grossman, 1997).

For the 1999 study, microbend fiber optic road top sensors were designed and tested for WIM system applications along with the embedded sensors previously tested. The road top sensor was made to be less sensitive since it took more direct pressure from the vehicle. The sensor was encased in a rubber tape for protection and could be placed in a heavily padded casing that secured it to the road surface. The road top sensor was designed to be part of a portable WIM system vs. the permanent installation application of the embedded sensors.

Three different methods were proposed for determining weights from the fiber optic signals. The three methods were referred to as the Basic Method, the Current Method and the Intensity Method (Cosentino & Grossman, 1997). For the 1997 study the method used by the Florida Tech researchers to determine weights from the fiber optic signal was the Basic Method, which required a field calibration that consisted of measuring tire pressures, widths, and using vehicle speed and tire/sensor contact time to calculate the

contact length. The Basic Method of determining a vehicle's weight used the following formula:

$$W_{ha} = A_t * P_t$$

Where: W_{ha} = weight on half-axle,

A_t = area of the contact patch, and

P_t = air pressure inside the tire.

This formula states that the tire's contact patch area multiplied by the tire's air pressure must be equal to the weight on the tire (Shuhy, 1999). The contact patch area was determined by breaking it down into the width and the length. The length of the tire's contact patch was measurable from the width of the pulse produced by the loss of light in the sensor when a vehicle passed over it. The width of the tire was not measured with this configuration and thus was estimated. For more details regarding the estimation of the contact patch area, please refer to Shuhy, 1999. The air pressure was also estimated based on the manufacturer's recommendations for the type of vehicle.

For the 1999 study Florida Tech researchers used the Basic Method as well as a method referred to as the Area Method for determining a vehicle's weight. The Area Method used the area of the pulse created by the vehicle that passed over a sensor and a conversion factor to calculate a vehicle's weight. The area of the pulse was calculated by trapezoidal approximation of the voltage drop values for all the samples. This method was based on the premise that heavier vehicles produced a larger loss due to larger microbends and longer contact lengths (Shuhy, 1999). The Area Method did not involve the estimation of any tire specifications or the air pressure in the tire, which could lead to more accurate results for a wider range of vehicles. However, a drawback of this method was that it had to be calibrated for the installed sensor pair with which it was used. In addition, this method depended heavily on the consistency of sensitivity along the length of the sensor.

For the 1999 study Florida Tech researchers conducted several tests with both road top and embedded sensors and with different types of test vehicles at speeds ranging from about 10 mph to about 40 mph. The vehicle weights were determined using both the

Basic Method and Area Method and were compared to static vehicle weights measured on a public scale.

Summary

The results from the Florida Tech 1997 study showed that prediction of vehicle weights by the Basic Method using embedded microbend fiber optic sensors was within 20% of the static half-axle loads.

The results from the 1999 Florida Tech study showed that prediction of vehicle weights by the Basic Method using *road top* microbend fiber optic sensors had errors as follows:

- From –11% to 7%, with an average of –1% for the front half-axle weight;
- From 8% to 36%, with an average of 22% for the rear half-axle weight; and
- From –1% to 18%, with an average of 8% for the combined weight.

For *embedded* sensors using the Basic Method for prediction of vehicle weights the errors were as follows:

- From 2% to 12%, with an average of 6% for the front half-axle weight;
- From 16% to 33%, with an average of 27% for the rear half-axle weight; and
- From 8% to 18%, with an average of 14% for the combined weight.

The results from the 1999 Florida Tech study showed that prediction of vehicle weights by the Area Method using *road top* microbend fiber optic sensors had errors from –43% to 37% for the combined front and rear half-axle weight. For *embedded* sensors using the Area Method for prediction of vehicle weights the results had errors from –22% to 27% for the combined front and rear half-axle weight. The researchers found indications that the large errors observed when using the Area Method may have been related to the vehicle velocity and was likely related to a low frequency bounce in the vehicle's tires (Shuhy, 1999).

Status-to-Date

In the interim between the end of the FDOT funded Florida Tech study and the present, Optical Sensors and Switches Inc. (OSS), a Florida company, has commercialized the

sensor technology and developed classification and WIM electronics to use with their portable and permanent fiber optic sensors. Researchers at Florida Tech under the direction of Dr. Barry Grossman, completed an initial study during 2002-2003 to determine the status of this equipment and to measure its accuracy. The researchers used portable fiber optic sensors (PSW-2) and a WIM system under development by OSS to perform the testing. Florida Tech supplied the research personnel and OSS supplied the sensors and equipment for the study.

The study was performed in two parts. The first part tested the accuracy of the system for speed and classification and the second part was the WIM accuracy. The sensors used in the study were the OSS PSW-2 portable two lane fiber optic WIM sensors. The WIM system was the OSS WIM 3000, which is currently under development and testing. Testing was performed at various locations in the Melbourne, Florida area.

As mentioned previously, the second phase of the study involved weight measurement. In this case the weight of a test vehicle, an SUV, was varied using concrete blocks to load it. The actual weights were determined using a public truck scale. The vehicle load was varied and the measured weight recorded.

The 2σ deviation between the measured and actual weight was 8.6%. A comparison of the WIM results from the OSS fiber optic system and conventional systems are shown in Figure 5.44.
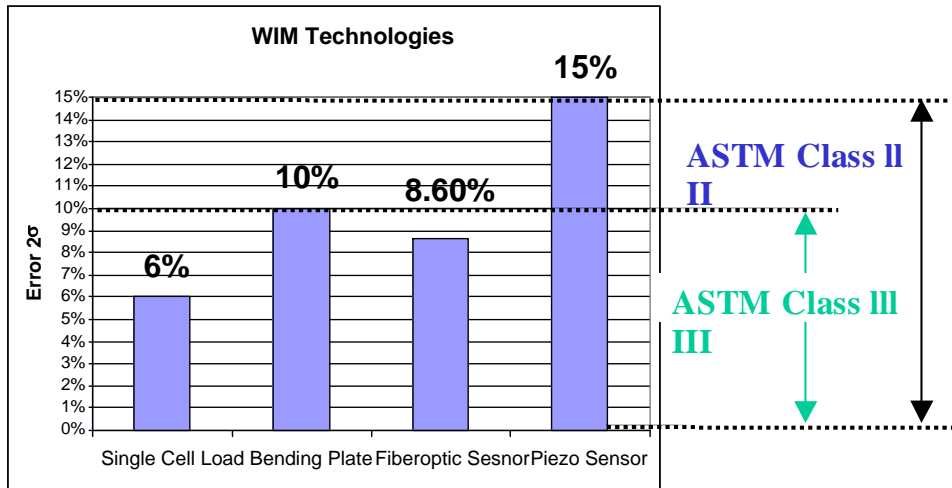
Figure 5.44. Comparison of 2σ deviation (error) from actual weight of results of the OSS fiber optic WIM system and conventional systems (Grossman, 2003).

These results, although preliminary, indicate that the OSS fiber optic sensor and processing technology have improved significantly since the last Florida Tech tests. The fiber optic system may prove to have accuracies comparable to or better than a bending plate. Further testing with calibrated trucks still needs to be performed. Since the cost of the fiber optic system is comparable to a piezo-based system, the fiber optics may provide a cost effective alternative having enhanced accuracy. Due to time constraints, the OSS permanent embedded sensors could not be tested. Since they use the same basic sensor construction, they are likely to have similar performance. Further testing needs to be performed to confirm the initial findings and tests should be made using an actual production model of the WIM unit when it becomes available.

Laboratoire Central des Ponts et Chaussees (LCPC)

Project Background

A WIM sensor based on the use of optical fiber was developed during the Weighing in motion of Axles and Vehicles for Europe (WAVE) project in a partnership with the Laboratoire Central des Ponts et Chaussees (LCPC), under the authority of the French Ministry of Transport, the Alcatel Group and the AML company as a sub-contractor of Alcatel. The sensor used light birefringence in optical fibers that undergo a mechanical

99

strain. Some transparent materials like fused silica have the property to become birefringent under external actions. Therefore, two waves can propagate independently with distinct polarizations. Furthermore, if one polarization direction is selected at the end of the fiber by the aid of a linear polarizer, the transmitting light intensity varies as the birefringence moves, resulting in a fading phenomenon. This is referred to as polarimetric fringes in optical systems because of the successive minima and maxima in light intensity (LCPC, 2000).

In the early 1990's LCPC and Alcatel assessed the feasibility of using a single mode optical fiber as the sensitive element for sensing and the interferometric principle. During the WAVE project a first generation prototype sensor was installed on the RN 10 close to Paris in 1995 and was used extensively to base further developments. A second fiber optic WIM strip sensor prototype system was developed that included two parallel 12.1 ft (3.7 m) optical sensors and an additional 4.9 ft (1.5 m) sensor was designed and a suitable optoelectronic system was developed. This prototype system was tested on a parking lot with a van and a few cars. The objective of this project was to achieve the design of an operational WIM station.

Equipment Used

This sensor used the photo-elastic effect in glass fiber: a vertical compressive force applied to glass changes the light velocity in an optical guide, because the refractive index moves. This induces the separation of two propagating modes: the fast mode (vertical) and the slower one (horizontal). The incident light, Ei, is a plane-polarized beam at an angle of 45° to the horizontal plane (see Figure 5.45).
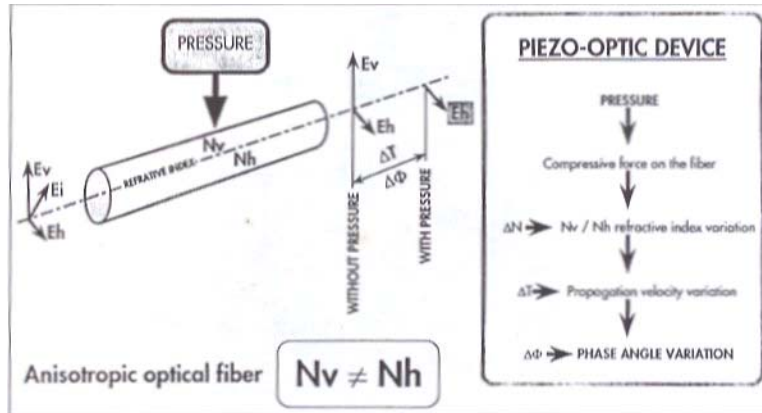
Figure 5.45. Optical beam propagation (Caussignac & Rougier, 1999).

At the fiber end, after light propagating along length L, a delay is caused between the two modes and creates a phase shift between the two transmitted waves. An optical receiver connected to the sensor end observes the sum of the two modes, and a photo-diode transducer converts light power into an electric current. After traveling through the sensitive optical fiber, the light is returned to the receiver by a non-sensitive fiber placed inside the same bar. This way, the sensor needs only one connecting cable to operate.

In order to measure a force this sensor was constructed by placing a single mode optical fiber between two metal ribbons joined together along the two edges. The effect of bending the ribbons exerts a compressive force on the fiber (see Figure 5.46).
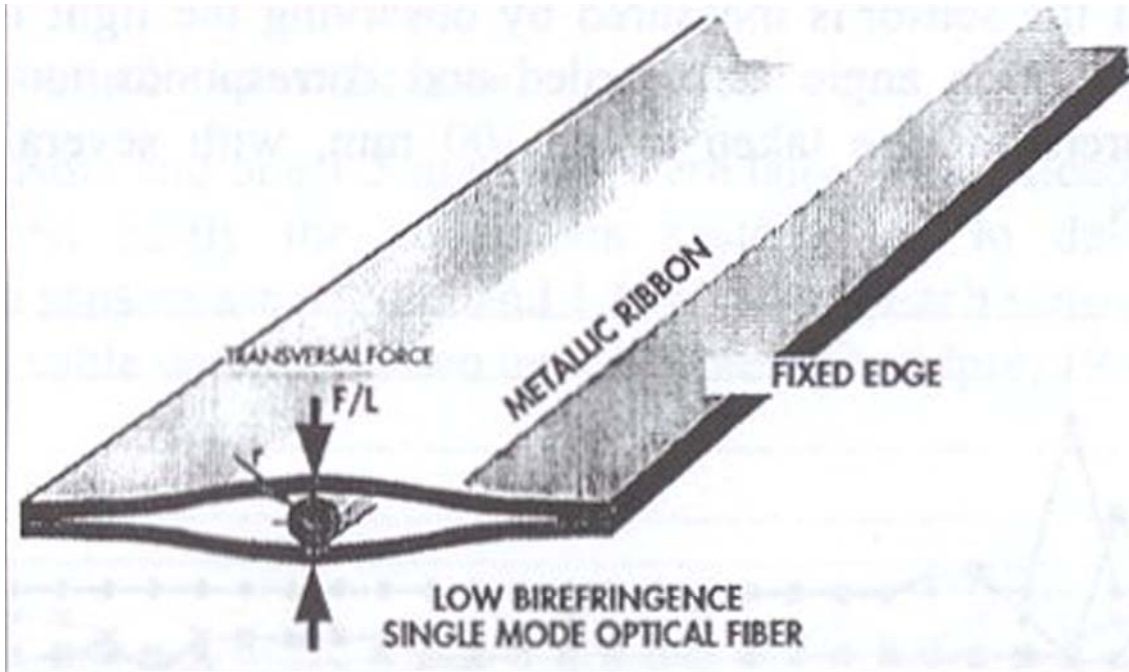
Figure 5.46. Sensitive element of the sensor (Caussignac & Rougier, 1999).

With these conditions the vertical axis of the fiber receives the force to be measured, while the horizontal axis does not. This causes a constant light velocity on the horizontal axis and a variable light speed on the vertical axis. A coherent, plane polarized light beam was introduced into the fiber at an angle of 45° to the vertical axis. The light beam travels along the fiber at two different speeds, as shown above, so at the end of the fiber, there is a delay between the two modes, and a rotation of the light polarization received is observed. To detect phase variations, an analyzer was placed in front of the receiver in order to select one polarizing direction. Under these conditions, minimum and maximum light intensity alternate as a function of the load applied to the sensor.

The period corresponds to a 2π phase-shift. The number of fringes, the frequency of fringes, the duration of the wheel print, and the speed of the vehicle characterize a typical vehicle signature, as illustrated in Figure 5.47.

102
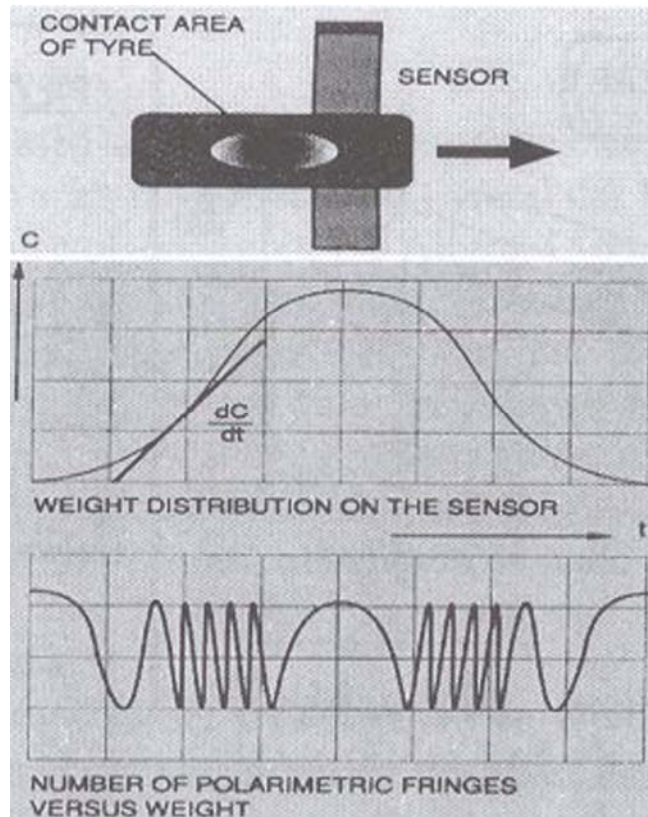
Figure 5.47. Example of weight signature (Caussignac & Rougier, 1999).

When a vehicle passes over the sensor the signature is interpreted as follows:

- The first fringe shift corresponds to an increasing load as the tire rolls on to the sensor;

- The constant signal indicates quasi-static pressure while the tire is centered on the sensor;

- The last fringe shift corresponds to a decreasing load as the tire rolls off the sensor; and

- The total vehicle dynamic load is calculated as the sum of the individual wheel weights.

Opto-electronic head

The Opto-electronic head included the following:

- One 1330 nm laser with its electronic driver,

- Two photodiodes with two electronic amplifiers, and

- One optical coupler, two light polarization filters.

The 4 electronic signals given by the opto-electronic head were connected to a data acquisition module, which digitized these signals at a 50 kHz/1MHz rate, with a 12 bit resolution. Data was then stored in the hard disk of a portable computer which recorded measurements, calculated weights, speeds, and displayed signals, and results.

Software Functions

The software read two series of measurements, sine and cosine. For each sensor, it found the beginning and the end of each wheel. It computed the phase of the optical signal coming from the sensor.

Using data from two sensors, the software calculated the wheel speed, the force applied by the wheel to the ground, the distance between two wheels, and the vehicle weight. Then it entered the results in an output file, and displayed them.

Experiment Details

In order to test easily the acquisition system and to develop the processing software, two 12.1 ft (3.7 m) optical sensors and one 4.9 ft (1.5 m) sensor were laid on the Alcatel plant site in Saintes, France in November 1998. The two strip sensors were parallel and 4.9 ft (1.5 m) apart. Each sensor was linked to its optoelectronic head with a cable containing two optical fibers. Figure 5.48 shows two periodic graphs given by two optical receivers linked to the sensor outputs.

The bar curve shows the instantaneous force received by the sensor, it was calculated by the portable computer, using the two previous graphs stored in the hard disk. The weight calculation was carried out 70 times for a car wheel, and up to 200 times for a truck wheel. These numbers are large enough to achieve the accurate shape of the impact force curve.
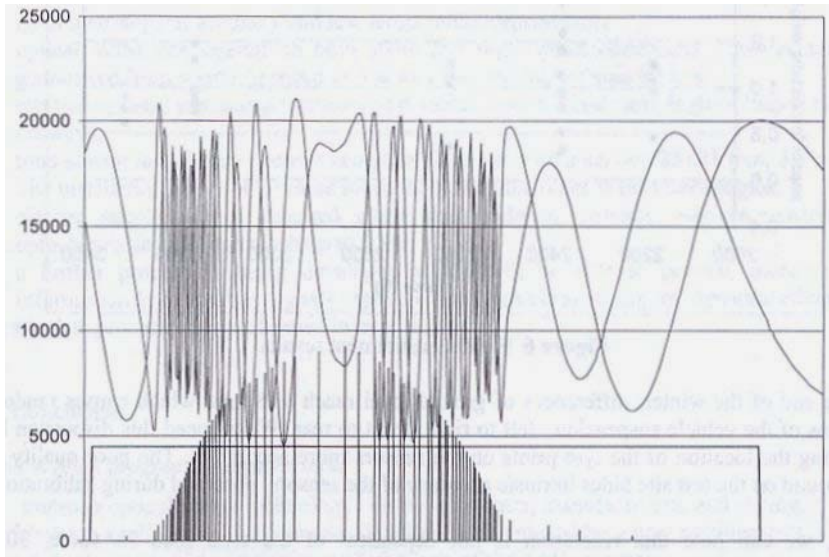
Figure 5.48. Load reconstruction for a van wheel (Caussignac & Rougier, 1999).

Measurements shown in Figure 5.49 were taken at the Saintes site when cars were traveling at speeds of 6.2 to 9.3 mi/hr (10 to 15 km/hr). The Y-axis indicates the ratio measured impact force/static weight. The X-axis indicates the static weight on the wheel. The accuracy of static weights is ± 22.5 lbf (± 100 N). During the calibration procedure on site, variability of results was observed due to deterioration of ground surfaces and extrinsic sensitivity of the sensor.
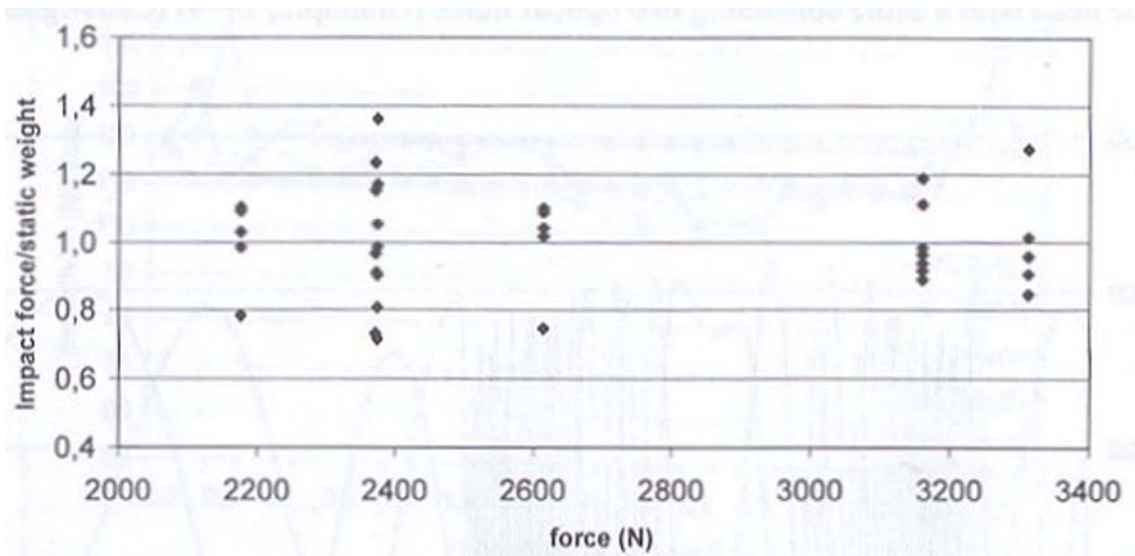
Figure 5.49. Field measurement results (Caussignac & Rougier, 1999).

At the end of the winter, differences of ground level reached ± 3.8 inches (± 15 mm), which caused random motions of the vehicle suspension. Checking the location of tire prints on the sensors more accurately reduced the variability. The researchers believed that the poor quality of the ground on the test site hid the intrinsic accuracy of the sensors, observed during calibration.

Summary

With test duration of two years and heavy traffic loads, this system has shown strong results in accuracy and low temperature dependence. The distance between sensors and optoelectronic head can reach up to 1.24 mi (2 km). Using the wealth of recorded signals research of other parameters such as tire pressure estimation, vehicle acceleration during measurement, and warning against lose vehicle suspension systems can be studied and applied in the next generation system.

Status to-date

During the WAVE project the whole fiber optic WIM system was completed and validated. However, only a small-scale test was carried out which was not under a real traffic flow. The signal processing methods for the fiber optic WIM system that will allow additional information such as tire pressure and width, vehicle accelerations and dynamics, suspension characteristics to be determined are still being developed. However, in order to speed up the completion of the development phase of this system and move on into the commercialization phase, the researchers must determine that a demand for this technology exists.

Virginia Polytechnic Institute and State University

1990 Strategic Highway Research Program (SHRP) Project

Project Background

The Strategic Highway Research Program (SHRP) supported this research project. The SHRP is a unit of the National Research Council that was authorized by section 128 of

the Surface Transportation and Uniform Relocation Assistance Act of 1987 (Safaai-Jazi, et al., 1990).

The research project studied the feasibility of an extrinsic fiber optic WIM sensor that consisted of a pneumatic tube filled with an incompressible fluid and embedded in a rubber pad, a diaphragm designed to convert pressure into displacement, and an optical displacement sensor. A prototype of the proposed sensor was designed, manufactured, and tested in the laboratory for different load-frequency combinations using a Materials Test Systems (MTS) machine. A micropositioner was used to simulate the deflection of the diaphragm. Statistical analyses of the data were performed to assess the sensor response to varying load frequencies. A piezoelectric cable was also tested under varying load frequencies for the purpose of comparison with the proposed fiber optic WIM sensor.

Equipment Used

The fiber optic WIM sensor that was proposed in this research project consisted of two main parts, the optoelectronics part and the mechanical part. The optoelectronics part included a light source, photodetector, Graded Index (GRIN) lens, optical fiber, and associated electronic circuits. As described previously, the essential elements of the fiber optic WIM sensor proposed for this research were a pneumatic tube filled with an incompressible fluid, a diaphragm to convert pressure into displacement and an optical displacement sensor. Figure 5.50 shows a block diagram of the system.
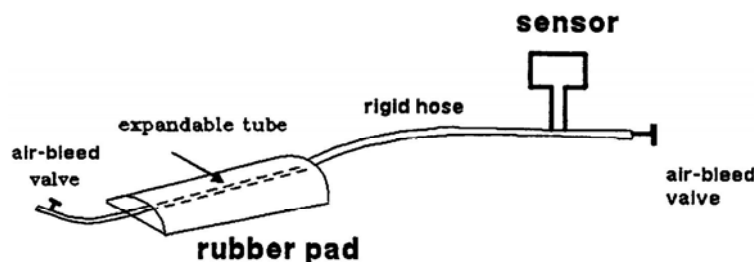
Figure 5.50. Block diagram of the fiber optic WIM sensor assembly (Safaai-Jazi, et al., 1990).

107

Optoelectronics

The principles of operation of the proposed sensor for this research were based on an extrinsic sensing mechanism where the pressure generated by the weight of a vehicle upon passing over a fluid-filled pneumatic tube was converted to displacement by means of a diaphragm. The deflection of the diaphragm modulated the light. The sensing technique used in the proposed sensor was based on the transmission of light where the detector measured the power of the transmitted light. Figure 5.51 shows a schematic diagram of a transmission-based pressure sensor. GRIN lenses as shown in Figure 5.51 were utilized to collimate the light beam, which helps the system respond more linearly.
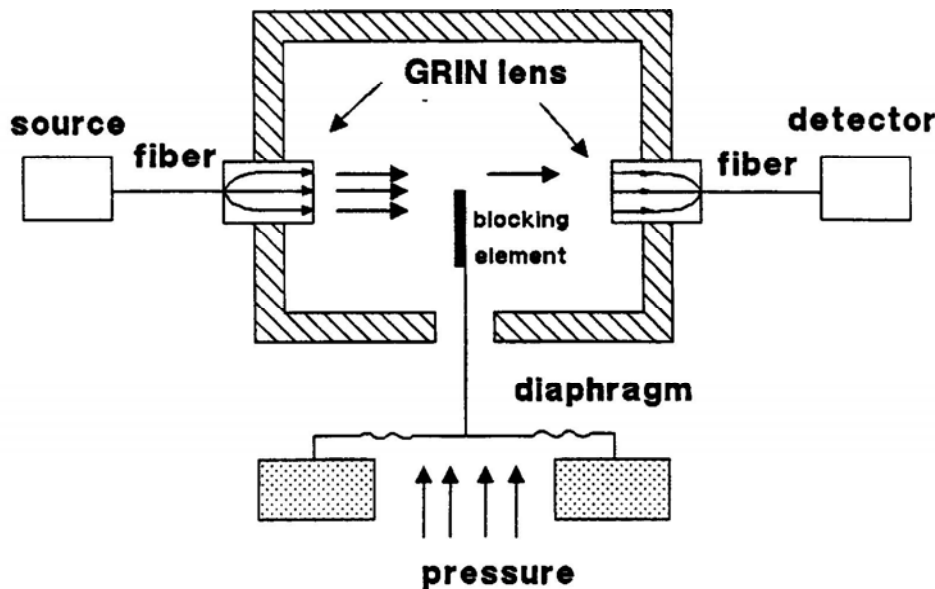
Figure 5.51. Schematic diagram of a transmission-based pressure sensor (Safaai-Jazi, et al., 1990).

A light emitting diode (LED) was used as the light source for this project. The LED used in the developed sensor emitted light at wavelength $\lambda = 850$ nm. Also, for the LED used in the pressure sensor, a current of 100 mA was recommended.

Another component of the optoelectronics portion of the sensor was the light detector. The light detector consisted of a semiconductor photodiode that converted the light energy into an electrical signal and used a PIN diode as a light detection element. The

PIN diode was reversed biased in order to create a strong electric field to separate the released electrons and holes in the intrinsic region of the PIN diode. The detector output signal was amplified using a two-stage amplifier to achieve a total voltage gain of 1000.

Mechanical

The tube was an expandable hose with an inner diameter of 0.25 inches. The tube was housed in a rubber pad, which served as a mechanical support. The tube was connected at both ends to flexible, but non-expandable, stainless steel hoses and was filled with an incompressible fluid.

A stainless steel diaphragm was placed at one end of the pneumatic tube between the optical displacement sensor and the flexible steel hose. The applied pressure (load) caused the diaphragm to deflect. One side of the diaphragm was attached to a light-blocking element, which served as a spatial light modulator. The pressure changes experienced by the pneumatic tube were ultimately converted into light intensity variations. The applied pressure caused the diaphragm to deflect. One side of the diaphragm was attached to a light-blocking element as that shown in Figure 5.51. Therefore, the diaphragm converted the pressure into displacement.

As previously mentioned, the rubber pad was used primarily for mechanical support and to transmit the applied pressure to the encased expandable tube. The material composition of the pad was resin, a softening agent and curing agent. The hardness of the rubber pad played a significant role in the operation of the sensor system, since the harder the pad, the greater the amount of loads that can be applied to it. Furthermore, the mechanical properties of the pad also influence the response of the system both quantitatively and qualitatively. However, the influence of the pad on the output voltage of the optical sensor can be accommodated through calibration.

Two steel hoses, one six feet long and another one foot long, were used. The function of the six-foot steel hose was to transmit the pressure from the load region to the diaphragm with minimal loss. The one-foot steel hose was used to facilitate the removal of trapped

109

air bubbles. Two air-bleed valves, one at each end of the sensor assembly, were used to remove trapped air in the fluid-filled part of the system.

Experiment Details

To evaluate the response of the displacement sensor performance under varying load frequencies, a series of laboratory experiments were performed using an MTS machine to simulate different vehicle weights and speeds. Statistical analyses of the data were performed to assess the dependence and the linearity of the sensor response.

Prior to the laboratory tests, the sensor assembly was packaged and filled with water as the incompressible fluid. A different type of fluid would need to be used for field type applications, since water is sensitive to extreme temperature variations. The block diagram is shown in Figure 5.50. Two metallic support plates each with an area of 72 in^2 were constructed to facilitate the application of the load by the MTS machine. Also, two wooden columns were made for supporting the steel hoses in order to dampen out undesired vibrations.

During the laboratory experiments the rubber pad was mounted onto the stationary upper plate of the MTS machine. Load was applied from below through the metallic support plates. The optical displacement sensor was powered with a power supply providing an output voltage of 30 volts. The MTS load signal and the output signal of the displacement sensor were both monitored using a dual channel oscilloscope. Figure 5.52 shows the block diagram of the laboratory experimental setup.
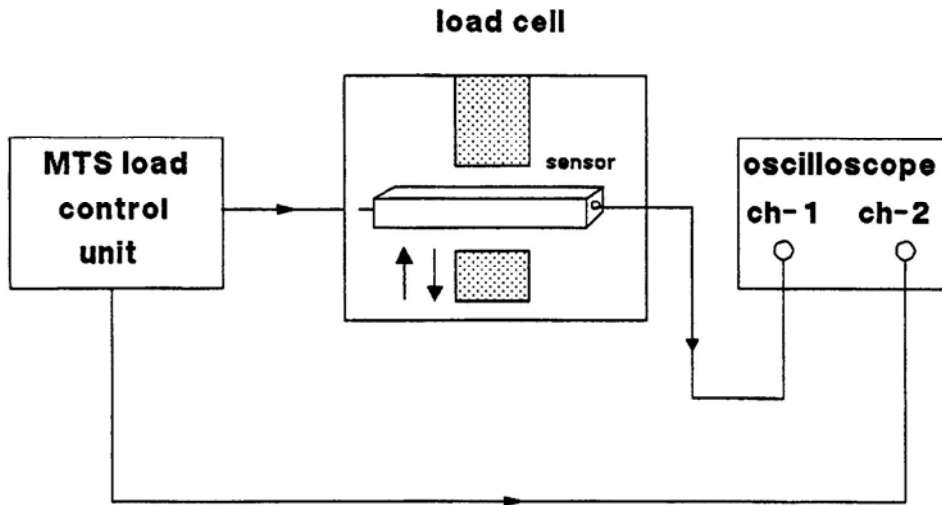
Figure 5.52. Block diagram of the experimental set up for the pressure sensor (Safaai-Jazi, et al., 1990).

A 20-Kip (20,000 lbs) MTS machine was used and ten levels of load were applied. Each load was applied at different frequencies of 0.25, 0.5, 1, 2, 5, and 10 Hz. The applied loads were 1 Kip (1,000 lbs) to 5.5 Kips (5,500 lbs) in 0.5 Kip (500 lbs) increments. For example, for a load at 1 Hz frequency (1-second period), each cycle is 1 second long, and the sensor is loaded for 0.5 seconds in each cycle. The input and output signals were monitored simultaneously and photographed following each load application. The output signals were obtained for fifty-eight load-frequency combinations summarized in Table 5.6. For 5 Kips and 5.5 Kips loads at 10 Hz, the pneumatic pad appeared to reach its maximum tolerance. Therefore, to avoid permanent deformation of the pad, tests at these load-frequency combinations were not performed over a long enough duration and consequently consistent readings for the output voltage were not obtained.

Similar tests were run on a piezoelectric sensor for comparison with the proposed WIM sensor. The experimental set up was similar to that used for the optical sensor shown in Figure 5.52. The piezoelectric sensor used consisted of a piezoelectric cable embedded in epoxied resin and housed in an aluminum frame of 20x20 mm cross section and was 3.5 meters long. The sensor was mounted onto the stationary upper plate of the MTS machine. The load was applied from below through a specially prepared metallic support plate of about 10 in^2.

111

Table 5.6. Experimental data for the proposed WIM sensor (Safaai-Jazi, et al., 1990).

Average Output Voltage (V)							
Load (Kips)	0.25 Hz	0.5 Hz	1.0 Hz	2.0 Hz	5.0 Hz	10.0 Hz	Coeff. of Variation
1.0	0.6	0.6	0.6	0.6	0.6	0.6	0
1.5	1.0	1.0	1.0	1.0	1.0	1.0	0
2.0	1.5	1.5	1.5	1.45	1.5	1.5	1.4%
2.5	2.0	2.0	1.8	1.8	1.8	1.8	5.5%
3.0	2.5	2.5	2.4	2.4	2.4	2.4	2.1%
3.5	3.0	3.0	2.9	2.9	2.9	2.9	1.8%
4.0	3.5	3.5	3.5	3.5	3.5	3.5	0
4.5	4.1	4.0	4.0	4.0	4.0	4.0	1.0%
5.0	5.0	5.0	5.0	5.0	5.0	-	0
5.5	6.0	6.0	5.8	5.8	5.8	-	1.9%

A 20-Kip (20,000 lbs) MTS machine was used and five levels of load were applied of one to five Kips in 1-Kip increments (1,000 to 5,000 lbs in 1,000 lbs increments). Each load was applied at different frequencies of 0.25, 0.5, 1, 2, 5, and 10 Hz. As with the optical sensor experiments, the input and output signals were monitored simultaneously and photographed after each load application.

Traffic Conditions Simulated

The loading conditions described previously represented a variety of combinations of speeds, axle spacings, and vehicle headways. For example, at 70 mph square waves like the ones used in this experiment, of 0.25, 0.5, 1, 2, 5, and 10 Hz approximately correspond to spacings of 200 ft, 100 ft, 50 ft, 25 ft, 10 ft, and 5 ft, respectively. The larger spacings that corresponded to the lower frequencies of 0.25, 0.5, and 1 Hz

generally represent vehicle headways, rather than axle spacing for most highway speeds. The higher frequencies of 2, 5, and 10 Hz were representative of typical truck axle spacings. As an example, a typical 3S2 semi-trailer truck may have axle spacings of 10 ft, 5 ft, 25 ft, and 5 ft between axles 1-2, 2-3, 3-4, and 4-5 from front to rear, respectively. At 70 mph, these axle spacings correspond to frequencies of 2, 5, and 10 Hz, respectively (Safaai-Jazi, et al., 1990).

Summary

The optical sensor proposed in the SHRP Virginia Tech study demonstrated that its response showed a high degree of linearity, thereby a high accuracy in correlating the sensor response to the actual vehicle weight. Figure 5.53 compares variations of the half-cycle average output voltage versus load at six different frequencies of application. It is evident from this figure that for loads higher than 5 Kips (5,000 lbs) the sensor response begins to exhibit nonlinearity, and, at a sufficiently high load, the expandable tube would buckle causing saturation of the output voltage. It was clear from the load study that the behavior of the sensor response was largely influenced by the performance of the rubber pad and the expandable tube, and to a less extent by the performance of the diaphragm. The rubber pad responds linearly only in a certain pressure range. Therefore, it is very important to design the pad such that it behaves linearly in response to the loads in the range of interest.

The best-fit regression line through the data in Figure 5.53 yielded the equation $y=-0.475+0.984x$, where y is the output signal in volts and x is the applied load in Kips. A coefficient of determination (R^2) equal to 99.5% was calculated for this best-fit line, which is an indication of high linearity of the sensor response.
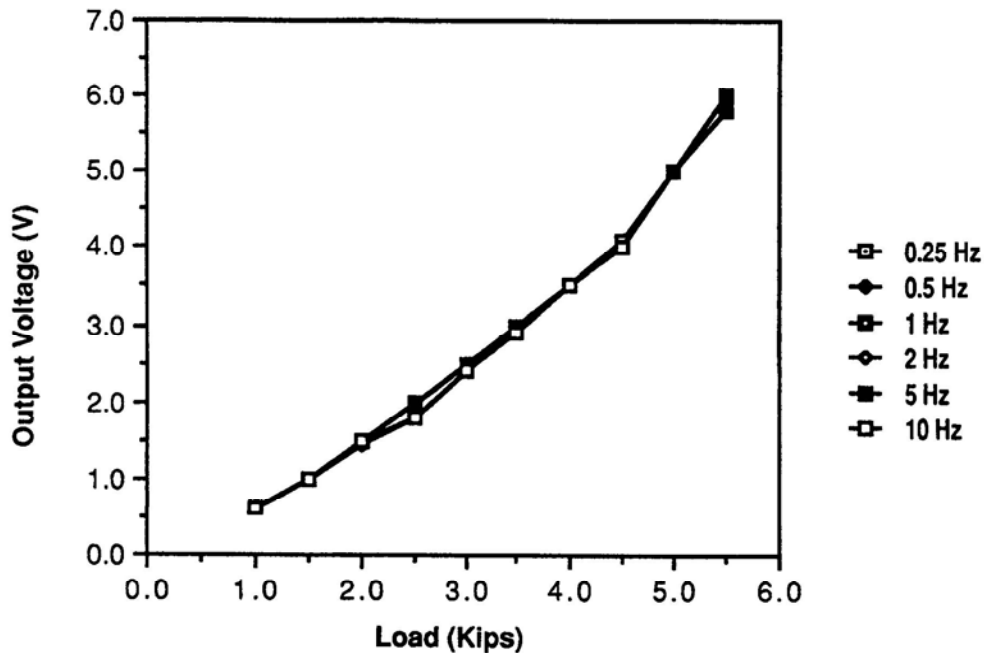
Figure 5.53. Variations of the sensor output voltage with load at different frequencies (Safaai-Jazi, et al., 1990).

An examination of the output waveforms of the piezoelectric experiment indicated that the initial application of the load induced a voltage which rose rapidly from zero to a maximum value, then decreased exponentially. Once the load was removed, the output voltage underwent another change reaching a negative peak, which also decreased exponentially with time. This type of behavior indicated that the response of the piezoelectric cable depended upon the time derivative of the applied load.

The results of the experiment carried out on the piezoelectric sensor yielded the equation $y=-5.08+12.6x$, where y is the output signal (mV) and x is the applied load (Kips) as the best-fit line. The coefficient of determination (R^2) for this best-fit line was 82.9%, which indicated a fairly linear relation between the applied load and the output signal.

When comparing the piezoelectric sensor to the optical sensor, the optical sensor reported a constant voltage reading as long as the MTS loading cell was in contact with the sensor. The piezoelectric sensor output signal, however, would peak to a maximum value proportional to the magnitude of the applied load but would drop back to zero regardless or if, or when, the load was removed. In processing the WIM sensor output signals, the

114

area underneath the output signal wave is a desirable piece of information in determining the axle weights. Therefore the fiber optic sensor wave output signal offers a significant advantage over the exponentially decaying output waves of the piezoelectric sensor.

Another advantage of the fiber optic WIM sensor over the piezoelectric sensor demonstrated in this study was in output signal variation with load frequency. The experimental data indicated that signal outputs varied considerably less with load frequency in the case of the fiber optic sensor. The waveforms generated clearly established that the response of the fiber optic sensor is less frequency dependent. This in turn indicated that the speed and axle spacing of vehicles could be a significant source of error in the piezoelectric WIM sensor, but not in the fiber optic case (Safaai-Jazi, et al., 1990).

Status to-date

The laboratory results described in this study yielded promising results for the proposed fiber optic WIM sensor. However, the researchers agreed that the sensor was not yet ready for field implementation. A number of issues needed to be addressed prior to the implementation phase. The sensor performance characteristics could be optimized through revisions in the design of the various sensor components. More importantly, the sensor performance needs to be monitored in the field and under actual traffic conditions. Other aspects such as calibration, signal processing, power utilization, and integration into existing vehicle monitoring and classification systems must also be undertaken.

As of the time of the present state-of-the-art study for fiber optic sensors in WIM system applications, no further literature was found documenting continuing studies of the proposed extrinsic fiber optic sensor in WIM system applications. In addition, this type of sensor was not found to be available commercially.

Project on Using Fiber Optic Sensors for Civil Infrastructure Monitoring

Project Background

Another study carried out by researchers from the Fiber & Electro Optics Research Center (FEORC) and the Bradley Department of Electrical Engineering at Virginia Polytechnic Institute (VPI) and State University was to investigate the use of fiber optic sensors in the acquisition of traffic data from the highway. Emerging applications of fiber optic sensors for vehicle flow, vehicle speed, and weigh-in-motion measurements were briefly discussed in this paper. At the time the paper by researchers at VPI was written fiber optic sensors were being developed for counting vehicles, measuring vehicle velocity, performing weigh-in-motion, and determining highway pavement conditions.

Equipment Used

Several cost-effective fiber optic sensor configurations were developed at FEORC for vehicle detection, vehicle velocity measurement, and weigh-in-motion systems. The sensors included Fabry-Perot type interferometric, modal domain and microbend sensitive sensors.

Experiment Details

To demonstrate the use of the fiber sensors for real life measurements, sensors, fixed inside three foot long tubing, were fabricated and embedded in a parking lot on campus at Virginia Tech. The sensors were placed at the entrance and exits of the parking lot, and asphalt was poured over them. As vehicles passed over the regions where the sensors were embedded, the output response showed intensity fluctuations as stress was transferred from the road surface to the embedded sensor (de Vries, et al, 1994).

Summary

No data on the weigh-in-motion system application was given in this paper. The paper stated that fiber sensors were being developed for weigh in motion measurements in cooperation with the Federal Highway Administration. The paper stated that such

sensors had been installed on Interstate 460 to study sensor reliability under various environmental conditions.

Status to-Date

After several telephone conversations and electronic mail communications with Dr. Richard Claus and Dr. Igor Kostic at VPI, the conclusion was that there were no current studies being performed using fiber optic sensors in WIM system applications. Furthermore, there were no published reports available at VPI on the WIM system study mentioned previously.

United Kingdom Highway Agency's Project

Project Background

A study carried out by researchers in the United Kingdom evaluated fiber optic interferometric-based sensors as a viable alternative to conventional WIM technology. The researchers involved in the study were D. J. Hill and P. J. Nash from QinetiQ Ltd. (formerly the Defense Evaluation & Research Agency), and N. Sanders from the UK's Highways Agency. During the course of the study, a multiplexed interferometric fiber optic sensor was developed to detect traffic and collect WIM data. An interrogation system was developed and the installation of the sensor on a roadway was achieved. The ultimate goal of the study was to establish an all optical sensing system that, as well as being capable of monitoring traffic flow, would also be able to perform high speed WIM and would be able to monitor the integrity of the road and thereby contributing to road maintenance programs (Hill et al., 2002).

Currently, there are over 6,500 miles of trunk road (major highway), of which approximately only 20% has detection equipment installed. This detection equipment is based predominantly on inductive loops buried beneath the road surface. Inductive loop hardware is relatively low in cost. However, the costs associated with installation, operation and maintenance, as well as their associated infrastructure cost, restricted

capabilities and unreliability, limit inductive loop systems' overall operational effectiveness (Hill et al., 2002).

Weigh-in-Motion devices are also installed at core census locations that gather data on vehicle weight, speed, axle configuration and vehicle classification. However, hardware costs of these systems can be substantial, as well as the installation and operation and maintenance costs (Hill et al., 2002).

As mentioned previously, the overall objective of this research project was to develop a fiber optic sensing technology that would be capable of monitoring traffic flow and also perform high-speed WIM. Some of the advantages of an all fiber optic sensing system include the following:

- Remote (>20km) interrogation of sensing points;

- Ability to multiplex many sensors on a single fiber (several hundred);

- Reduced costs due to the adoption of cheap components from the telecommunications industry;

- Passive operation requiring electrical power only at the interrogation point;

- Sensor immunity from electrical and magnetic interference; and

- Improved reliability due to simplicity/ruggedness of sensor design.

Equipment Used

As mentioned previously, the technology developed for this study was a multiplexed interferometric fiber optic sensor system to detect traffic and collect WIM data. Interferometric based systems using sensors comprised of a coil of fiber wound upon a compliant mandrel have been under development for the past two decades. However, past work has largely focused on the development of large-scale fiber optic hydrophone arrays for military applications (Hill et al., 2002). The basic operating principle of these types of sensors is shown in Figure 5.54.

118

Applied Pressure

$P = P_o \cos \omega_s t$

Light in

Fiber Coil

$\phi = \gamma \cos \omega_s t$

$i \propto (1 + \cos \phi)$
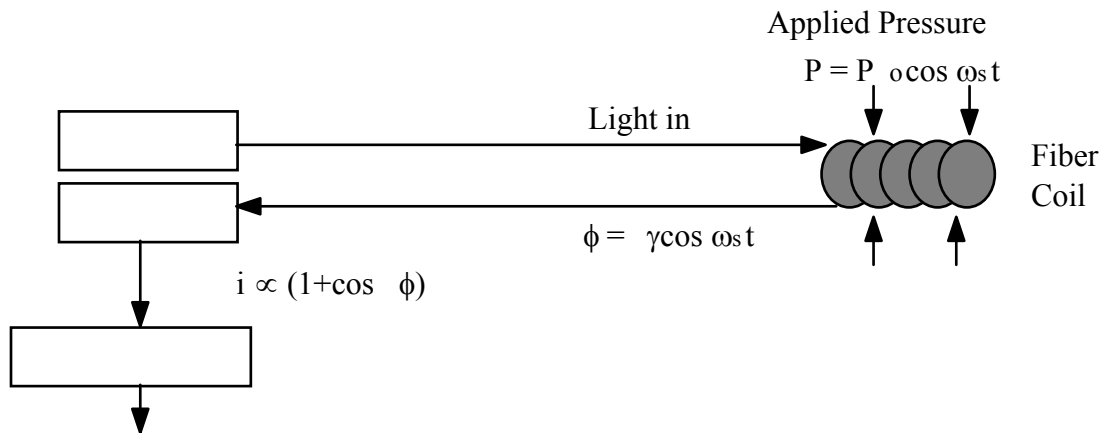
Figure 5.54. Operating principle of an interferometric sensor (Hill et al., 2002).

Injected light passes through a long coil of optical fiber. As pressure is applied to the coil both the physical length of the coil and the refractive index of the optical fiber undergo minute changes. These changes cause a phase change in the light that is passing through which is detected at a receiver. The detected phase change is measured using a phase demodulator, which in turn gives an output proportional to the original pressure applied to the sensor. For a traffic monitoring system, the strain induced in the sensor as a vehicle passes above it will cause a phase modulation (Hill et al., 2002).

Another major benefit of this type of sensor is in the ability to multiplex a large number of sensors together over very long distances as shown in Figure 5.55. By using a combination of Spatial, Time and Division Multiplexing (SDM/TDM/WDM), several hundred sensors can be multiplexed on a single optical fiber.

>20km
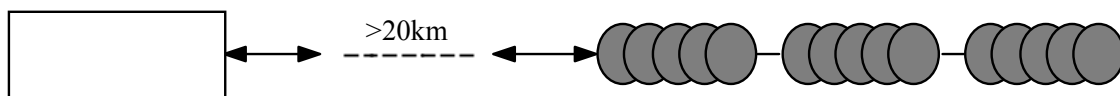
Figure 5.55. Interferometric sensor multiplexing (Hill et al., 2002).

For the application of traffic monitoring this has particular importance since it offers the potential to have over a thousand sensors interrogated from a single conveniently located interrogation node. This node could contain all the opto-electronics necessary and would

be the only point within the system requiring any form of electrical power and access to a communication network (Hill et al., 2002).

The prototype sensor design used in the tests for this study was based upon a long thin coil as shown in Figure 5.56. One of the advantages of this type of sensor is that being a long extended sensor it can sense traffic evenly across the entire width of each lane of the highway. In addition, the sensor sensitivity can be easily adjusted by using a different stiffness supporting structure and by altering the types of encapsulated material used in the sensor construction.
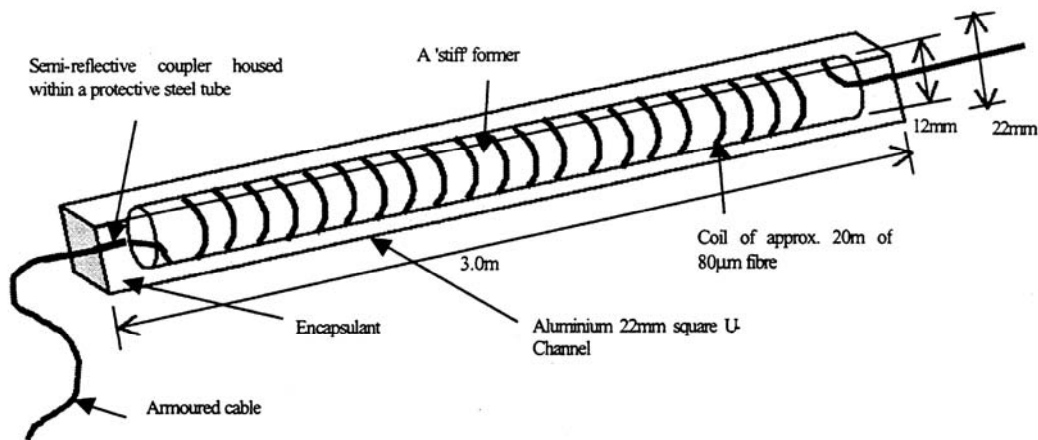
Figure 5.56. Prototype fiber optic interferometric sensor (Hill et al., 2002).

As part of the interferometric design it was necessary to include a semi-reflective element with each sensor. This was accomplished by using semi-reflective fiber couplers. Using these reflectors allowed the multiplexing of a larger number of sensors with a low level of optical crosstalk.

Each sensor was made up of a fiber coupler of a predefined split ratio connected to an 18m long fiber coil laid into a helical groove cut into the surface of a 2.6m long polyurethane bar. One port of the coupler was silvered to form a mirrored end. At either end the fiber was fed through a loose tube that in turn was inserted into a length of

reinforced hosepipe. The cable, coupler and coil were laid in a 22mm square channel and then potted in soft polyurethane.

Each sensor was connected to the next sensor by a 4.5m interconnect length of fiber cable. In addition, 0.5m of spare fiber was added to each sensor resulting in a total sensor length of 23m.

Also, a 200m-delay coil, made using standard telecom grade fiber, was used between the sensors and interrogation unit to simulate interrogation over a large distance. In later tests this was greatly extended by the addition of a further 20km of optical fiber. This was to demonstrate that it would be possible to use the optical fiber of existing fiber optic highway communication systems to link sensor stations over large distances.

Experiment Details

During March 2001 a number of field trials were arranged at the Winfrith Technology Centre site to determine the sensitivity and performance of the sensor, and to demonstrate the ability to multiplex sensors together while interrogating them over large distances. The test results were obtained using the prototype sensor described previously. Unfortunately, the researchers were unable within the period of the study to calibrate the sensor output, given in terms of Radians, into a measurement of weight. However, the form and amplitude of the test results strongly indicated that fiber optic sensors of this type might be viable alternative WIM sensors.

Unfortunately, the test road used during the field tests was not ideal, being only 6m wide. Hence the 3m length of each sensor, to get optimal coverage pairs of sensors on each lane were interlaced as shown in Figure 5.57. Each pair was offset by 0.2m, with a 2m separation between sensors on each lane. Four slots were cut to accommodate the four prototype fiber optic sensors. Three of these slots were extended to the far side of the road by additional slots (Hill et al., 2002).
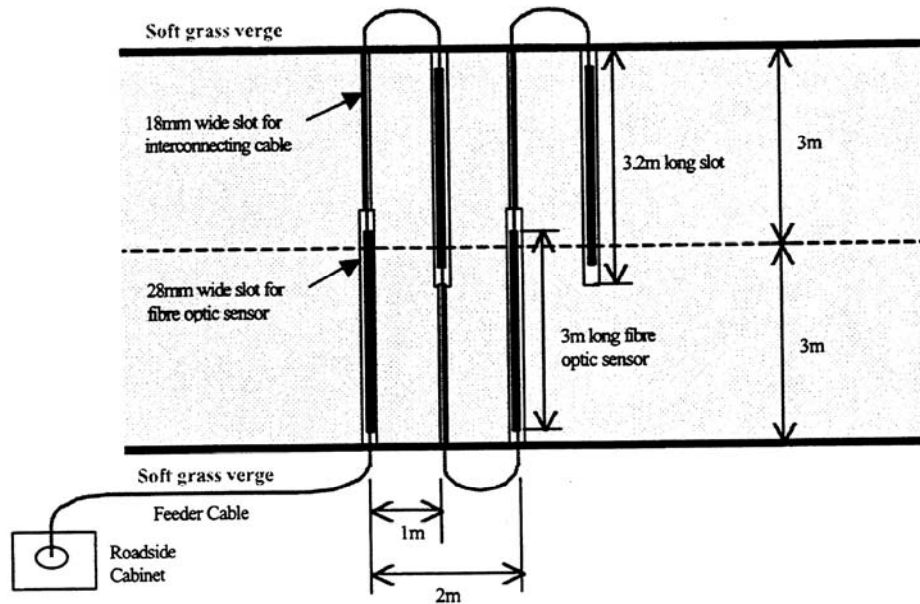
Figure 5.57. Multiplexed sensor deployment (Hill et al., 2002).

The four sensors arrived on site pre-connected, with interconnecting cable lengths of 4.5m. Once the slots were cut the multiplexed sensors were lowered into the slots supported off the bottom by resting on screw heads 45mm below the road surface. Once the slots containing the sensors and the interconnecting cable were in place they were back filled with Polyurethane resin until flush with the road surface.

The feeder cable was brought back to the roadside cabinet and the end of the cable spliced into a sealed box containing a 200m-delay coil of standard fiber. A fiber optic connector on the outside of this box allowed for easy connection to the demultiplexing and demodulation electronics.

Figure 5.58 shows the response of a single sensor to two passes of a car traveling at different speeds. This plot shows that the form of the signal differs with speed in regard to the peak spacing, pulse width and differing amplitudes. Also, the so called "bow wave" in the data, due to the sensor responding to horizontal pressure can be clearly seen before the start of each signal corresponding to a wheel impact.
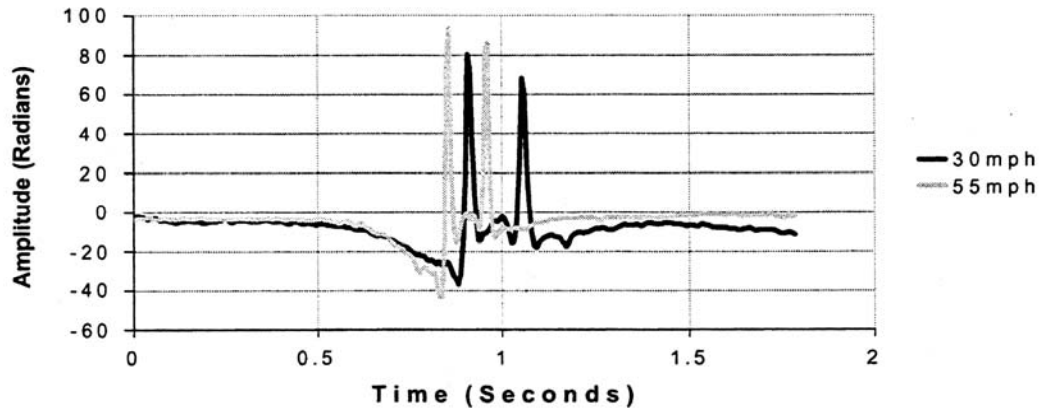
Figure 5.58. Response of the prototype sensor to a passing car (Hill et al., 2002).

During the field study an additional 20km of standard telecom fiber was connected between the sensors and the interrogation system. This added an additional 40km of optical path round trip to the optical signals within the system. The returned signal remained strong and the processing unit continued to demultiplex and demodulate the signals from the four multiplexed sensors.

Figure 5.59 shows the response of a sensor pair to a passing car followed, 2.25 seconds later, by a bicycle. This data was collected over the 20km optical fiber downlink. The response of the two sensors was closely matched with excellent signal to noise. Given the separation distance between sensors, speed estimation can easily be achieved by measuring the peak-to-peak separation between sensor signals. The researchers believe that this data demonstrated the dynamic range of this sensor and its potential at being able to discriminate between different vehicle types.
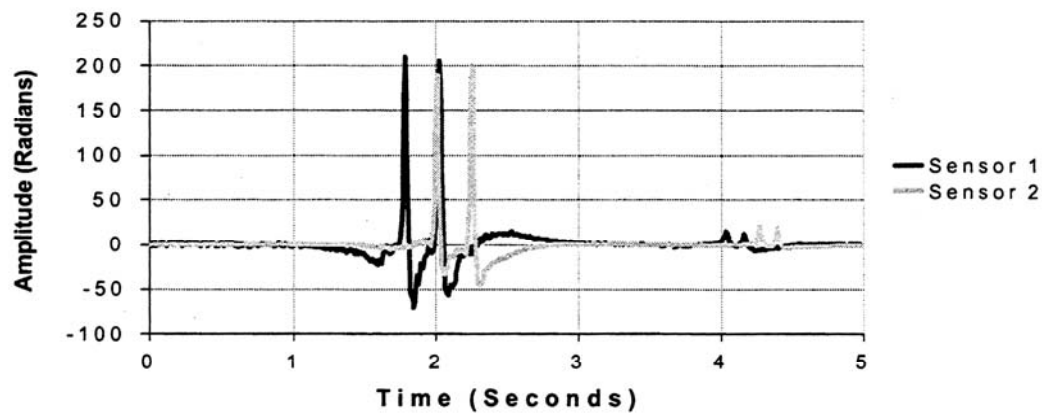
Figure 5.59. Car followed by a bicycle passing over a sensor pair, interrogated over a 20km optical fiber (Hill et al., 2002).

In addition, Figure 5.60 shows the low frequency response of the system. Specifically, a car was slowly driven and parked over the sensor pair. The front axle remained over the first sensor for five seconds before slowly driving off. According to the researchers, this test confirmed that the system has a DC response, thus allowing static measurements that can be calibrated to give a direct value for the vehicle weight.
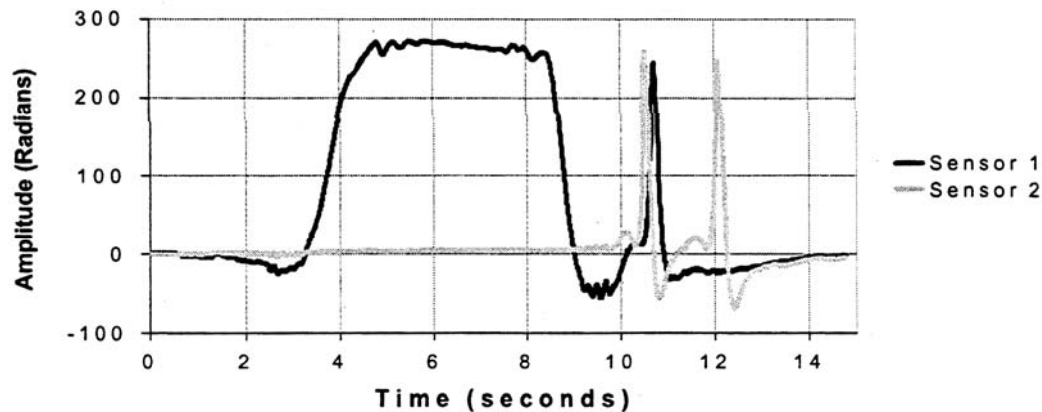
Figure 5.60. Front axle of a car stopping over first sensor before moving off (Hill et al., 2002).

<u>**Summary**</u>

The researchers believe that the advantages of the type of sensor developed for this study will be fully realized when deployed within a multiplexed network. Due to the inherently

124

high bandwidth capability and low signal attenuation of optical fiber, a multiplexed network will remove the requirements for roadside electronics along with all the associated power needs and access to telecommunications infrastructure. Very preliminary estimates at the time of this study suggested that the manufactured hardware cost for a networked system of 32 fiber optic WIM sensors could be in the region of $75,000, with the proportional cost reducing as the size of the network increases (Hill et al., 2002).

The researchers believe that test results from this study showed that with the sensors, connected to a specially designed digital multiplexer/demodulator, it is possible to perform traffic monitoring and weigh-in-motion measurements. Tests on four of these sensors multiplexed together onto a single fiber showed that it is possible to interrogate sensors over a distance of at least 20km. Results also showed that the sensors were sensitive enough to detect a person running over them and a DC response enabling static weighing of a vehicle wheel and axle unit if positioned directly above the sensor.

Status to-Date

As a follow up phase to this project, the researchers would like to demonstrate a large area network of approximately 100 sensors, deployed at the Winfrith Technology Centre. This deployment would be used to refine sensor designs and evaluate multiplexing techniques and optical architectures required to facilitate the interrogation of the network via a pair of standard telecomm grade optical fibers from a conveniently located central location, which in this case would be the Winfrith Technology Centre.

In addition, the researchers would also deploy 32 fiber optic WIM sensors in four separate groups along a three-lane highway. This deployment would utilize the available so-called "dark fiber" within the UK's National Motorway Communications System (NMCS) to optically link the four sensor stations together and carry the signals back to the interrogation system.

As of the date of completion of this report on fiber optic sensors utilized in WIM

systems, the authors were unaware of any further advancement to this study. However,

that does not mean that the future projects discussed previously are not being carried out.

Chapter 6 – Evaluation and Testing Criteria

Evaluation and testing of newly installed weigh-in-motion (WIM) systems is typically carried out by the vendors installing the equipment in conjunction with one or several representatives of the agency that will be using the system. The evaluation and testing procedure of WIM equipment includes the calibration of the system and testing to insure the calibration is satisfactory. Calibration ensures that the estimation of static weight by the WIM system closely approximates the measured static weight. Calibration accounts for site-specific effects such as pavement temperature, vehicle speed, and pavement condition. Calibration procedures may include an acceptance testing phase and a recalibration phase.
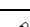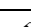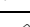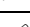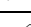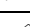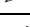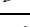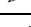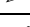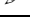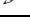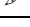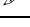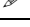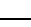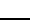
The FHWA strongly encourages State Highway agencies to allocate resources to the calibration of their WIM systems. As mentioned previously, calibration of WIM sensors is extremely important, because even small errors in vehicle weight measurements caused by poorly calibrated sensors result in significant errors in estimated pavement damage when those axle weights are used in pavement design analyses (FHWA, 2001).

Several techniques have been developed for WIM system calibration. The most common of these techniques is to make multiple passes over the WIM sensors with one or more test trucks of known weight. The WIM sensor performance is then compared with the known weights and adjustments are made to the WIM sensor's calibration as necessary. Additional passes are then made to confirm that the performance of the WIM sensors has improved to the level of accuracy desired.

The American Society for Testing and Materials (ASTM) has developed a standard specification for "Highway Weigh-in-Motion (WIM) Systems with User Requirements and Test Methods," designated as E1318-02. This standard includes a common test truck calibration procedure and an acceptance test that requires that the WIM system being offered by the vendor pass a rigorous one-time Type-Approval Test. The categories

(types) of WIM systems according to ASTM are listed in Table 6.1, along with the corresponding data they provide.

Table 6.1. WIM System Categories, Applications, and Data Items (Mimbela & Klein, 2000).

	Category			
	Type I	**Type II**	**Type III**	**Type IV**
Speed range	16 to 113 km/h (10 to 70 mi/h)	16 to 113 km/h (10 to 70 mi/h)	24 to 80 km/h (15 to 50 mi/h)	24 to 80 km/h (15 to 50 mi/h)
Application	Traffic data collection	Traffic data collection	Weight enforcement	Weight enforcement
Number of lanes	Up to 4	Up to 4	Up to 2	Up to 2
Bending plate	✎	✎	✎	✎
Piezoelectric	✎	✎		
Load cell	✎	✎	✎	✎
Wheel load	✎		✎	✎
Axle load	✎	✎	✎	✎
Axle-group load	✎	✎	✎	✎
Gross vehicle weight	✎	✎	✎	✎
Speed	✎	✎	✎	✎
Center-to-center axle spacing	✎	✎	✎	✎
Vehicle class (via axle configuration)	✎	✎		
Site identification code	✎	✎	✎	✎
Lane and direction of travel	✎	✎	✎	✎
Date and time of passage	✎	✎	✎	✎
Sequential vehicle record number	✎	✎	✎	✎
Wheelbase (front-to-rear axle)	✎	✎		
Equivalent single-axle load	✎	✎		
Violation code	✎	✎	✎	✎
Acceleration estimate			✎	✎

The Type-Approval Test is to be conducted under excellent site conditions, which are specified in the standard, to demonstrate that the system is capable of performing under such conditions. This test verifies the functionality of all features of the system, as well

as the highest potential accuracy when the sensors are subjected to loads from a wide range of vehicle types. However, if the vendor provides credible evidence that the type and model of system being offered has already successfully passed the applicable Type-Approval Test and the user provides site conditions as specified in the standard for acceptance testing, the system will be expected to perform at the site within the tolerances shown in Table 6.2 (ASTM E1318-02, 2002).

Table 6.2. ASTM performance requirements for WIM systems.

Function	Tolerance for 95% Probability of Conformity				
	Type I	Type II	Type III	Type IV	
				Value ≥ lb (kg)[a]	± lb (kg)
Wheel load	± 25%		±20%	5,000 (2,300)	300 (100)
Axle load	±20%	±30%	±15%	12,000 (5,400)	500 (200)
Axle load group load	±15%	±20%	±10%	25,000 (11,300)	1,200 (500)
Gross vehicle weight	±10%	±15%	±6%	60,000 (27,200)	2,500 (1,100)
Speed	±1 mi/h (±2 km/h)				
Axle spacing	±0.5 ft (±150 mm)				

[a] Lower values are not usually a concern in enforcement.
Source: *Standard Specification for Highway Weigh-in-Motion* (*WIM*) *Systems with User Requirements and Test Method*, Designation E 1318-02, 2002 Annual Book of ASTM Standards, Vol. 04.03, West Conshohocken, PA: ASTM.

Each type of fiber optic sensor WIM system would need to be submitted to the Type-Approval Test if the ASTM WIM standard is to be used to evaluate its performance. Once the fiber optic sensor WIM system's Type is determined during the Type-Approval test, the less rigorous acceptance test can be used to evaluate its performance for future installations.

One important aspect of ASTM WIM standard E1318-02, is that it includes a detailed section on user requirements for both the Type-Approval Test and the Acceptance Test since under current equipment constraints, the collection of WIM data based on calibrated equipment and comparable to static weight data may only be possible on smooth and flat pavement (FHWA, 2001).

The two main differences between the Type-Approval Test and the Acceptance Test are differences in the stricter user requirements for the Type-Approval Test and the use of 51 test vehicles from the traffic stream of specified classes in addition to two test trucks. The calibration procedure is basically identical for both types of tests and requires that two loaded, pre-weighed and measured test vehicles each make multiple runs over the WIM-system sensors in each lane at specified speeds. Road-surface profiles and sensor installation are different at every WIM site, and every vehicle has unique tire, suspension, mass, and speed characteristics. Therefore, it is necessary to recognize the effects of these site-specific, speed-specific, and vehicle-specific influences on WIM-system performance and attempt to compensate for their adverse effects as much as practicable via on-site calibration (ASTM E1318-02, 2002).

The ASTM WIM standard E1318-02 includes testing of WIM systems used for enforcement at weigh stations. The tolerances for these two types are shown in Table 6.2 under Types III and IV. The testing and calibration procedures for these two types of WIM systems is slightly different from the other two types due to their location off of the main highway as well as the equipment they have readily available, such as static weigh scales, etc., and personnel available on site for monitoring the equipment. Please refer to ASTM E1318-02 for complete details of calibration, Type-Approval Testing and On-Site Acceptance Testing.

As mentioned previously, the ASTM WIM standard E1318-02 is the only standard available for use in the calibration and testing of WIM systems. However, some State Highway departments have developed their own set of performance requirements (tolerances) for WIM data and guidelines for the calibration and testing of WIM systems. Table 6.3 shows performance requirements for WIM systems used by the California Department of Transportation (Caltrans).

Table 6.3. California Department of Transportation (Caltrans) performance requirements for WIM systems[a].

Parameter	Mean	Standard Deviation
Vehicle weight		
Single axle	±5 %	8%
Tandem axle	±5 %	6%
Gross weight	±5 %	5%
Axle spacing	±150 mm (6 in)	300 mm (12 in)
Vehicle length	±300 mm (12 in)	460 mm (18 in)
Vehicle speed	±1.6 km/h (1 mi/h)	3.2 km/h (2 mi/h)

[a] *Source*: McCall, W. and W.C. Vodrazka Jr., *States' Successful Practices Weigh-In-Motion Handbook*, Center for Transportation Research and Education (CTRE), Iowa State University, Dec. 15, 1997, http://www.ctre.iastate.edu/research/wim_pdf/index.htm.

The acceptance testing phase used by Caltrans and reported in the *State's Successful Practices Weigh-in-Motion Handbook* (McCall & Vodrazka, 1997) has three stages: system component operation verification, initial calibration process, and a 72-h continuous operation verification.

- System component testing verifies the transmission of signals by the roadway sensors to the on-site controller and the conversion of the signals into the desired WIM data.

- Initial calibration consists of comparing data obtained when one or more trucks pass over the WIM sensors with measurements taken on a static scale. Several runs are made to measure weight and axle spacing in each lane equipped with WIM sensors at speeds that encompass the expected operational range. These data are utilized to compute the WIM weight factors that convert the dynamic measurements into static weights. The test vehicles make additional runs at each speed to verify the weight factor values. Weight factors can be adjusted to account for seasonal variations, changes in pavement condition, and unique vehicles.

- The 72-h calibration monitors WIM system operation to ensure continuous functioning within the required specifications. When this phase is completed, the system is ready for online operation.

The recalibration phase occurs throughout the design life of the WIM site. Weight factors are adjusted or repairs made to the system when problems are identified during regularly scheduled data reviews.

Chapter 7 – Conclusions

The importance of weigh-in-motion (WIM) data to help determine effective and safe life of the world's transportation infrastructure such as bridges and pavements was presented in the earlier chapters of this report. For example it was mentioned previously that for bridges WIM data can be analyzed to estimate the probability that the maximum load rating of the bridge is being exceeded or to calculate the fatigue cycles experienced by the structure, which can in turn be used to predict remaining service life (Ansari, 1998). For pavements, WIM data are used for new pavement design and to predict remaining service life of existing roadways.

The earlier chapters of this report also mentioned that although WIM systems are commercially available at this time, fiber optic based WIM systems offer the potential to measure actual dynamic loads while offering sensors that are light weight, immune to electromagnetic interferences, offer the ability to be imbedded under hostile environments, and have extremely high bandwidth capability (Udd, 1995). Furthermore, it is anticipated that fiber optic WIM systems, once developed, will eventually be lower in overall cost relative to conventional systems, due to the inherently low cost of the fiber optic sensors.

In addition to the uses of WIM data for assessing useful and safe life of structures and pavements, WIM data can also be utilized as part of the National Intelligent Transportation System (ITS) Architecture, which is a framework for Integrated Transportation into the 21st century (FHWA, 2003). Many states in the U.S. have developed or are developing local ITS Architecture plans and WIM systems can play a major role in providing real-time data that can be used to achieve the goals of these plans. For example, one of the goals of the National ITS Architecture is to "manage traffic." The "manage traffic" process, which includes traffic signal control functions, interacts with the following eight other processes (FHWA, 2003):
1. Provide Vehicle Monitoring and Control,
2. Provide Electronic Payment Services,
3. Provide Driver and Traveler Services,

4. Manage Emergency Services,
5. Manage Commercial Vehicles,
6. Manage Archived Data,
7. Manage Transit, and
8. Manage Maintenance and Construction.

In order for WIM systems to play a major role in achieving the goals of the national and local ITS Architecture plans, deployment of these systems must be dramatically increased and their real-time monitoring capabilities need to be improved. In order to satisfy the deployment needs and real-time monitoring capabilities of WIM systems for ITS purposes (includes traffic monitoring) lower cost alternatives must be developed with higher bandwidth capacity. Fiber optic sensor WIM systems have the potential to offer these two key capabilities once the technology has been well developed.

One of the specific objectives of this project was to perform a comprehensive review of the literature for fiber optic sensors for measurement of in-motion weight or weigh-in-motion (WIM) applications; performance criteria (precision, accuracy and durability); and applications of weigh-in-motion (WIM) data for fatigue in pavements and structures. As mentioned previously, a state-of-the-art study was carried out for this project, which included a literature review for fiber optic sensors in WIM system applications. During the state-of-the-art study documentation for a total of ten different studies was reviewed from the following entities:

1. New Mexico State University (NMSU) / Naval Research Laboratory (NRL)
11. Blue Road Research (BRR)
12. Oak Ridge National Laboratories (ORNL)
13. New Jersey Institute of Technology (NJIT)
14. University of Connecticut (UCONN)
15. Florida Institute of Technology (FL Tech)
16. Laboratoire Central des Ponts et Chaussees (LCPC)
17. Virginia Polytechnic Institute and State University - 1990 Strategic Highway Research Program (SHRP) Project
18. Virginia Polytechnic Institute and State University - Project on Using Fiber Optic Sensors for Civil Infrastructure Monitoring
19. United Kingdom Highway Agency's Project

No official readily available documentation was encountered from other entities to support additional studies of WIM systems using fiber optic sensors or commercially available WIM systems using fiber optic sensors other than the ones listed previously.

However, the state-of-the-art study was conducted mainly for U.S.-based technologies and foreign technologies that were presented in the U.S. at appropriate technical conferences. Several World Wide Web based searches were conducted to locate technologies in other countries and in all cases no credible documentation was found using this medium. However, this does not mean that there are no studies or commercially available fiber optic sensor WIM systems available in other countries.

Table 7.1 shows the results of the state-of-the-art study for fiber optic sensors in WIM system applications. The accuracy was compared to gross vehicle weight (GVW) and the speed was the speed at which the vehicles passed over the sensors.

Table 7.1. Results of State-of-the-Art Study for Fiber Optic Sensors in WIM System Applications

Entity – Year	Method	GVW Accuracy Speed	Status
NMSU/NRL – 1998	Multiple Bragg Grating	Not determined	Research – No plans to continue at this point
Blue Road Research (BRR) – 1998 to present	Multiple Bragg Grating	Not determined	Research – Field study stage in progress
ORNL – 1990 to 1991	Transparent Rubber	±0.5% to ±3% 5km/hr (3 mph)	Research – No plans to continue at this point
NJIT – 1996	Polarimetry	Lab testing w/o vehicles	Research – No plans to continue at this point
UCONN – 1997 to present	FTDM Dual Core fiber	±4% to ±12% static (0 mph)	Research – Laboratory testing is ongoing
FL Tech –1999 to present	Microbend	8% to 14% 10-40 mph	Commercial Deployment of Fiber Optic WIM System
LCPC – 1999	Low birefringence single mode optical fiber	±22.5 lbf (lbs) 6.2-9.3 mph	Research – On hold until demand for product is determined
VPI & State University			
SHRP Project – 1990	Extrinsic pressure sensor	Lab testing w/o vehicles	Research – No evidence of plans to continue at this point
Civil Infrastructure Monitoring Project – 1994	Fabry-Perot	Not determined	Research – No evidence of plans to continue at this point
United Kingdom Hwy. Agency – 2002	Interferometry	Not determined	Research – No evidence of plans to continue at this point

The results of the state-of-the-art study for the use of fiber optic sensors in WIM system applications clearly demonstrated that this technology is in the research stages with the exception of FL Tech's microbend sensor WIM system (highlighted). At the beginning

134

of the state-of-the-art study, the FL Tech study was also in the research stage. However, in late 2002 and early 2003 the researchers made a breakthrough and a commercially available fiber optic WIM system was developed and marketed. As of the date of this report a WIM system using microbend fiber optic sensors (WIM 3000) was commercially available from Optical Sensors and Switches, Inc. and had been deployed in at least one location in the U.S.

The results from the state-of-the-art study revealed at least 9 different types of fiber optic sensor methods used in WIM system applications. Therefore, the potential for the development of at least 8 additional different types of fiber optic sensor WIM systems is high. The research study results using the 9 methods of fiber optic sensors in WIM system application revealed advantages and disadvantages of each application. This in turn would make some of these systems suitable for different types of uses. For example, the more accurate systems would be suitable for enforcement uses, while the least accurate would be suitable for traffic monitoring purposes.

The results for four of the 10 different studies of fiber optic sensor WIM systems regarding accuracy are listed in column three of Table 7.1. The reader should be cautioned that these accuracy values cannot be compared to each other directly since they were obtained at different speeds and site conditions, and the GVW figures used for comparison were not all obtained by the same method.

Gathering specific information on durability of the 10 studies of the different types of fiber optic sensor WIM systems was not the focus of the studies and for 8 out of the 10 studies would not be directly applicable to real life applications due to the type of testing (e.g. laboratory, parking lot, etc.) employed. However, the two Multiple Bragg Grating systems were deployed on existing bridges and a highway system under actual traffic conditions. For the bridge installations the sensors did not come in contact with the vehicle since they were located underneath the bridge on supporting beams, etc. It is anticipated that the durability of this type of non-intrusive system would be higher in comparison to the intrusive (in or on-pavement) systems. The highway installation had

135

only been in place several months as of the time of this report, thus no official data was yet available on durability issues.

Information on performance criteria (precision, accuracy, and durability) for WIM systems using fiber optic sensors is clearly lacking. However, it is obvious that once the technology matures to the demonstration phase, acquiring this type of information should be top priority since this will allow providers of this technology to find the niche for their specific product.

Another specific objective of this study was to conduct a review of the literature for applications of WIM data for the determination of fatigue in pavements and structures. Chapter 3 of this report describes the use of WIM data for determining fatigue on bridges using WIM data vs. simplified AASHTO methods that use estimated values of truck weights (HS15 fatigue truck) and number of trucks crossing the bridge.

The results from this literature review demonstrated that using an HS15 fatigue truck and using GVW's computed with WIM data for determining fatigue in steel bridges yielded similar conservative figures for service life when compared to using actual field measurements of individual stress ranges. One conclusion made from this particular study was to first estimate the fatigue life of a bridge using an HS15 fatigue truck, which would give a conservative estimate. If the safe life was found to be shorter than the desired service life, the fatigue analysis using actual field measurements of individual stress ranges should be performed.

The final objective of this state-of-the-art study for fiber optic sensors in WIM system applications was to develop recommended criteria for testing and evaluating commercial fiber optic sensors and measurement systems for weigh-in-motion. Chapter 6 of this report describes the use of ASTM WIM standard E1318-02 for calibration and testing of the entire WIM system (sensors and measurement system combined). The reader is also referred to the *State's Successful Practices Weigh-in-Motion Handbook (WIM Handbook)* by McCall, et al for guidelines on evaluating commercial WIM systems. The ASTM

WIM standard and the WIM Handbook offer criteria for evaluating and testing WIM systems as a whole and do not separate the sensors and the measurement system. For testing only the sensors portion of the system, the users of WIM systems rely on the vendors' guidelines. This will be the case as well for the evaluation and testing of fiber optic sensors in WIM system applications. Furthermore, if there should be a problem with the sensors this will most likely show up as a problem during the calibration and evaluation and testing of the entire WIM system.

In conclusion fiber optic sensors in WIM system applications show considerable promise for meeting both traffic monitoring needs and as part of the national and local ITS architecture plans. However, the technology is not mature with only one type of system commercially available and several others in various stages of development. These potentially innovative and practically significant fiber optic WIM systems need to be encouraged and supported so that they can be developed into maturity and thus make a broader fiber optic WIM system technology base available from which the best ones can be selected for real-life highway testing and practical use.

Chapter 8 – Recommendations

Based on the results of this study, a more detailed phase of work is needed to address the following in order to consider the use of fiber optic sensors in WIM system applications a mature and proven technology:

1. Select fiber optic sensor WIM systems that are fully developed and install, calibrate, and evaluate and test the systems at selected test sites according to the ASTM WIM standard or other standard and determine system accuracy under optimum site conditions.

2. Once the fully developed systems have been initially tested, conduct a series of field demonstrations under low and high volume traffic conditions and low and high-speed scenarios and compare the data to data obtained from conventional WIM systems at the same location.

3. Select fiber optic sensors complete with optoelectronics systems whose outputs are in terms of an electrical or digital signal and solicit conventional WIM system manufacturers to attempt to hook up their measurement systems to these to obtain a complete WIM system. Next, work together to develop the algorithm for calculating weight and proceed as in items 1 and 2 above.

Item 3 is desirable since established WIM system manufacturers will offer higher credibility to potential users of innovative technologies than newly developed companies whose sole product is the new sensor technology being offered. However, this approach might result in the established WIM manufacturer buying the rights to the sensor technology instead of purchasing the sensor components from the sensor developer. This is due to the fact that established WIM system manufacturers will have larger facilities and economies of scale will result in lower production cost of the sensor system components. This type of situation may not be desirable to the sensor system developer who is looking to become a provider of sensor system components and ultimately an entire WIM system.

At the time of this study SWTDI was partnering with the Border Technology Deployment Center (BTDC), New Mexico State Highway and Transportation Department, other State and Federal Agencies, and a conventional WIM system manufacturer from Canada, International Road Dynamics (IRD), on a proposal to conduct a field demonstration project of fiber optic sensor WIM system technologies.

The proposed project would install, evaluate and test several fiber optic sensor systems hooked up to IRD's WIM measurement system by comparing ease of calibration, functionality and performance criteria (precision, accuracy and durability) to a conventional WIM system at the same site. The selected demonstration site is located at the Santa Teresa, New Mexico international port of entry and would be considered a low speed, low traffic site during the demonstration. However, the selected port of entry has the potential to become a high traffic port due to predicted increased growth of the area. Results of this proposed demonstration of fiber optic sensors in WIM system applications are expected to determine performance criteria (precision, accuracy, and durability) for the systems evaluated under the real-life application scenario at the selected site.

References

Ansari, F., Wang, J., <u>Fiber Optic Polarimetric Dynamic Force Sensor</u>. Experimental Techniques Vol 20, pgs. 20-23, January-February, 1996 SEM – Society for Experimental Mechanics, Inc., Bethel, Connecticut.

Blue Road Research (BRR), <u>Overview of Fiber Optic Sensors</u>, (October 2000). [On-Line]. Available: http://www.blueroadresearch.com/images/overview_of_FOS2.pdf

Blue Road Research (BRR), <u>Experimental Results</u>, Personal correspondence, March 18, 2003.

Caussignac, J., Rougier, J., <u>Fibre Optic WIM Sensor and Optoelectronic System – Preliminary Tests, In Weigh-in-Motion of Road Vehicles</u>, Proceedings of the Final Symposium of the project WAVE (1996-99), Paris, May, 1999.

Cosentino, P. J., Grossman, B. G., <u>Development of Fiber Optic Dynamic Weigh-in-Motion Systems,</u> Florida Institute of Technology, Melbourne, Florida, August, 1997.

Daniels, J. H., Wilson, J. W., Yen, B. T., Lai, L. Y., Abbaszadeh, R., <u>Weigh-in-Motion and Response Study of Four In-service Bridges</u>, Report No. FHWA/RD-86/045, October 1987.

De Vries, M., Arya, V., Grinder, C., Murphy, K., Claus, R., <u>Civil Infrastructure Monitoring for IVHS Using Optical Fiber Sensors</u>, *In* The International Society for Optical Engineering (SPIE) Vol. 2344 Intelligent Vehicle Highway Systems, 1994 Proceedings.

Federal Highway Administration (FHWA), <u>Key Concepts of the National ITS Architecture.</u> 2003. [On-Line]. Available: http://www.iteris.com/itsarch

Gagarine, N., Albrecht, P., <u>Advances in Weigh-in-Motion Using Pattern Recognition and Prediction of Fatigue Life of Highway Bridges</u>, Report No. FHWA-RD-92-046, September 1992.

Grossman, B. G., <u>Real Time Speed, Classification and WIM Using Portable Fiberoptic Sensors</u>, Personal correspondence, March 19, 2003.

Hill, D. J., Nash, P. J., Sanders, N., <u>Networked Fibre Optic WIM Sensors.</u> *In* Pre-Proceedings of the Third International Conference on Weigh-in-Motion (ICWIM3), May 13-15, 2002, Orlando, Florida.

Lee, C. E., Ferguson, P. M., Concepts of Weigh-in-Motion Systems. *In* National Weigh in Motion Conference Proceedings, July 11-15, 1983, Stapleton Plaza Hotel, Denver, Colorado.

Lin, Y., Development of a Dual Core FTDM Fiber Optic WIM System. *M.S. Thesis*, (Major Thesis Advisor: R. Malla), Dept. of Civil & Environmental Engineering, Univ. of Conn., Storrs, CT, December 2000.

Malla, R., Garrick, N., Sen, A., and Dua, P., A Dual Core Forward Time Division Multiplexing Optical Fiber for Weigh-in-Motion System, *Fiber Optic Sensors for Construction Materials and Bridges (F. Ansari, Ed.), (Proceedings of the NSF/FHWA/ASCE/NJDOT International Workshop on Fiber Optic Sensors for Construction Materials and Bridges*, NJIT, Newark, NJ, U.S.A., May 3-6, 1998) Technomic Publishing Co., Lancaster, PA, May 1998, pp 251-262.

Malla, R., Garrick, N., Dual Core FTDM Fiber Optic WIM System, Final NCHRP-IDEA Project Report (Grant # NCHRP-42), Transportation Research Board, National Research Council, June 15, 2000.

Malla, R., and Lin, Y., Application of a New Dual Core Fiber Optic Sensor for Weighing Vehicles in Motion, *Procs., Connecticut Symposium on Microelectronics & Optoelectronics*, United Technologies Research Center, E. Hartford, CT, March 14, 2001, P25 (Abstract).

Malla, R. B., Research on Fiber Optic Weigh-in-Motion Sensor at University of Connecticut, Personal correspondence, August 2002.

McCall, W. and W.C. Vodrazka Jr., States' Successful Practices Weigh-In-Motion Handbook, Center for Transportation Research and Education (CTRE), Iowa State University, Dec. 15, 1997, [On-line], Available: http://www.ctre.iastate.edu/research/wim_pdf/index.htm

Mimbela, L. Y. and Klein, L. A., Summary of Vehicle Detection and Surveillance Technologies Used in Intelligent Transportation Systems (ITS), Vehicle Detector Clearinghouse (VDC), October, 2001.

Muhs, J. D., et al., Portable Weighing System – A Vehicle Weigh-in-Motion System Based on Fiber Optics, Applied Technology Division, Oak Ridge National Laboratory, July 1991.

Oak Ridge National Laboratory (ORNL). DP 121 Weigh-in-Motion Technology. (April 2001). [On-Line]. Available: http://www.ornl.gov/dp121/

Safaai-Jazi, A., Ardekani, S. A., Mehdikhani, M., A Low-Cost Fiber Optic Weigh-in-Motion Sensor, Strategic Highway Research Program, National Research Council, Washington, DC, 1990. [On-Line]. Available:

http://www4.trb.org/trb/onlinepubs.nsf/web/Long-Term_Pavement_Performance_Reports

Sen, A., Weigh-in-Motion Using a Special Forward Time Division Multiplexing Fiber Optic, *M.S. Thesis* (Major Thesis Advisor: R. Malla), Dept. of Civil & Environmental Engineering, Univ. of Conn., CT, August 1999.

Shuhy, J. F., Analysis of Fiber Optic Microbend Sensors for Use in Vehicle Classification and Weigh-in-Motion Systems, *M.S. Thesis* (Major Thesis Advisor: B. G. Grossman), Dept. of Electrical Engineering, Florida Institute of Technology, Melbourne, FL, January 1999.

Stein, P. P., Friedrichs, D. A., Wiley, M. M., The Overweight Truck in Wisconsin-its Impact on Highway Design, Maintenance and Enforcement Planning, Madison, Wisconsin, Wisconsin Department of Transportation, October 1988.

Udd, E., et al., Fiber Grating Systems for Traffic Monitoring, Paper for Poster Session, The International Society for Optical Engineering (SPIE) Technical Conference – Smart Systems for Bridges, Structures and Highways, March, 2001.

Udd, E., et al., Fiber Optic Sensors for Infrastructure Applications, Report No. FHWA-OR-RD-98-18, February 1998.

Udd, E., et al., Fiber Optic Sensors – An Introduction for Engineers and Scientists, John Wiley & Sons, Inc., New York, 1991.

U.S. Department of Transportation Federal Highway Administration (FHWA), Automated Traffic/Truck Weight Monitoring Equipment (Weigh-in-Motion) – An Overview of Issues and Uses, Report No. FHWA-DP-90-076-002, March 1990.

Wyman, J. H., Weigh In Motion Instrumentation of a Bridge. *In* National Weigh in Motion Conference Proceedings, July 11-15, 1983, Stapleton Plaza Hotel, Denver, Colorado.